AD-A200 560

③

DOT/FAA/CT-88/16

FAA Technical Center
Atlantic City International Airport
N.J. 08405

Wheel Performance Evaluation

Phase I — Analysis

P.C. Durup
T.R. Brussat
L. Bakow

Prepared by
Lockheed Aeronautical Systems Company
Burbank, California 91520

September 1988

Final Report

This document is available to the U.S. public
through the National Technical Information
Service, Springfield, Virginia 22161.

DTIC
ELECTE
NOV 0 4 1988
S   H   D

U.S. Department of Transportation
Federal Aviation Administration

88 11 4 030

Technical Report Documentation Page

1. DOT/FAA/CT88/16	2. Government Accession No.	3. Recipient's Catalog No.

4. Title and Subtitle	5. Report Date
WHEEL PERFORMANCE EVALUATION	September 1988
PHASE I - ANALYSIS	6. Performing Organization Code
	8. Performing Organization Report No.

7. Author's)
P. C. Durup; T.R. Brussat; L. Bakow

9. Performing Organization Name and Address	10. Work Unit No. (TRAIS)
LOCKHEED CALIFORNIA COMPANY	
BURBANK, CA 91520	11. Contract or Grant No.
	DTFA03-84-C-00044
	13. Type of Report and Period Covered

12. Sponsoring Agency Name and Address	
U.S. Department of Transportation	
Federal Aviation Administration	
Technical Center	14. Sponsoring Agency Code
Atlantic City International Airport, NJ 08405	

15. Supplementary Notes

A follow-on report, Wheel Performance Evaluation - Phase II, will provide for an evaluation and comparison of flight and dynamometer test results.

16. Abstract

This report describes the procedures of analysis and dynamometer testing that may be used to develop data and supporting technology for improving aircraft wheel performance. As related to current wheel standards and in-service inspection procedures, load/test spectras which characterize wheel operating environments (associated with long, medium and short haul aircraft) are defined. These spectra may be applied as a basis for effective dynamometer testing and to the verification of wheel service limits taking into account stress corrosion and crack growth conditions.

17. Key Words	18. Distribution Statement
wheel stress fatigue damage dynamometer test	Document is available to the U.S. public through the National Technical Information Service, Springfield, VA 22161

19. Security Classif. (of this report)	20. Security Classif. (of this page)	21. No. of Pages	22. Price
Unclassified	Unclassified	106	

Form DOT F 1700.7 (8-72)   Reproduction of completed page authorized

PREFACE

This report was prepared by the Lockheed Aeronautical Systems Company under Contract DTFA03-84-C-00044 and contains a description of the effort performed in Phase I. This work was sponsored by Federal Aviation Administration Technical Center, with Richard Johnson as Technical Monitor.

The program leader is Paul Durup of the Lockheed Aeronautical Systems Company. Dr. Thomas Brussat and Leon Bakow of the Lockheed Aeronautical Systems Company performed the work connected with fatigue and crack growth. Important contributions were made to the program by B. F. Goodrich, which is participating as subcontractor under the direction of Mark Owen and Robert Spofford. Valuable assistance was supplied by them in service experience, testing of wheels, and in the cost effectiveness studies. Lt. Greg Fisher of Hill AFB provided logistic services in having drawings, tire, wheel, and associated parts shipped for the test program. Preliminary wheel tests were performed at Wright/Patterson AFB under the direction of Igors Skriblis.

1

CONTENTS

FIGURES

FIGURES (Continued)

TABLES

SYMBOLS

D	=	Damage
E	=	Young's modulus, psi
K_rS	=	Measured stress at critical area, psi
L_L	=	Lateral load, pounds
L_R	=	Radial load, pounds
M	=	Walker's constant
N	=	Number of cycles to failure
n	=	Cycles for a given effective stress and for one flight
n_f	=	Number of flights
P,A	=	Constants
P_A	=	Tire pressure, psi
R	=	Ratio of maximum to minimum stress
S_L	=	Tubewell stress due to lateral load, psi
S_P	=	Tubewell stress due to tire pressure, psi
S_R	=	Tubewell stress due to radial load, psi
S_T	=	Total tube well stresses due to tire pressure, radial load and lateral load, psi
TSO	=	Technical Standard Order
ϵ	=	Strain, inch per inch
δ	=	Stress, psi
$\bar{\delta}$	=	Effective stress, psi
$\bar{\delta}_{sp}$	=	Effective stress shop peened, psi

EXECUTIVE SUMMARY

The life of an airplane wheel is affected mostly by the severity of the operational loads imposed on it, increased tire pressure encountered during operations from tire heating, and corrosion pitting in the critical areas of the wheel. The "Wheel Performance Evaluation" program, of which Phase I, Analysis, is the subject of this report, addresses these factors. A method is given to develop loads spectra for the wheels during expected operations of airplanes taking into account the missions to be performed. These spectra are converted into test loading and crack growth spectra using the stresses developed in the critical areas of the wheels. Phase I also includes a comparison of the present TSO-C26c and the test spectrum developed in this program. In addition, inspection procedures are discussed along with a study of cost effectiveness as it pertains to test procedures, inspection procedures and roll-on rim requirements.

Phase II will cover an evaluation of flight and dynamometer test results, applications of the wheel test procedures developed in Phase I, test requirements, and the benefits derived from the qualification test requirements.

SECTION 1

INTRODUCTION

1.1 PURPOSE

In addition to the TSO-C26c test requirements, airframe manufacturers and aircraft wheel manufacturers are devising different tests to increase the assurance that wheels will perform their function with a reduced probability of failure in service. The pupose of this program is to provide and verify, by use of service experience and dynamometer tests, a procedure by which a new wheel can be shown, by tests, that it will provide the service life projected for it. Phase I involves that development of loads and test spectra, a comparison of the TSO and proposed wheel test spectra, review of inspection procedures and a cost effectiveness study.

1.2 BACKGROUND

A comparison of tire, wheel, antiskid and brake system failures from 5229 reported operational failures during the years 1970 to 1975 was made by the FAA. The results indicated that, of the total tire and wheel failures, over thirty percent were wheels. This failure percentage does nut include the number of wheels removed from service ahead of their planned life as a result of cracks found during inspection periods. Since that time there have been some changes to requirements such as the roll-on-rim to provide some roll capability in the event of tire failure. However, other than work performed by individual wheel and airframe manufacturers to provide a safer wheel, there has not been a significant change in qualification requirements.

To be assured of a safe wheel, two factors must be satisfied. The first is that the qualification test must show that the predicted fatigue life of the wheel has been met and the second is that in the event of development of a flaw, such as a corrosion pit, the subsequent crack growth rate is sufficiently slow that the crack is detected prior to failure.

A test program for demonstrating the fatigue life of a wheel requires that all the loads experienced by the wheel in its intended operations be represented for the proposed number of roll miles. These loads are not only the radial and lateral but also the loads imposed by the pressure of the contained gas of the tire which fluctuates with the temperature of the tire. These loads can be developed by a series of scenarios depicting the operational use of the airplane taking into account varying loads acting on the wheel from differences in gross weight and from ground maneuvering requirements.

In dynamometer tests of wheels, the tires govern the rapidity in which the tests are performed because of the tires tendency to overheat and fail if the roll speed is too high. For a wheel designed to provide a 50,000 mile roll life, a calendar time of over 400 days would be needed using 24 hours per day for 7 days a week. This figure does not allow for tire changes and inspection periods performed during the course of the test program. As a consequence it is necessary to reduce the calendar test time and yet provide a test spectrum that is representative of the wheels service life.

The method used in Phase I is to develop a detailed operational scenario, for a given airplane, using the different missions of the airplane. The critical stress area is determined and strain gages applied. Equations are developed relating loads and stresses from the data obtained by rolling the instrumented wheel under various load conditions. These equations are used to determine the critical wheel stresses for the loads spectra. Using the fatigue curves for the wheel material, scenario loadings that have stresses that will not affect the fatigue life are eliminated. In addition, for loads that have stresses that are affected by fatigue, the number of load applications is reduced by increasing the level of stress. The corresponding loads and load applications are then used to define the test spectra.

SECTION 2

DISCUSSION

Three wheels, having different characteristics, are used in the program. The first wheel is representative of a wide body large transport airplane for which substantial service history data are available. In addition, inspection procedures are being used for crack detection which provide data for evaluating the reliability of methods for predicting crack growth. The second wheel is from a smaller transport which also is used as a patrol airplane. Because the airplanes missions have changed and the life of the airplane is being extended, tests are being run on a load spectrum that is considered to be representative of a flight-by-flight loading to the predicted mission of the airplane. In this program, a test spectrum using the same missions but reducing the number of loading cycles to one-fourth of that of the pseudo flight-by-flight technique, using the method developed in this program, is employed. The results of the two test spectra will be compared. The third wheel is that of a tactical airplane. The uniqueness of this wheel is that because of the growth of the airplane's weight and the limitation of the wheel well size, the tires have to be operated well in excess of the rated pressure and loads. This requirement results in the wheels being exposed to much greater loads than the original design requirements.

2.1 DEVELOPMENT OF LOADS SPECTRA

2.1.1 Transport Airplanes

The loads spectra for the transport airplanes are developed using the mission mixes for the long-range, medium range and short haul airplanes. The mission mixes (see Table 2-1) are a composite of predicted flights by potential operators condensed to provide a means by which representative loadings can be established for the life of the airplane.

TABLE 2-1. MISSION MIXES FOR TRANSPORT AIRPLANES

a. LONG-RANGE

Non-Dimensional Weight ①		Percent of Flights	Flight Time Hours
Takeoff	Landing		
0.940	0.611	5.2	9.4
0.846	0.616	17.4	6.8
0.818	0.690	12.2	3.6
0.736	0.615	12.2	3.6
0.729	0.690	26.5	1.0
0.652	0.615	26.5	1.0

b. MEDIUM-RANGE

Non-Dimensional Weight ①		Percent of Flights	Flight Time Hours
Takeoff	Landing		
0.958	0.711	15.2	5.6
0.900	0.808	10.9	1.9
0.847	0.808	30.2	0.6
0.787	0.704	10.4	1.9
0.745	0.708	33.3	0.6

c. SHORT HAUL

Non-Dimensional Weight ①		Percent of Flights	Flight Time Minutes
Takeoff	Landing		
0.916	0.871	20	60
0.865	0.834	20	45
0.820	0.798	20	45
0.792	0.747	20	60
0.741	0.711	20	45

① Weight of interest divided by design takeoff weight

Knowing the airplane weight for the various missions allows the calculation of the taxi loads associated with each mission. One main wheel is selected for determining taxi loads by ascertaining which wheel will most likely experience the greatest loads. On a four wheel bogie it is usually the aft inboard wheel because of the crown of the runways. On a dual mount, the inboard wheel is critical for the same reason. In calculating the wheel loads, the pavement/tire interface, torsional stiffness of the strut, tire deflection, lateral stiffness of the strut, tire characteristics and tire gas pressure are taken into account. Tables A-1 through A-6 are examples of the loads, taxi speeds and single flight cycles for the heavy weight takeoff mission given in Table 2-1a. Tables A-7 through A-11 and A-12 through A-16 show the same data for the medium and short haul transports, respectively.

2.1.2 Small Transport/Airplane

Inasmuch as the small transport is an older airplane, it is being used for many diverse operations which makes it very difficult to define a set of missions. The patrol airplane version has defined missions which provides the data needed to define operational, fatigue and crack growth spectra which can be compared with experience. The tests to be performed with this wheel will augment the tests to be performed on the long range transport airlpane wheel. The mission definitions for the patrol airplane are complex involving landings during the flight as well as optional deviations in the mission. Figures 2-1 through 2-7 illustrate the various missions of the patrol airplane.

Once the missions are defined, the loading spectra can be determined. Table A-17 is an example load spectrum for the patrol airlpane tracking mission. During touch-and-go landings, the gear is left down which cools the tire such that contained gas pressure does not rise.

2.1.3 Tactical Airplane

The missions for the tactical airplane are derived from the Standard Aircraft Characteristics Charts. Table 2-2 shows the takeoff and landing weights, mission flight time, and the percentage of flights represented by each mission. The ground taxi scenario is developed from a tactical airplane base, wherein weapons are loaded and unloaded.

2-3
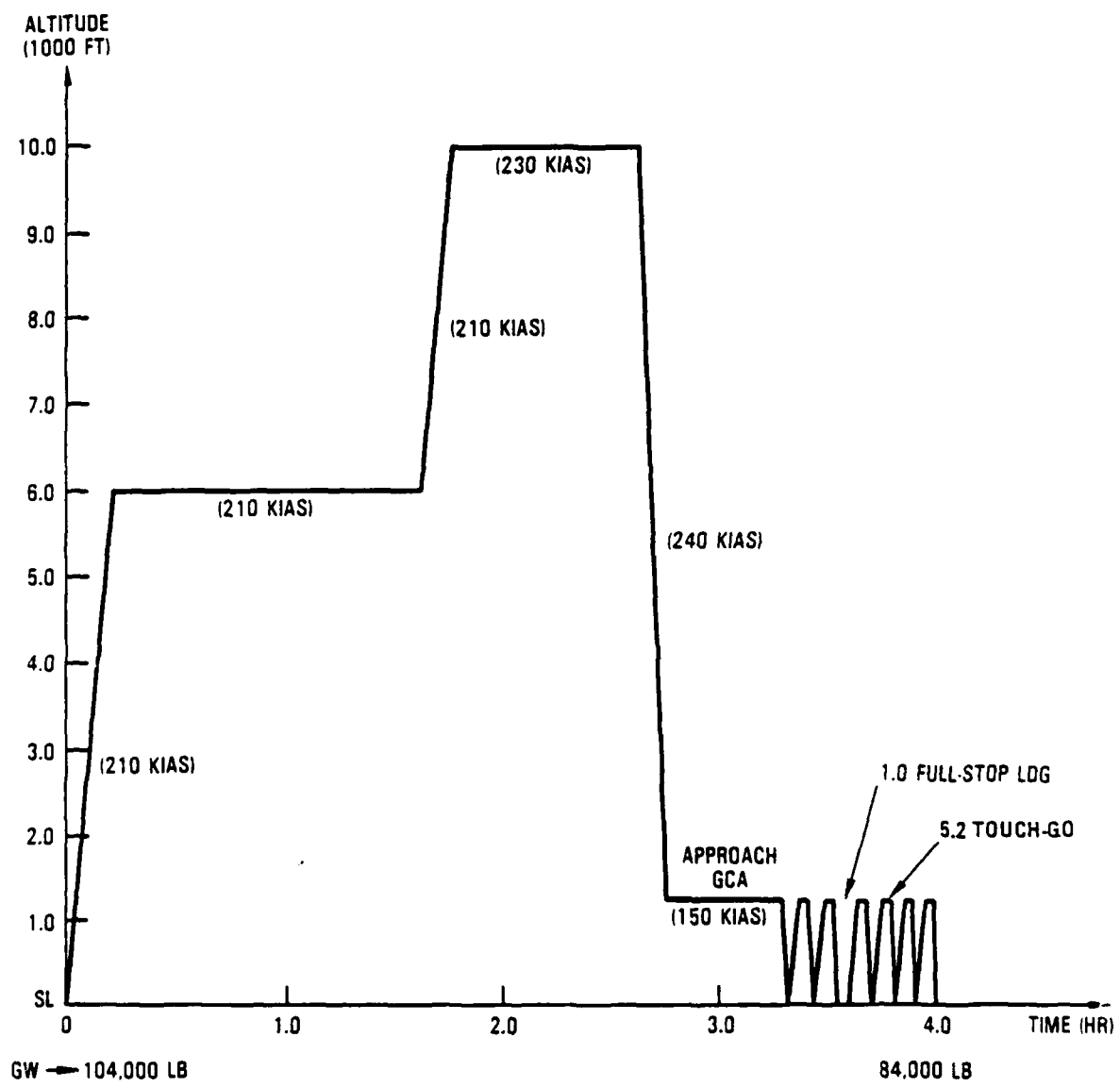
Figure 2-1. Patrol Airplane, Training/Fundamentals,
24.3 Percent of Flights
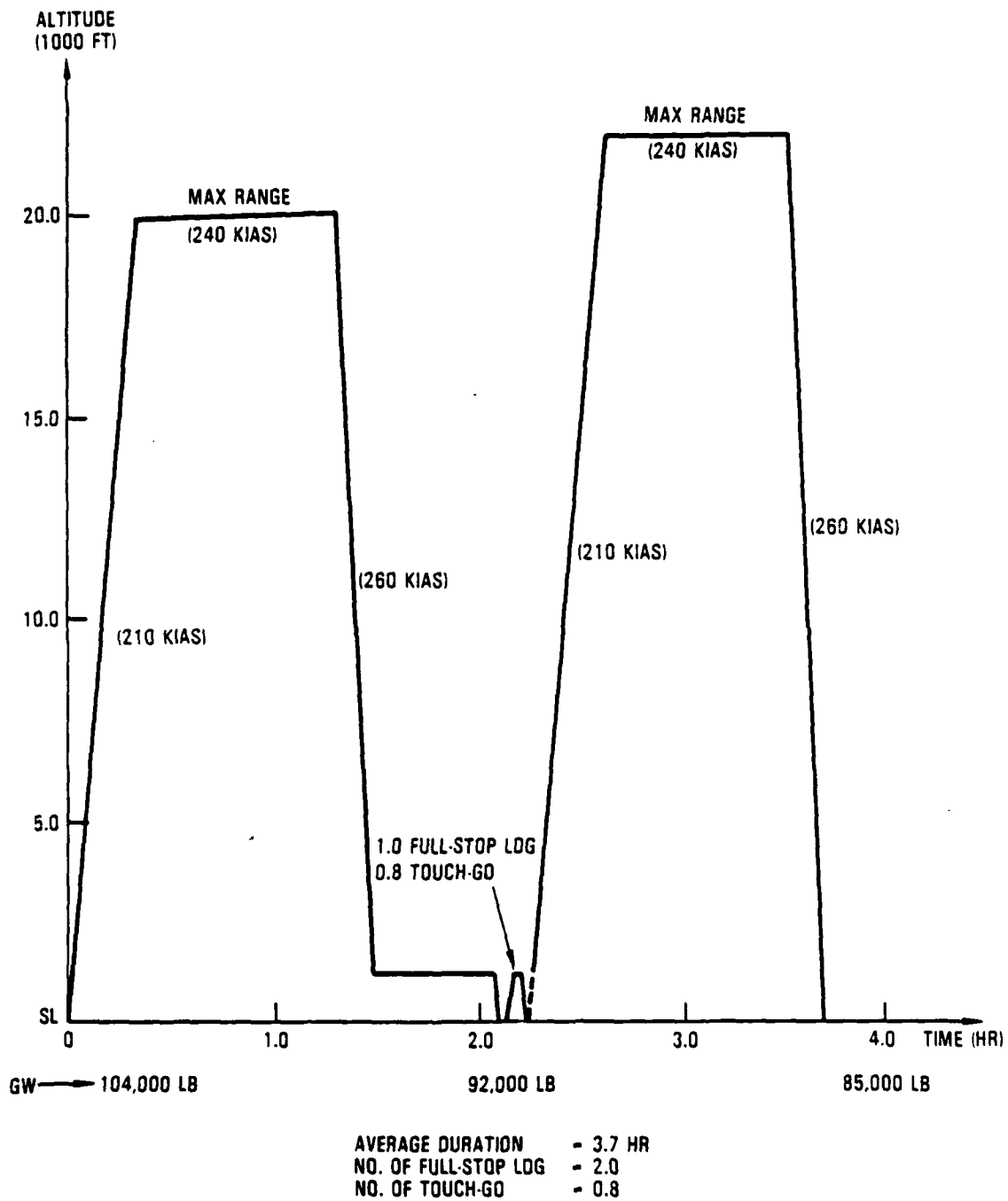
Figure 2-2. Patrol Airplane, Training/Instruments, 16.2 Percent of Flights
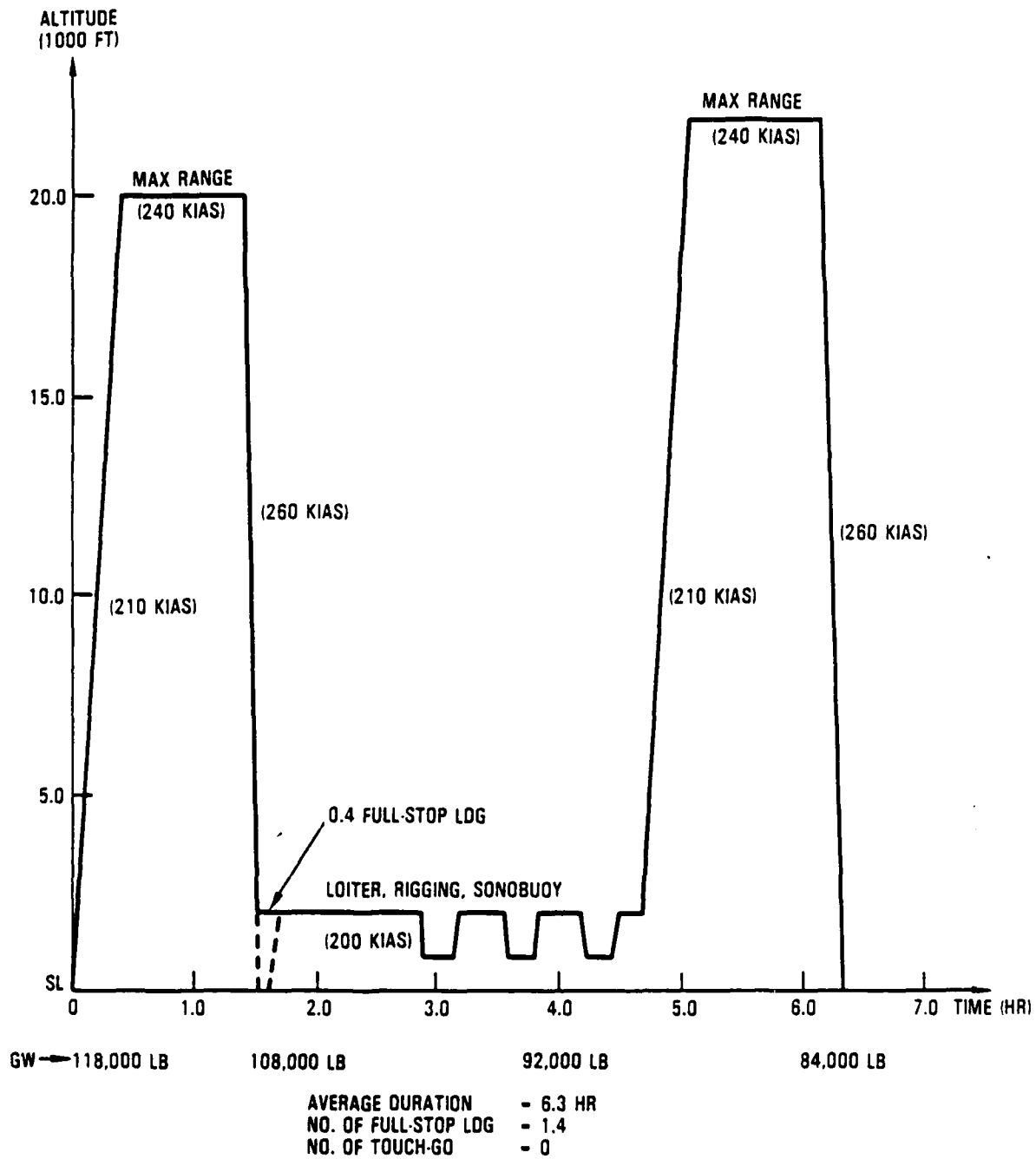
Figure 2-3. Patrol Airplane, ASW Training/Operational,
22 Percent of Flights
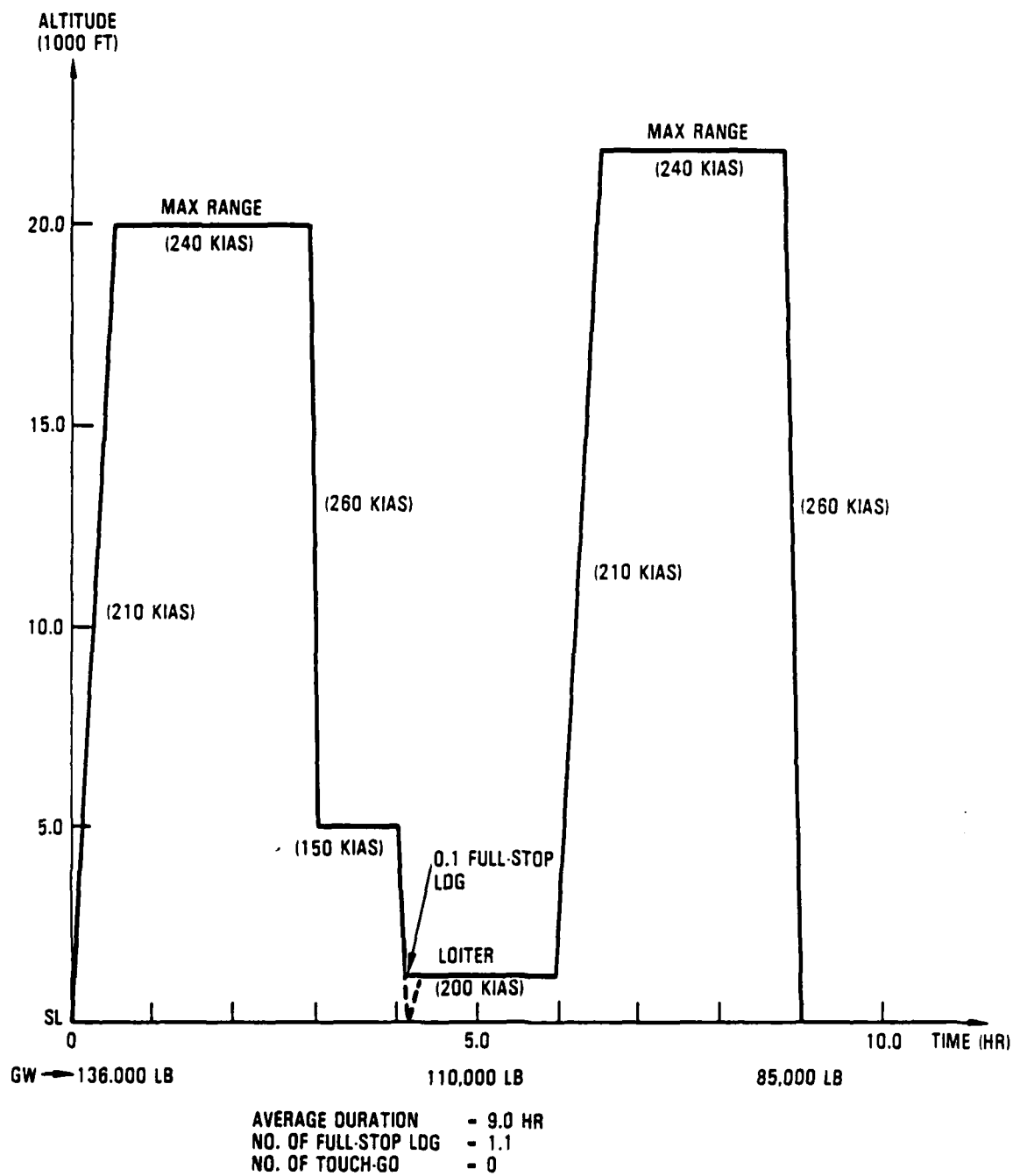
Figure 2-4. Patrol Airplane, Patrol/Search/Reconnaissance, 26.4 Percent of Flights
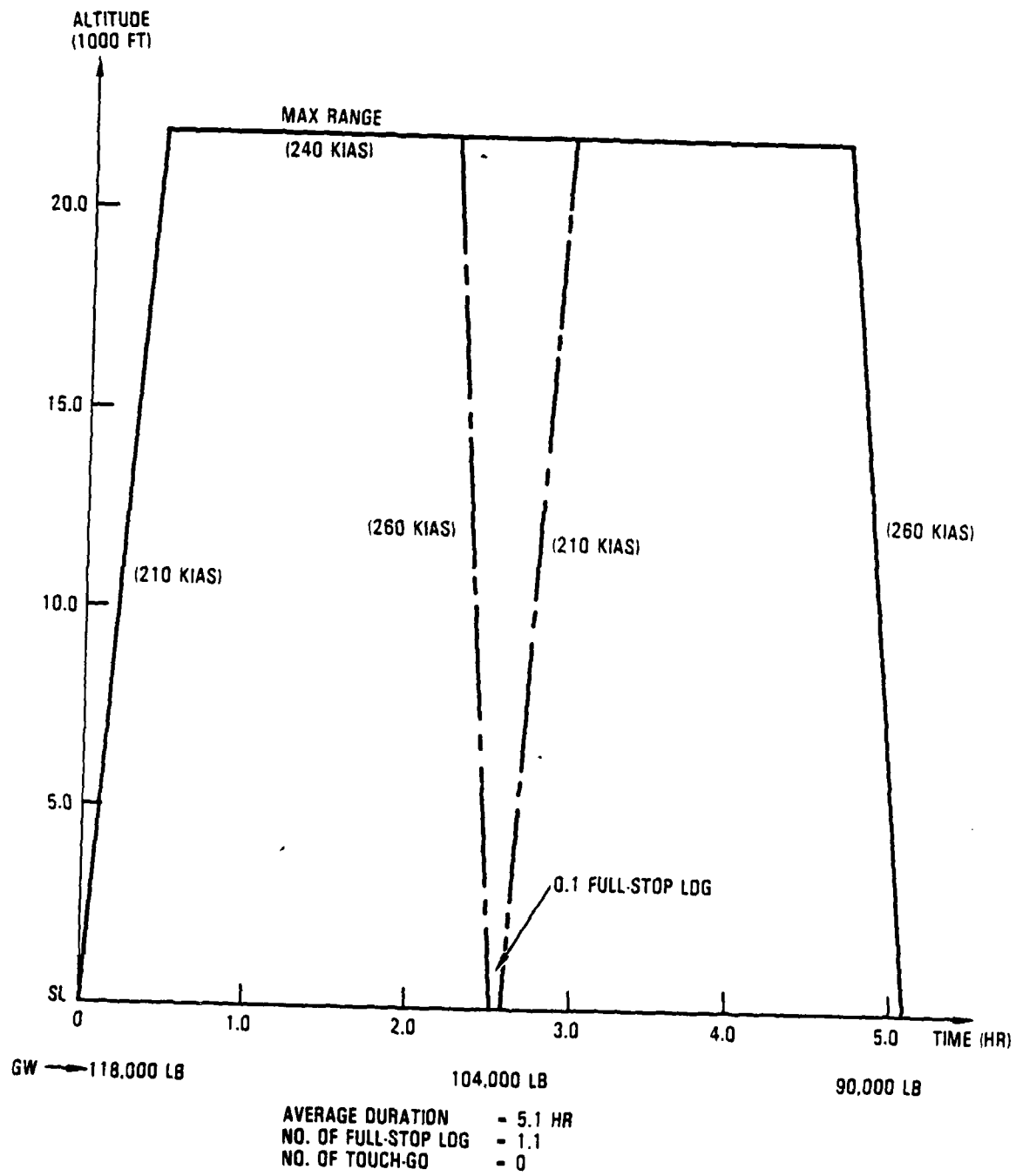
Figure 2-5. Patrol Airplane, Transport/Utility/Service,
4.8 Percent of Flights
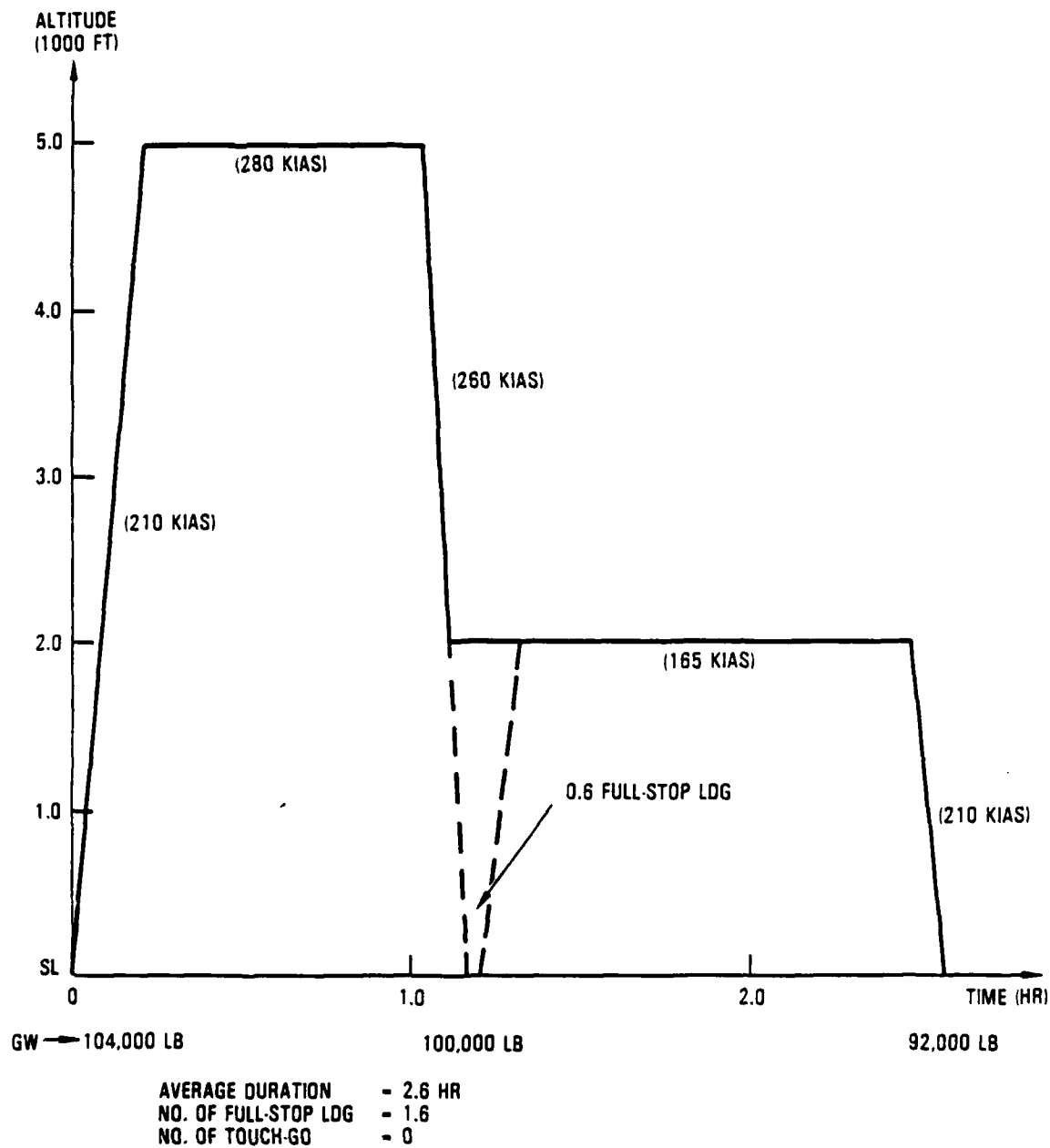
Figure 2-6. Patrol Airplane, Functional Check/Experimental/
Development/Evaluation, 5.3 Percent of Flights
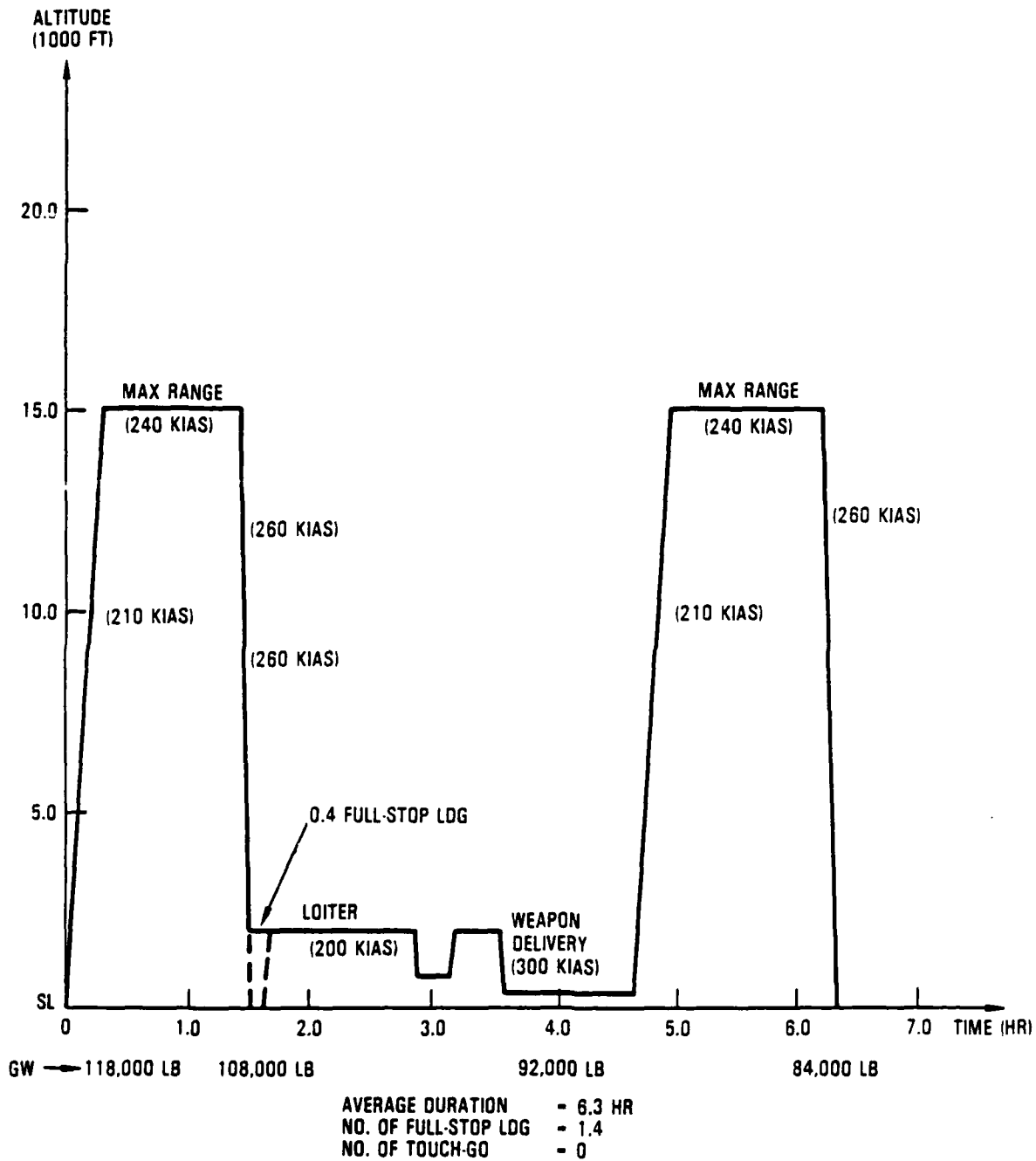
Figure 2-7. Patrol Airplane, ASW Training/Operational (with External Stores), 1.0 Percent of Flights

TABLE 2-2. TACTICAL AIRPLANE MISSIONS

WEIGHT-POUNDS		PERCENT OF FLIGHTS	FLIGHT TIME HOURS
TAKEOFF	LANDING		
53,848	35,871	20.0	1.9
53,848	35,871	20.0	1.8
53,848	35,871	9.0	1.9
61,505	36,858	13.0	2.3
61,651	36,982	13.0	1.6
53,848	35,871	13.0	3.6
55,957	33,019	9.0	2.6
54,137	34,181	3.0	3.2

Table A-18 is an example of the loads, taxi speeds, tire pressures, and cycles per flight for the tactical airplane mission. Lateral wheel loads are low and are a function of the forward speed of the airplane.

2.2 DEVELOPMENT OF WHEEL TEST SPECTRA

There are two concerns regarding showing that a wheel will not fail in service use. The first is to verify the life of the wheel by providing a test program that is representative of the operating conditions and the service life of the wheel. The second is to assure that if a flaw, such as stress corrosion pits, is introduced into a critical area on the wheel, that any cracks that might be developed will not grow to a catastrophic size prior to the next inspection period.

2.2.1 Test Spectra

Because of the great number of different values of loads acting on the wheels during ground operations, it is desirable to reduce them to a much lower number but yet represent them in a test spectrum. Loads are imposed on the wheel from radial, lateral and drag forces, by the torque loads imposed on the tie bolts, and from the pressure in the tire. It is not practical to combine the loads from these sources by examination because it is not known how much of the load is contributed to the stresses by each source of loading. Inasmuch

as the stresses from each of the load sources can be considered linear and additive, the following equation can be assumed to provide the total stresses acting on a given point on the wheel.

$$S_T = S_P + S_{TB} + S_L + S_R$$

Where

S_T = Total stress

S_P = Stress due to tire pressure

S_{TB} = Stress due to tie-bolt torque

S_L = Stress due to lateral load

S_R = Stress due to radial load

The stresses due to tie-bolt torque for this program have been assumed to be constant and are obtained after the tire is mounted on the wheel and the bolts tightened. However, to make this assumption, it is necessary to determine if the tie bolt and wheel materials have a different thermal coefficient of expansion, and if they do, whether or not the wheel and tie bolts will heat up prior to landing, close to the temperature at which the original torque was applied after the wheel and tie bolt have cold soaked at altitude. The stresses due to tire pressures are obtained by increasing the pressure in steps up to pressures' that are fifty percent greater than the rated pressure for the tire.

The critical stress areas on the wheel are determined either by finite element methods or by the use of stress coat. In the case of the wheels used in this program the stress coat method is employed. The tire is mounted on the wheel and the stress coat is applied. A series of loads, which envelope those developed in the load spectra, are applied. Table 2-3 is an example of the types of loads applied in the stress coat tests for the patrol and tactical airplane main landing gear wheels. Figures 2-8 through 2-11 show the results of the stress coat tests for the small transport/patrol airplane. The arrows point to some of the higher stress areas at which strain gages are applied.

TABLE 2-3.   EXAMPLE LOADING FOR STRESS COAT
AND STRAIN GAGE TESTS

AIRPLANE	LOADS - KIPS		TIRE PRESS
	RADIAL	LATERAL	PSI
SMALL TRANSPORT /PATROL	35.2	--	235
	30.5	--	230
	26.9	--	225
	22.1	--	210
	33.4	+3.3	230
	33.4	-3.3	230
	27.6	+6.3	225
	27.6	-6.3	225
	29.0	+2.9	225
	29.0	-2.9	225
	25.7	+5.9	240
	25.7	-5.9	240
	25.6	+2.6	225
	25.6	-2.6	225
	21.3	+5.0	230
	21.3	-5.0	230
TACTICAL	29.3	--	380
	25.6	--	325
	17.6	--	320
	17.0	--	290
	33.7	+6.6	360
	33.7	-6.6	360
	29.5	+5.8	310
	29.5	-5.8	310
	18.7	+2.0	320
	18.7	-2.0	320
	18.2	+1.7	285
	18.2	-1.7	285
	17.9	+0.5	320
	17.9	-0.5	320
	17.3	+0.5	290
	17.3	-0.5	290
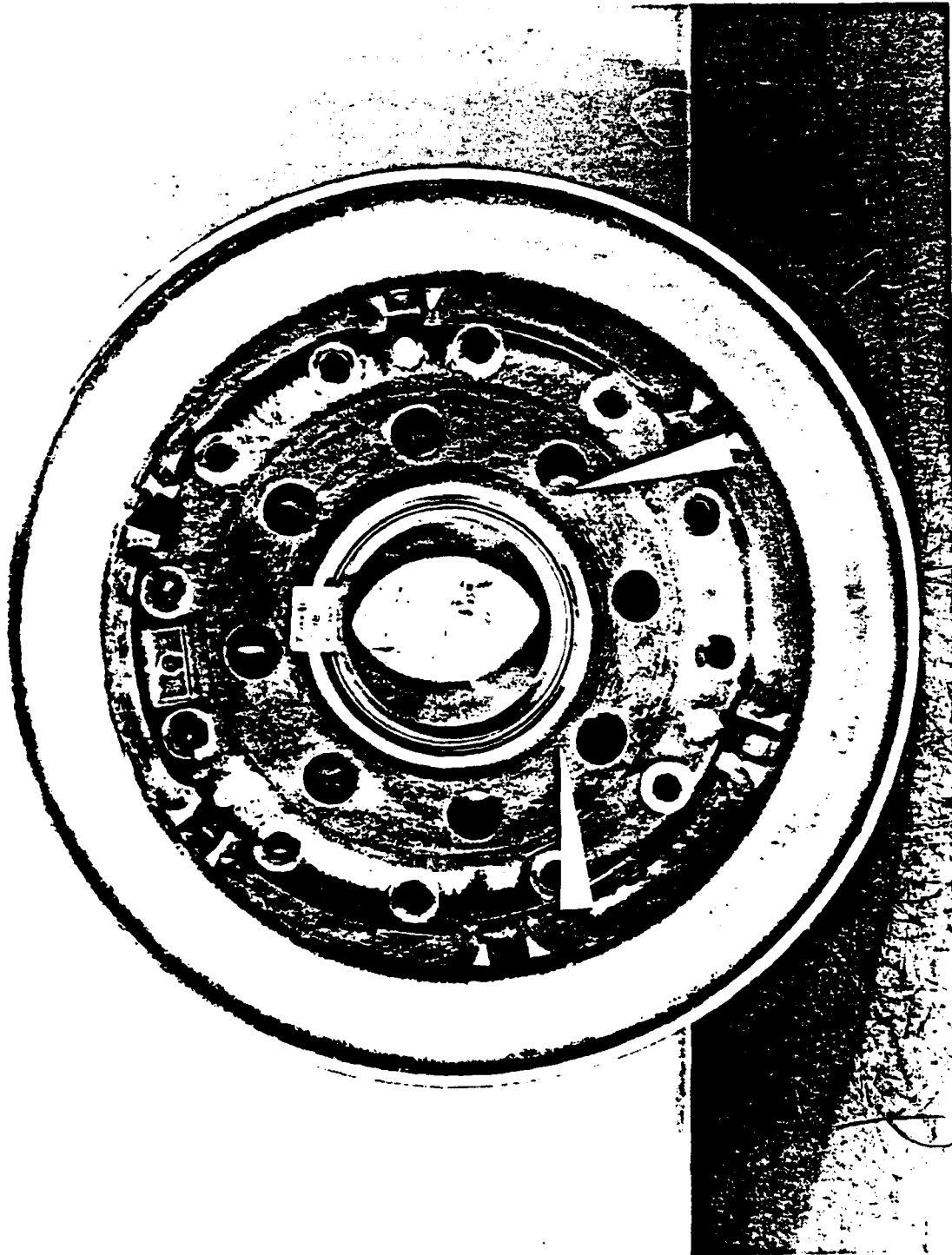
Figure 2-8. Stress Coat, Results, Inboard Wheel Half
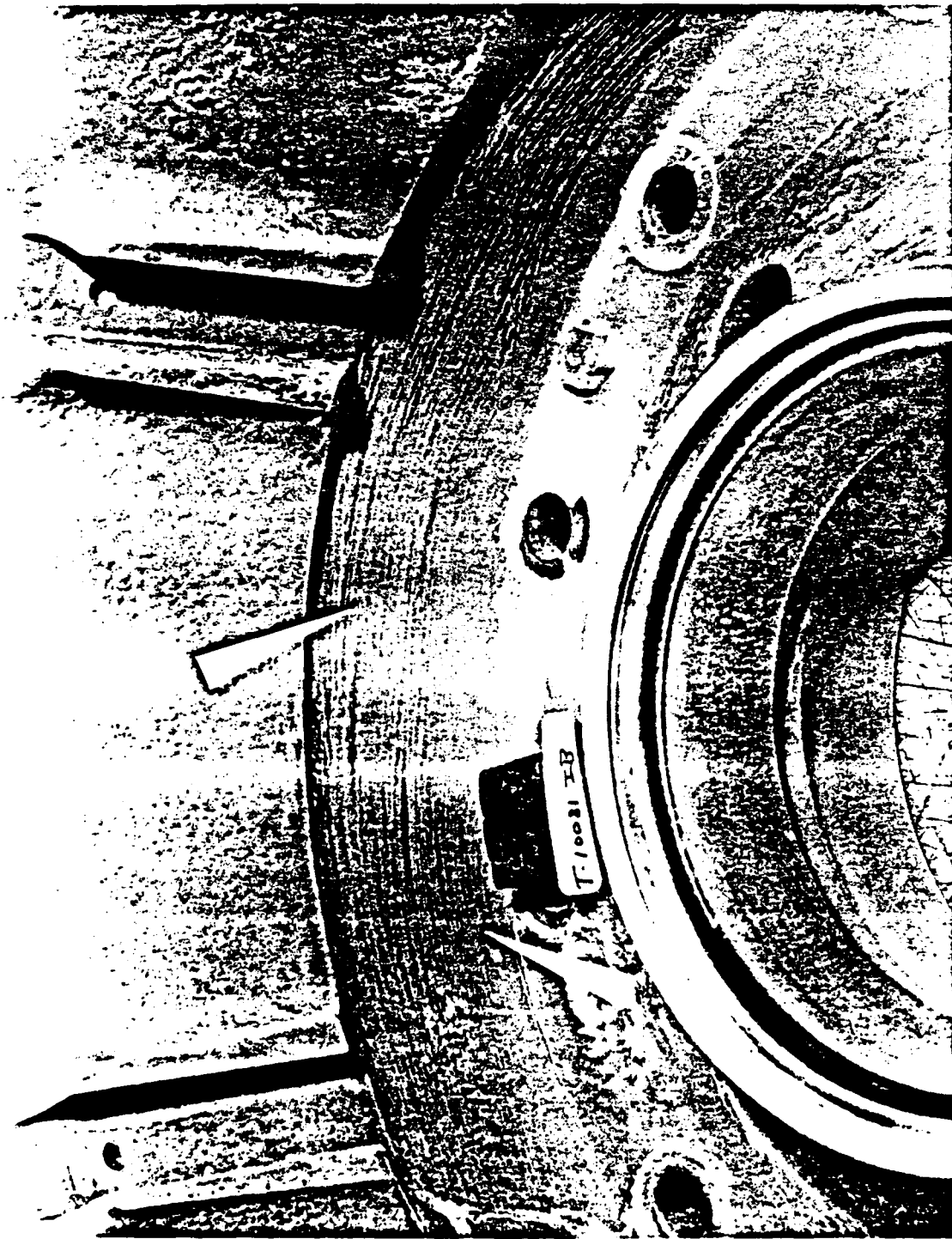
Figure 2-9. Stress Coat Test Results, Inboard Wheel Half Hub Area

2-15
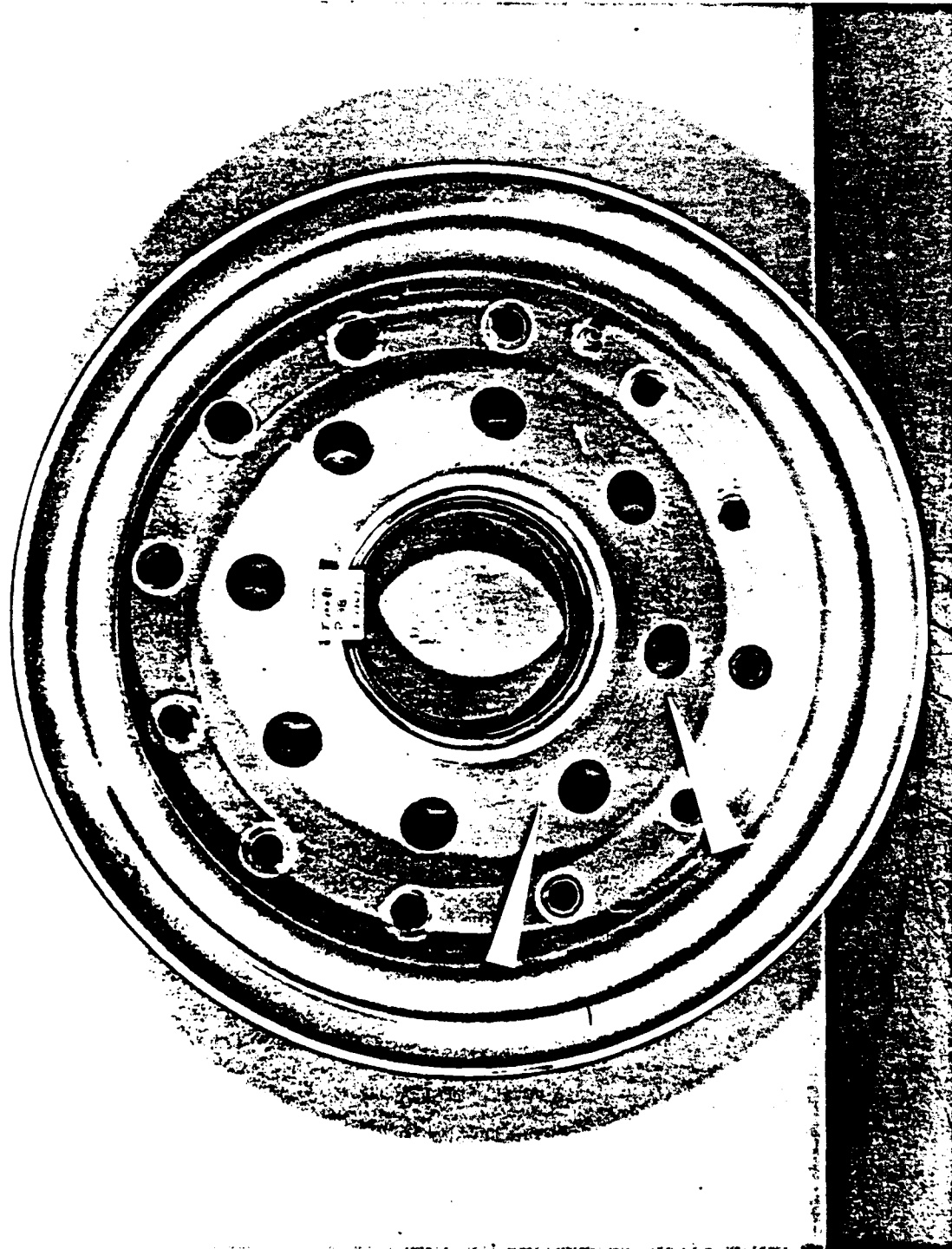
Figure 2-10. Stress Coat Test Results, Outboard Wheel Half
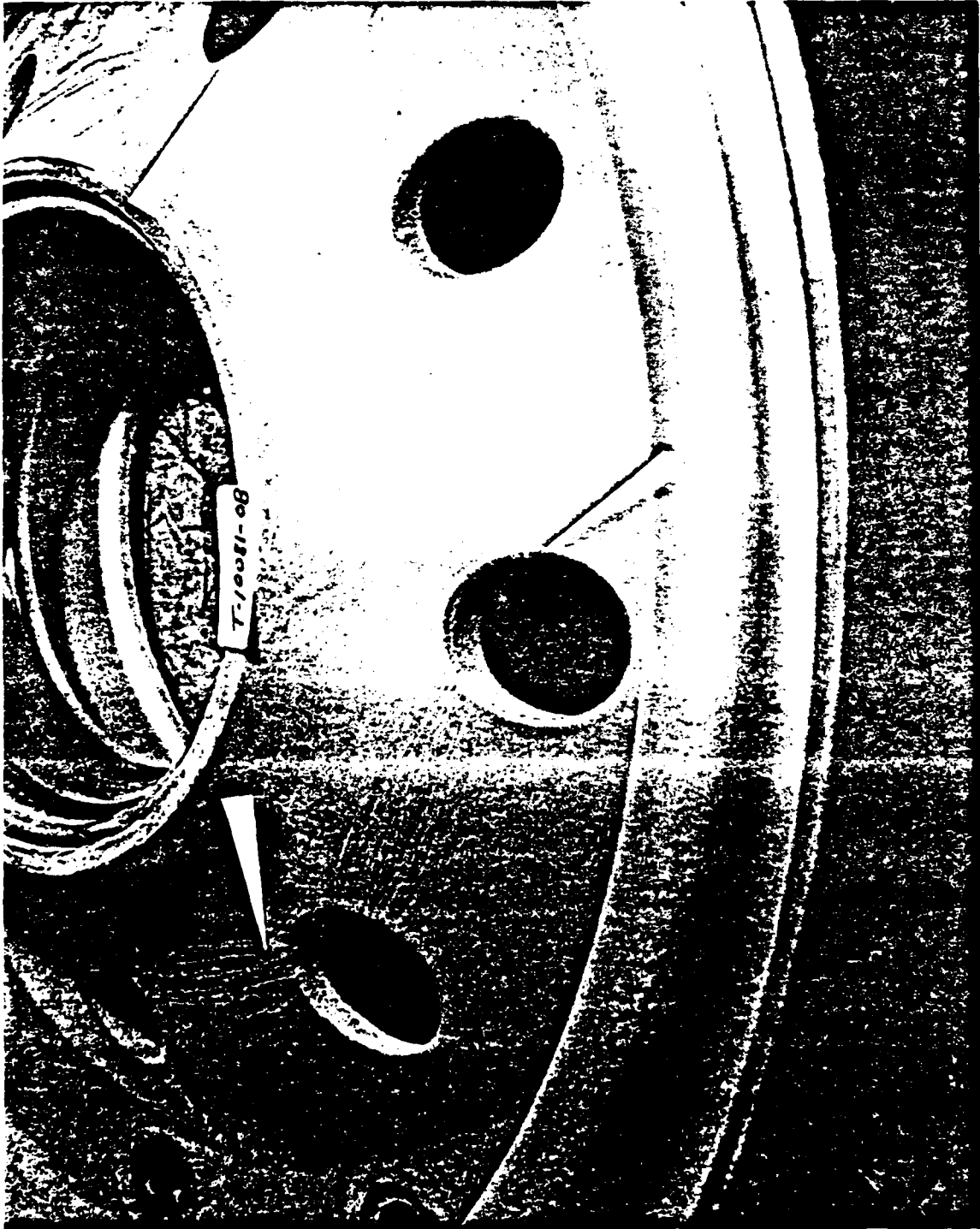
Figure 2-11. Stress Coat Test Results, Outboard Wheel Half Hub Area

After strain gages are applied to the critical areas, the wheel is rolled on a dynamometer using the same loads as in the stress coat tests. The data obtained from these tests are used to develop equations relating loads with stresses for critical areas of the wheels. Table 2-4 shows typical results for the wheels of the wide bodied transport.

These data are used to develop equations that provide stresses for any other set of loads and tire pressures. For example, by plotting the tubewell stresses as a function of tire inflation pressure as shown in Figure 2-12, the following equation is developed for the variation of tubewell stresses with tire pressure.

$$S_P = 47.78 \; P_A \tag{1}$$

where P_A = Tire pressure - PSI

Using the radial load data for the cases of no lateral load, the variation of both maximum and minimum tubewell stresses attributed to radial load only are plotted as shown in Figure 2-13. The corresponding equations are:

$$S_{R_{MAX}} = 0.1452 \; L_R \tag{2}$$

$$S_{R_{MIN}} = -0.1248 \; L_R \tag{3}$$

where

L_R = Radial load.

By subtracting the stresses due to the radial loads from the roll stresses for the combined radial and lateral loads, the stresses attributed to the lateral load only are obtained. For example, in Table 2-4 the combined maximum tubewell roll stress for condition Takeoff 1 is 14,430 PSI. By subtracting the radial stress of 8250 PSI attributed to the radial load of 56,650 pounds as given in Figure 2-13, a lateral stress of 6,180 PSI is obtained. Figure 2-14 shows the variation of lateral stresses with lateral loads for other combinations of radial and lateral loads. The corresponding equations are:

2-18

TABLE 2-4. TYPICAL ROLL TEST STRESS DATA FOR LONG-RANGE TRANSPORT

LOAD CONDITION	TEST RAD.LOAD (POUNDS)	TEST SIDE LOAD (POUNDS)	INFL. PRES. (PSI)	TIEBOLT TORQ.	GAGE 3 - O.B. ① WEB INFL.	ROLL MAX	ROLL MIN	GAGE 17 - I.B. WEB TORQ	INFL	ROLL MAX	ROLL MIN	GAGE 23 - I.B. ② TUBEWELL TORQ	INFL	ROLL MAX	ROLL MIN
Takeoff 1	56,650	9,280	250	12,210	3020	17150	- 7050	5460	-470	14540	-24580	1530	11790	14430	-4380
Takeoff 2	55,850	-9,250	250	12,210	3020	10280	-15580	5460	-470	5310	- 3350	1530	11790	3940	-8050
Takeoff 3	44,200	7,610	246	12,210	2910	12920	- 4900	5460	-450	11170	-18940	1530	11530	10990	-4820
Takeoff 4	43,500	-7,675	246	12,210	2910	8680	30	5460	-450	6910	- 3390	1530	11530	3120	-7170
Takeoff 5	55,600	0	267	12,210	3410	4710	- 320	50	-450	7340	- 8270	1530	12970	8070	-6300
Takeoff 6	42,150	0	263	12,210	3320	3790	- 2	5460	-470	5530	- 6410	1530	12690	6130	-5410
Landing 1	40,100	10,790	263	12,210	3320	17740	- 6050	5460	-470	12890	-23090	1530	12690	12100	-4250
Landing 2	39,650	-10,500	263	12,210	3320	9430	-188	5460	-470	8010	- 4990	1530	12690	3200	-6670
Landing 3	34,700	10,300	246	12,210	2910	14490	- 8720	5460	-450	11150	-20870	1530	11530	11470	-3010
Landing 4	34,750	-10,160	246	12,210	2910	9870	-17930	5460	-450	8360	- 6720	1530	11530	2940	-6790
Landing 5	41,900	0	263	12,210	3320	3790	- 2360	5460	-470	5510	- 6390	1530	12690	6240	-5450
Landing 6	36,050	0	258	12,210	3250	3280	- 1780	5460	-450	4540	- 5880	1530	12340	5390	-4770

STRESS (PSI) DUE TO:

① Outboard wheel half
② Inboard wheel half

2-19
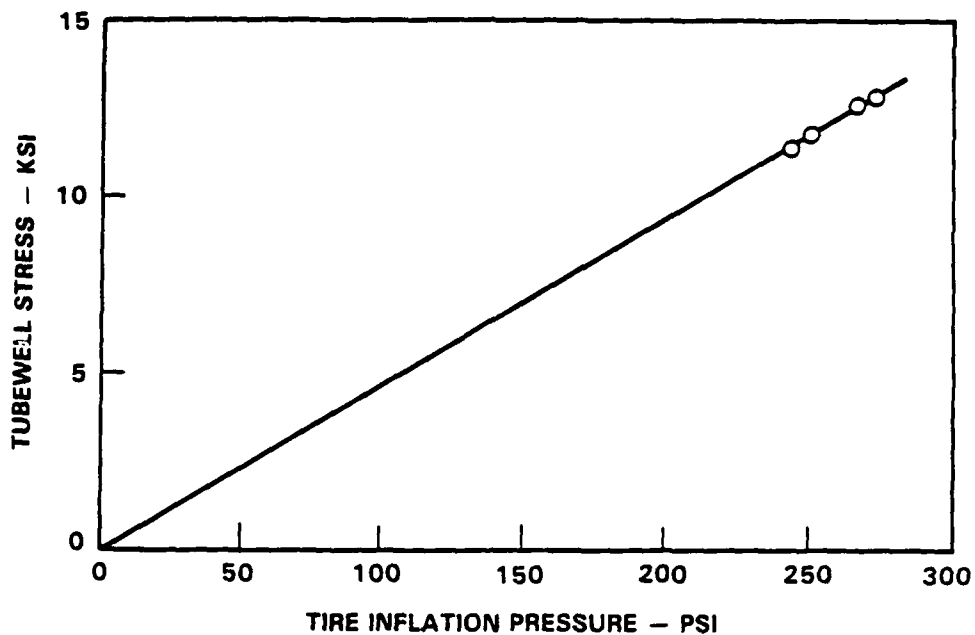
Figure 2-12.   Tubewell Stress Variation with Tire Pressure
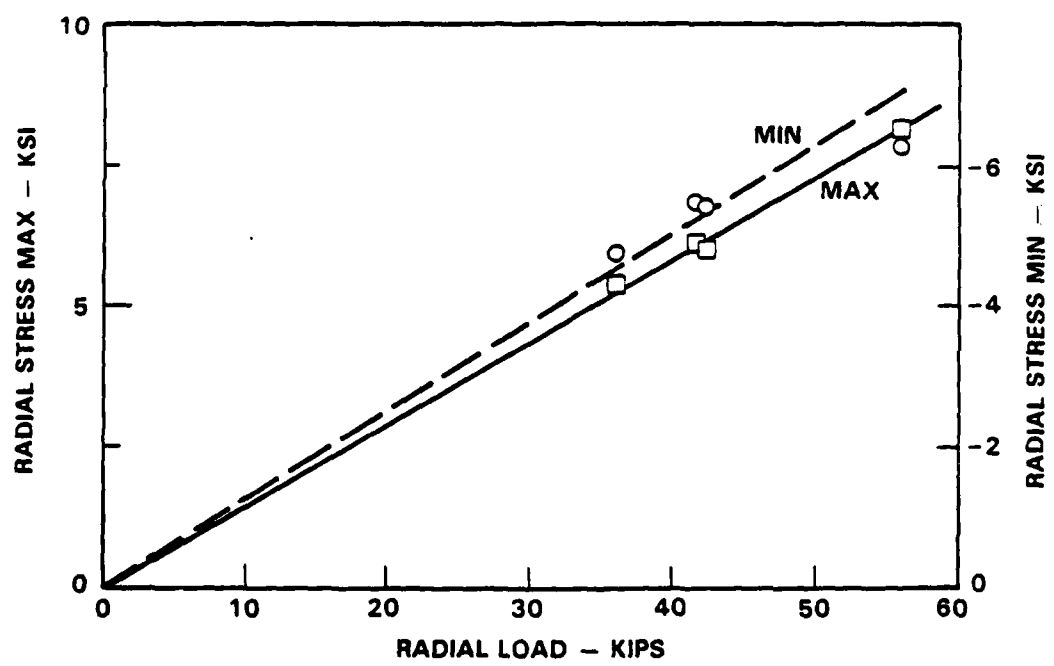
Figure 2-13.   Tubewell Maximum and Minimum Stresses from
Radial Loads with No Lateral Loads
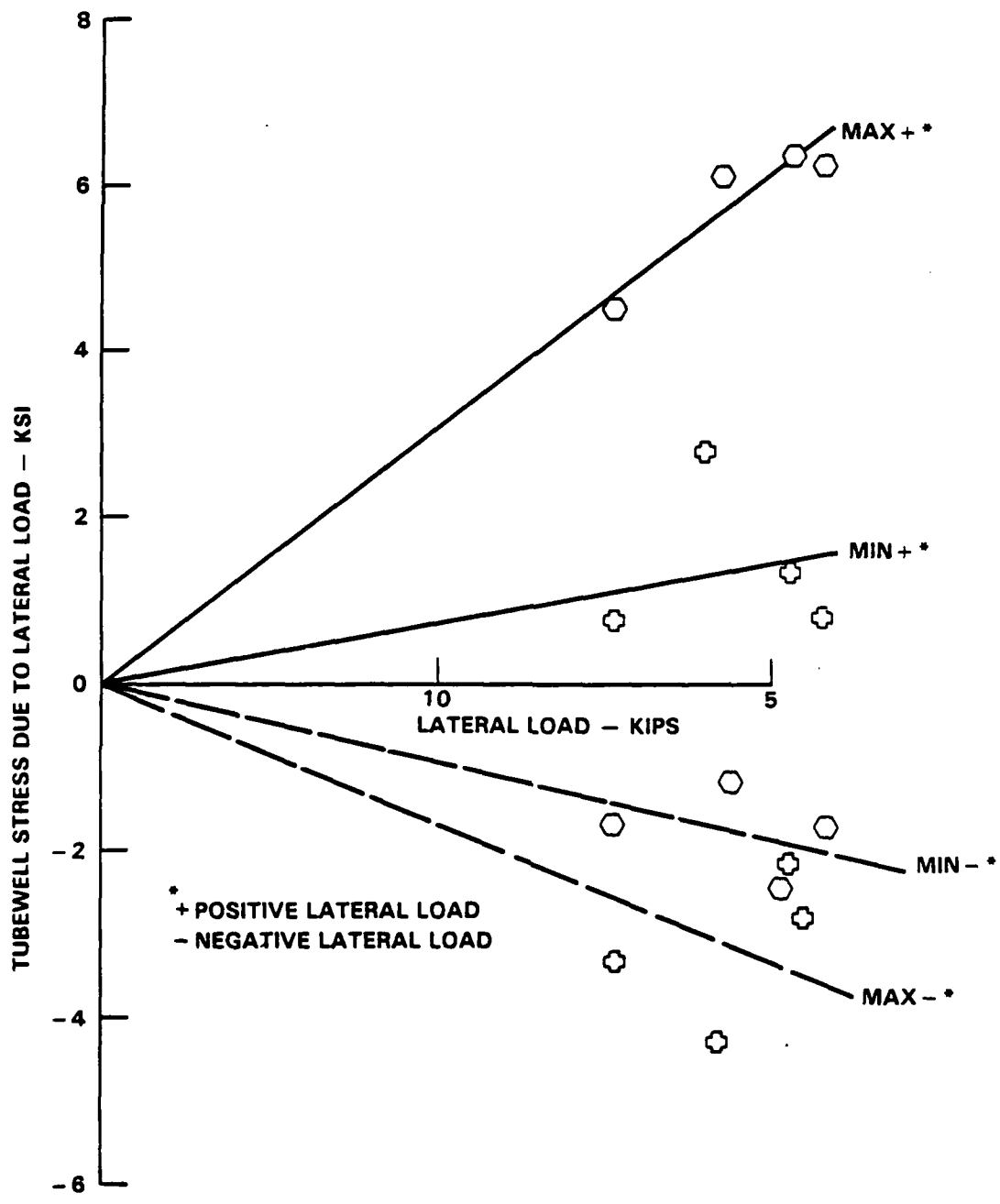
Figure 2-14. Tubewell Maximum and Minimum Stresses
from Lateral Loads with No Radial Loads

2-21

$$S_{L_{MAX+}} = 0.6119\ L_{L+} \tag{4}$$

$$S_{L_{MAX-}} = 0.3271\ L_{L-} \tag{5}$$

$$S_{L_{MIN+}} = 0.1507\ L_{L+} \tag{6}$$

$$S_{L_{MIN-}} = 0.1792\ L_{L-} \tag{7}$$

where

L_{L+} = Positive lateral load

L_{L-} = Negative lateral load

By substituting the foregoing equations into equation (1), the following equations are derived for calculating tubewell stresses for any combinations of radial and lateral loads:

$$S_{T_{MAX+}} = 47.78\ P_A + 1530 + 0.1452\ L_R + 0.6119\ L_{L+} \tag{8}$$

$$S_{T_{MIN+}} = 47.78\ P_A + 1530 - 0.1248\ L_R + 0.1507\ L_{L+} \tag{9}$$

$$S_{T_{MAX-}} = 47.78\ P_A + 1530 + 0.1452\ L_R + 0.3271\ L_{L-} \tag{10}$$

$$S_{T_{MIN-}} = 47.78\ P_A + 1530 - 0.1248\ L_R + 0.1792\ L_{L-} \tag{11}$$

By using these equations the maximum and minimum stresses can be derived for each of the taxi events. Table 2-5 shows the stresses encountered for various taxi events of a wide bodied transport during one mission. By applying the equations to all the missions, a complete spectrum is obtained relating stresses to loads. Because these stresses are measured, they include the effects of the local geometry. Therefore, geometric stress concentrations do not have to be considered in fatigue analyses.

The number of stress cycles in the taxi spectra is reduced by the use of the cyclic stress-strain formulation, Neuber's rule and Walker's equation to transform the measured stresses into effective stresses. Because cyclic stress-strain data are not available, 2014-T6 forged aluminum cyclic tests were

TABLE 2-5. WHEEL STRESSES RESULTING FROM TAXI AND TIRE PRESSURE LOADS

EVENT	WHEEL LOAD - KIPS			SPEED MPH	TIRE CONTAINED GAS		CYCLES PER FLIGHT*	STRESSES - KSI					
								TUBEWELL		FLANGE		WEB	
	RADIAL	LATERAL	DRAG		TEMP °F	PRESS PSI		MAX	MIN	MAX	MIN	MAX	MIN
90' LFT TURN	54.4	6.0	--	10	101.1	200.4	11.4	22.68	4.32	17.09	10.91	26.92	8.01
90' RT TURN	56.7	6.4	--	10	104.5	201.6	15.4	17.30	2.94	22.95	10.29	23.14	1.30
1500' TAXI	55.6	--	--	25	112.3	204.4	118.5	19.37	4.36	18.33	11.75	19.71	11.63
150' LFT TURN	54.6	4.1	--	10	115.9	205.7	18.9	21.80	4.54	17.74	11.47	24.67	9.22
3000' TAXI	55.6	--	--	25	134.1	212.2	236.9	19.74	4.73	18.87	12.30	19.81	11.73
150' LFT TURN	54.6	4.1	--	10	137.2	213.3	18.9	22.16	4.91	18.26	11.99	24.76	9.32
9000' TAXI	55.6	--	--	25	187.6	231.3	710.8	20.65	5.64	20.20	13.63	20.04	11.97
65' RT TURN	56.7	9.3	--	10	189.8	232.1	12.3	17.81	3.88	25.92	12.62	25.05	-2.96
65' RT TURN	56.7	9.3	--	10	199.5	235.6	12.3	17.98	4.04	26.16	12.86	25.09	-2.92
7010' T.O.	63.0	--	--	0-170	207.6	238.5	552.0	22.07	5.06	21.71	13.86	20.80	11.64
1805' LDG	50.8	--	--	160	6.1	166.4	142.7	16.86	3.14	15.03	9.23	18.81	11.43
3619' BRK	46.4	--	9.7	160-25	19.7	171.3	284.8	16.92	3.53	15.21	9.66	18.77	11.56
1800' TAXI	42.8	--	--	25	44.3	180.1	140.9	16.35	4.79	14.89	10.52	18.27	12.05
150' LFT TURN	35.5	3.4	--	10	47.3	181.2	13.6	17.42	5.76	13.52	10.51	21.81	12.47
65' LFT TURN	34.8	11.0	--	10	49.4	181.9	8.2	22.01	5.88	12.46	9.82	31.08	5.85
5000' TAXI	36.2	--	--	25	71.8	189.9	388.6	15.86	6.09	14.68	11.43	17.80	12.54
150' RT TURN	36.7	3.1	--	10	73.1	190.4	22.5	14.94	5.49	18.49	9.98	19.48	7.56
3000' TAXI	36.2	--	--	25	85.3	194.8	233.0	16.09	6.32	15.02	11.78	17.86	12.60
150' LFT TURN	35.5	3.4	--	10	87.4	195.5	18.6	18.11	6.44	14.52	11.51	21.98	10.59
1500' TAXI	36.2	--	--	25	93.9	197.8	116.5	16.24	6.46	15.23	11.98	17.82	12.69
90' LFT TURN	35.3	5.1	--	10	95.1	198.2	11.2	19.25	6.60	14.45	11.53	24.08	9.60
35' RT TURN	36.7	9.6	--	10	96.5	198.8	8.4	13.22	4.73	20.97	11.04	23.01	-2.74

9.4 Hour Flight

* 1 cycle equals 1 revolution of the wheel

2-23

performed using 2014-T6 specimens fabricated directly from a wide-bodied transport wheel. Figure 2-15 presents the results of two specimens as half the stress range versus half the strain range. The curve shown is the average curve of the two specimens.

The cyclic stress-strain formulation has the form

$$\varepsilon = \frac{\sigma}{E} + \left(\frac{\sigma}{A}\right)^P \tag{12}$$

where

ε = Strain

σ = Stress

E = Young's modulus

P, A = Constants

for describing the first portion of loading, with the point ① (see Figure 2-16) being defined by the intersection of line (A) and the line representing Neuber's rule

$$\frac{\left(K_t S\right)^2}{E} = \sigma\varepsilon \tag{13}$$

where

$K_t S$ = Measured stresses at critical locations.

The second portion of loading ① to ② (Figure 2-16) is described by

$$\Delta\varepsilon = \frac{\Delta\sigma}{E} + 2\left(\frac{\Delta\sigma}{2A}\right)^P \tag{14}$$

with the value at ② being defined by the intersection of ③ and

$$\frac{\left(K_t \Delta S\right)^2}{E} = \Delta\sigma\Delta\varepsilon \tag{15}$$

where

$\Delta S = S_{MAX} - S_{MIN}$

$\Delta\sigma = \sigma_{MAX} - \sigma_{MIN}$

2-24
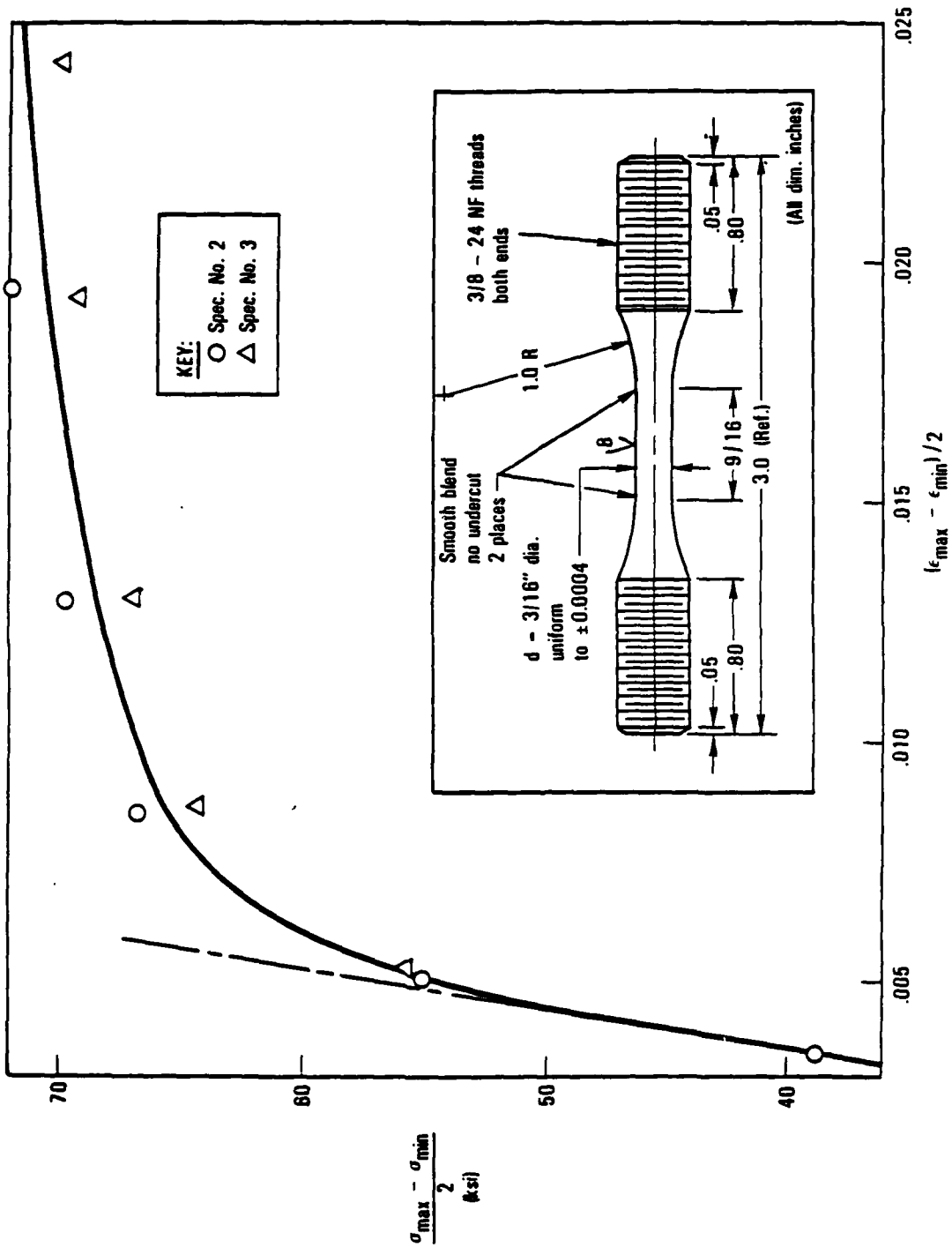
Figure 2-15. Results of Cyclic Stress-Strain Tests for 2014-T6 Wheel Forging

$$\varepsilon = \frac{\sigma}{E} + \left(\frac{\sigma}{A}\right)^P$$

(A)

$$\sigma\varepsilon = \frac{\left(K_t S\right)^2}{E} \; ; \; \text{(NEUBER'S RULE)}$$

$$\Delta\varepsilon = \frac{\Delta\sigma}{E} + 2\left(\frac{\Delta\sigma}{2A}\right)^P$$

$$\Delta\sigma\cdot\Delta\varepsilon = \frac{\left(K_t \Delta S\right)^2}{E}$$
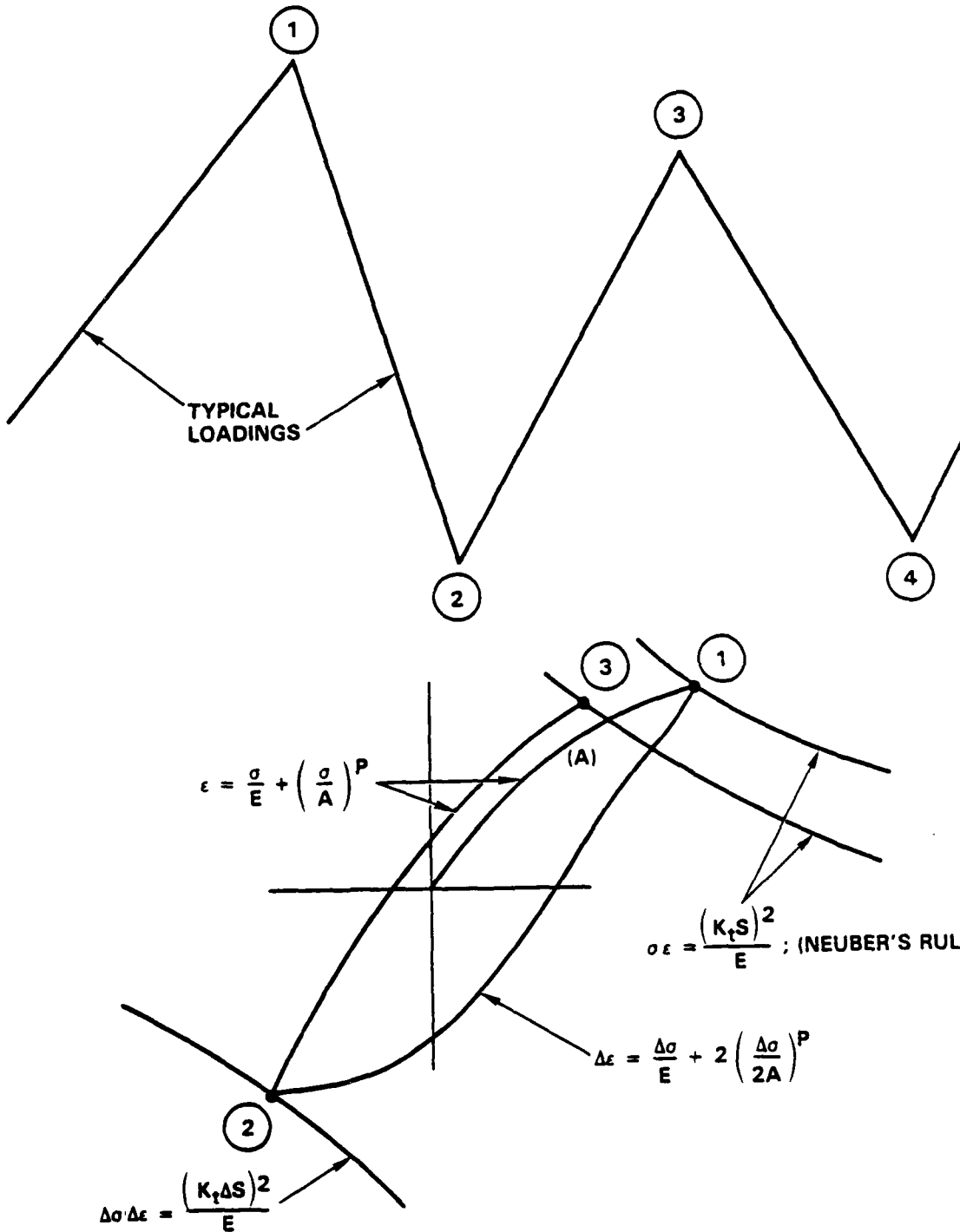
Figure 2-16. Local Stress-Strain for Typical Loadings

2-26

The above formulations provide σ_{max} and σ_{min}. Using Walker's equation,

$\bar{\sigma}$ = Effective stress

$$\bar{\sigma} = \sigma_{MAX} (1-R)^m \qquad\qquad (16)$$

where

$$R = \frac{\sigma_{min}}{\sigma_{max}} \qquad\qquad (17)$$

M = Walker's constant

Constant amplitude fatigue test data are reduced to a single curve of $\bar{\sigma}$ vs N by using the above formulations (see Figure 2-17). This curve provides the allowable curve for computing damages for the stress spectra which are to be made into wheel fatigue test spectra. Comparisons of the original stress spectra may be made by simply converting local stresses to effective stresses and comparing their respective damage summations. Also shown in Figure 2-17 are reduced allowable curves for peened (dashed) and unpeened material that provide the best correlation with the fatigue test lives of small coupon specimens tested under flight-by-flight loading spectra.

A cyclic trade-off procedure is used to reduce the number of loading cycles in developing the wheel fatigue spectrum. This reduction is achieved by replacing lower stress levels, having a large number of cycles, with higher stress levels having fewer cycles. The plot of effective stress, $\bar{\sigma}$, in Figure 2-17 has a four line fit. Stresses at the critical locations peened or unpeened, are transformed to effective stresses, $\bar{\sigma}$, with subsequent manipulation to higher stress levels, seen by the wheel, and less cycles by using the formulations in Figure 2-16. Subsequently, the effective stresses are converted back to stresses at the critical locations. The wheel operational load spectra thus derived are given in Tables 2-6 through 2-10 for the long range, medium range and short haul transports, and for the patrol and fighter airplanes, respectively. The areas of interest on the wheels have not all been shot peened, accordingly, the appropriate curve is used in Tables 2-6 through 2-10.

2-27
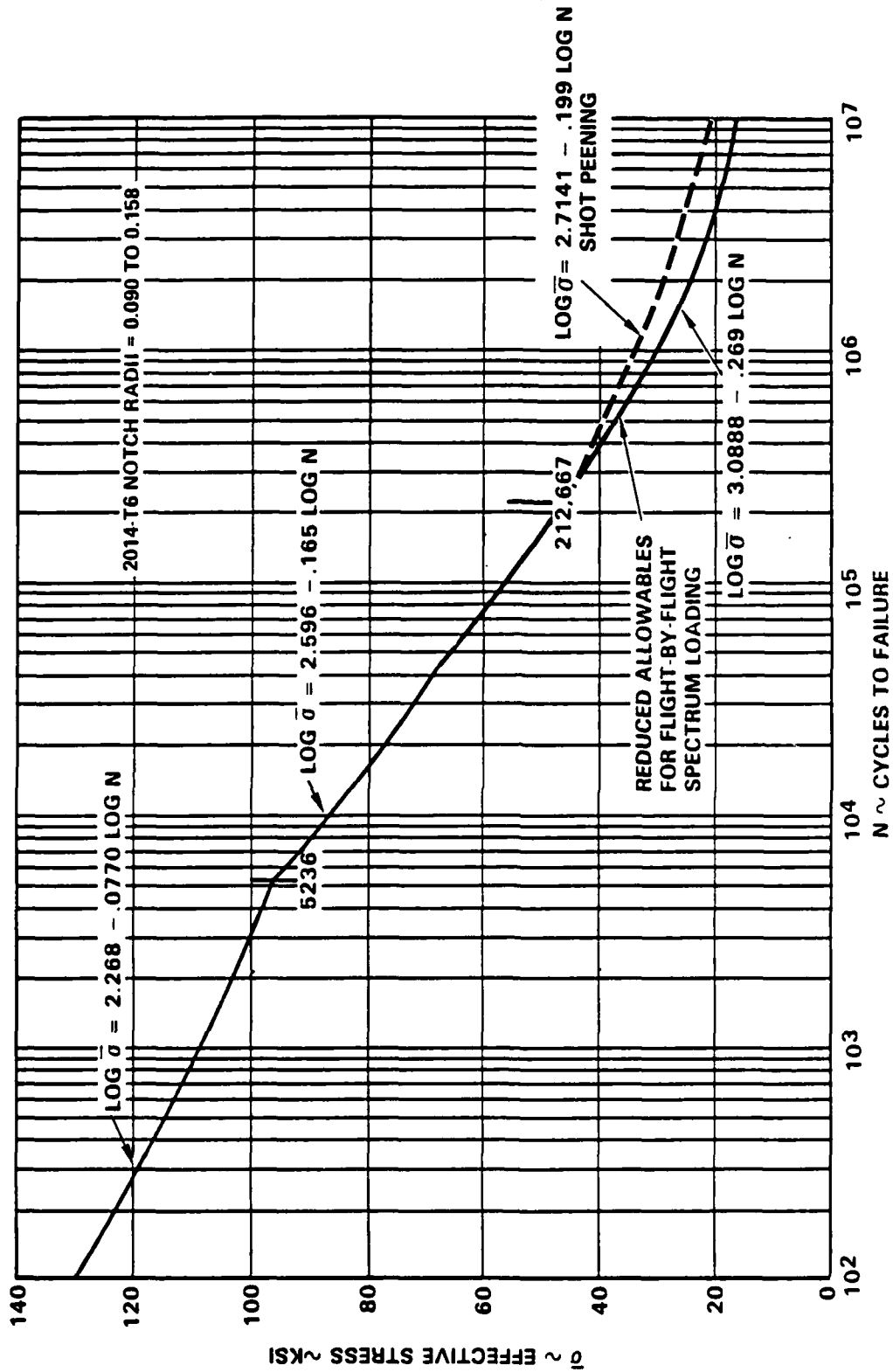
Figure 2-17. Fatigue Allowables for 2014-T6.

TABLE 2-6. WHEEL LOAD OPERATIONAL SPECTRUM, LONG-RANGE TRANSPORT

| CONDITION | LOADS - KIPS | | TIRE PRESS PSI | TUBEWELL* STRESS - KSI | | CYCLES PER FLIGHT | CYCLES PER 50,000 MILES |
	RADIAL	LATERAL		MAX	MIN		
1. T.O. TURN	54.6	4.1	213	18.31	4.17	23.55	0.1747 E6
2. T.O. TURN	56.7	-9.3	236	26.71	7.11	11.03	0.0818 E6
3. T.O. TAXI	63.0	-	239	22.07	5.06	552.29	4.0969 E6
4. LDG. TURN	41.3	3.0	214	18.04	7.33	29.04	0.2154 E6
5. LDG. TURN	41.5	-10.3	249	25.74	9.79	12.67	0.0940 E6
6. LDG. TAXI	51.3	-	219	20.07	5.09	634.56	4.7072 E6
					TOTAL	1,263.14	9.3700 E6

* SHOT PEENED

TABLE 2-7. WHEEL LOAD OPERATIONAL SPECTRUM, MEDIUM-RANGE TRANSPORT

| | CONDITION | LOADS – KIPS | | TIRE PRESS PSI | FLANGE STRESS* – KSI | | CYCLES PER FLIGHT | CYCLES PER 50,000 MILES |
		RADIAL	LATERAL		MAX	MIN		
1.	T.O. TURN	47.0	3.5	208	30.85	19.07	26.00	0.1929 E6
2.	T.O. TURN	46.8	-5.2	205	35.11	19.58	21.54	0.1598 E6
3.	T.O. TAXI	54.2	–	223	35.62	20.76	674.89	5.0063 E6
4.	LDG. TURN	40.8	3.0	223	31.54	21.30	26.36	0.1955 E6
5.	LDG. TURN	39.3	-10.8	215	38.55	21.71	17.84	0.1323 E6
6.	LDG. TAXI	55.5	–	211	34.46	19.24	621.35	4.6092 E6
						TOTAL	1387.98	10.2960 E6

* SHOT PEENED

TABLE 2-8. WHEEL LOAD OPERATIONAL SPECTRUM, SHORT HAUL TRANSPORT

| | | LOADS — KIPS | | TIRE PRESS | FLANGE STRESS* — KSI | | CYCLES PER | CYCLES PER |
	CONDITION	RADIAL	LATERAL	PSI	MAX	MIN	FLIGHT	50,000 MILES
1.	T.O. TURN	38.3	1.2	184	27.06	16.94	31.33	0.2324 E6
2.	T.O. TURN	38.3	-1.2	184	28.29	17.17	26.57	0.1971 E6
3.	T.O. TAXI	40.3	—	186	28.22	17.17	928.65	6.8887 E6
4.	LDG. TURN	35.4	0.1	181	26.53	16.86	31.57	0.2342 E6
5.	LDG. TURN	36.9	-2.5	187	29.16	17.75	19.28	0.1430 E6
6.	LDG. TAXI	38.5	—	175	26.51	15.96	877.21	6.5072 E6
						TOTAL	1914.61	14.2026 E6

* SHOT PEENED

TABLE 2-9. WHEEL LOAD OPERATIONAL SPECTRUM, PATROL AIRPLANE

	CONDITION	LOADS - KIPS		TIRE PRESS PSI	"O" RING SEAL STRESS - KSI		CYCLES PER FLIGHT	CYCLES PER 8,000 MILES
		RADIAL	LATERAL		MAX	MIN		
1.	TAKEOFF TAXI	35.2	-	242	41.81	31.94	898.57	0.8051 E6
2.	TAXI TURN	33.4	3.3	240	43.64	30.36	19.61	0.0176 E6
3.	TAXI TURN	33.4	-3.3	240	37.40	33.17	9.28	0.0083 E6
4.	LANDING TAXI	28.6	0	205	37.88	29.86	2165.17	1.9400 E6
5.	TAXI TURN	27.6	6.3	231	44.20	28.99	22.73	0.0204 E6
6.	TAXI TURN	27.6	-6.3	231	36.82	32.62	4.63	0.0041 E6
						TOTAL	3119.99	2.7955 E6

TABLE 2-10. WHEEL LOAD OPERATIONAL SPECTRUM, TACTICAL AIRPLANE

CONDITION	LOADS - KIPS		TIRE PRESS PSI	FLANGE STRESS - KSI		CYCLES PER FLIGHT	CYCLES PER 8,000 MILES
	RADIAL	LATERAL		MAX	MIN		
1. TAKEOFF TAXI	29.3	-	379	25.41	14.45	610.84	1.1038 E6
2. TAXI TURN	33.7	+6.6	360	29.38	14.70	4.58	0.0083 E6
3. TAXI TURN	28.8	-1.5	354	24.82	13.55	12.63	0.0228 E6
4. LANDING TAXI	17.6	-	334	19.86	13.08	1,063.29	1.9213 E6
5. TAXI TURN	18.7	+2.0	321	20.62	12.79	13.66	0.0246 E6
6. TAXI TURN	14.9	-3.2	312	19.86	12.94	15.68	0.0283 E6
					TOTAL	1,720.58	3.1091 E6

While this procedure does reduce the number of cycles seen by the wheel under actual operations, the reduction is not sufficient to provide a practical test spectrum. Accordingly, a further reduction in test cycles is needed. Inasmuch as the straight taxi provides the greatest number of cycles, the method used for consolidating the loadings to several representative loadings is employed. As a consequence, a much higher loading condition is used for the straight taxi such that the number of cycles for the entire spectrum is reduced to a practical test level. A comparison of the test and operational spectra are made by comparing the results of fatigue analyses. If the damage summations for the test spectra are not significantly different from the damage summations for the operational loading spectra, then the developed test spectra are satisfactory. If the damage summations are significantly different, an iteration is required.

Damage is calculated as follows.

$$D = \frac{n \times n_F}{N} \tag{18}$$

where

D = Damage

n = Cycles for a given effective stress and for one flight

n_F = Number of Flights

The number of cycles to failure is derived from Reference (1). From Figure 2-17.

$$\bar{\sigma} = 1227 N^{-0.269} \tag{19}$$

$$\bar{\sigma}_{SP} = 518 N^{-0.199} \tag{20}$$

where

$\bar{\sigma}$ = Effective stress

$\bar{\sigma}_{SP}$ = Effective stress shot peened

N = Number of cycles to failure

Solve for N:

$$N = \left(\frac{\bar{\sigma}}{1227}\right)^{3.7175} \quad (21) \qquad\qquad N = \left(\frac{\bar{\sigma}_{SP}}{518}\right)^{5.0327} \quad (22)$$

Substitute equations (7) in equation (6) for N

$$D = n_F n \left(\frac{\bar{\sigma}}{1277}\right)^{3.7175} \quad (23) \qquad D_{SP} = n_F n \left(\frac{\bar{\sigma}_{SP}}{518}\right)^{5.0327} \quad (24)$$

Table 2-11 shows a comparison of fatigue damage developed from the test and operational spectra for the airplanes. The greater values for the medium-ranged and short haul transports from that of the long range transport reflects the thinner flange used in those wheels and is representative of service experience. The results of the development of the test spectra are given in Tables 2-12 through 2-16 of the long range, medium range and short haul transports and for the patrol and tactical airplanes, respectively.

TABLE 2-11. COMPARISON OF TEST AND OPERATIONAL DAMAGE

AIRPLANE	WHEEL FATIGUE DAMAGE CRITICAL AREA	
	OPERATIONAL SPECTRUM	TEST SPECTRUM
Long-Range Transport (Shot Peened)	0.524	0.526
Medium-Range Transport (Shot Peened)	2.158	2.159
Short Haul Transport (Shot Peened)	0.732	0.732
Patrol	0.721	0.727
Tactical	0.064	0.064

TABLE 2-12. WHEEL LOAD TEST SPECTRUM, LONG-RANGE TRANSPORT

CONDITION	LOADS - KIPS		TIRE PRESS PSI	TUBEWELL* STRESS - KSI		CYCLES PER FLIGHT	CYCLES PER BLOCK
	RADIAL	LATERAL		MAX	MIN		
1. T.O. TURN	54.6	4.1	213	18.31	4.17	23.55	3,485
2. T.O. TURN	56.7	-9.3	236	26.71	7.11	11.03	1,632
3. T.O. TAXI	76.8	-	276	25.86	5.13	228.51	33,820
4. LDG. TURN	41.3	3.0	214	18.04	7.33	29.04	4,298
5. LDG. TURN	41.5	-10.3	249	25.74	9.79	12.67	1,875
6. LDG. TAXI	65.9	-	269	23.95	6.16	262.51	38,852
					TOTAL	567.31	83,962

* SHOT PEENED

NOTES:

1. Fifty (50) blocks required for complete test representing 50,000 roll miles.

2. The tire is to be deflated after each block and reinflated prior to start of next block.

3. Each condition will be applied once per block for the indicated number of cycles per the sequence given.

TABLE 2-13. WHEEL LOAD TEST SPECTRUM, MEDIUM-RANGE TRANSPORT

CONDITION	LOADS – KIPS		TIRE PRESS PSI	FLANGE STRESS* – KSI		CYCLES PER FLIGHT	CYCLES PER BLOCK
	RADIAL	LATERAL		MAX	MIN		
1. T.O. TURN	47.0	3.5	208	30.85	19.07	26.06	3,857
2. T.O. TURN	46.8	-5.2	205	35.11	19.58	21.54	3,188
3. T.O. TAXI	40.0	-	246	41.75	22.56	247.04	36,562
4. LDG. TURN	90.8	3.0	223	31.54	21.30	26.36	3,901
5. LDG. TURN	39.3	-10.8	215	38.55	21.71	17.84	2,640
6. LDG. TAXI	69.0	-	246	41.53	22.62	227.45	33,662
					TOTAL	566.29	83,810

* SHOT PEENED

NOTES:

1. Fifty (50) blocks required for complete test representing 50,000 roll miles.

2. The tire is to be deflated after each block and reinflated prior to start of next block.

3. Each condition will be applied once per block for the indicated number of cycles per the sequence given.

2-37

TABLE 2-14. WHEEL LOAD TEST SPECTRUM, SHORT HAUL TRANSPORT

	CONDITION	LOADS - KIPS		TIRE PRESS PSI	FLANGE STRESS* - KSI		CYCLES PER FLIGHT	CYCLES PER BLOCK
		RADIAL	LATERAL		MAX	MIN		
1.	T.O. TURN	38.3	1.2	184	27.06	16.94	31.33	4,637
2.	T.O. TURN	38.3	-1.2	184	28.29	17.17	26.57	3,932
3.	T.O. TAXI	54.1	-	229	36.32	21.49	235.66	34,878
4.	LDG. TURN	35.4	0.1	181	26.53	16.86	31.57	4,672
5.	LDG. TURN	36.9	-2.5	187	29.16	17.75	19.28	2,854
6.	LDG. TAXI	50.0	-	227	35.21	21.50	222.61	32,946
						TOTAL	567.02	83,919

* SHOT PEENED

NOTES:

1. Fifty (50) blocks required for complete test representing 50,000 roll miles.

2. The tire is to be deflated after each block and reinflated prior to start of next block.

3. Each condition will be applied once per block for the indicated number of cycles per the sequence given.

TABLE 2-15. WHEEL LOAD TEST SPECTRUM, PATROL AIRPLANE

| | CONDITION | LOADS - KIPS | | TIRE PRESS PSI | "O" RING SEAL STRESS - KSI | | CYCLES PER FLIGHT | CYCLES PER BLOCK |
		RADIAL	LATERAL		MAX	MIN		
1.	TAKEOFF TAXI	58.0	-	243	46.12	29.85	333.51	11,953
2.	TAXI TURN	33.4	3.3	240	43.64	30.36	19.61	703
3.	TAXI TURN	33.4	-3.3	240	37.40	33.17	9.28	332
4.	LANDING TAXI	44.1	-	251	43.86	31.50	803.60	28,801
5.	TAXI TURN	27.6	6.3	231	44.20	28.99	22.73	815
6.	TAXI TURN	27.6	-6.3	231	36.82	32.62	4.63	166
						TOTAL	1193.36	42,770

NOTES:

1. Twenty-five (25) blocks required for complete test representing 50,000 roll miles.

2. The tire is to be deflated after each block and reinflated prior to start of next block.

3. Each condition will be applied once per block for the indicated number of cycles per the sequence given.

2-39

TABLE 2-15. WHEEL LOAD TEST SPECTRUM, TACTICAL AIRPLANE

| CONDITION | LOADS – KIPS | | TIRE PRESS PSI | * FLANGE STRESS – KSI | | CYCLES PER FLIGHT | CYCLES PER BLOCK |
	RADIAL	LATERAL		MAX	MIN		
1. TAKEOFF TAXI	36.8	–	380	27.46	13.83	305.42	22,076
2. TAXI TURN	33.7	+6.6	360	29.38	14.70	4.58	331
3. TAXI TURN	28.8	-1.5	354	24.82	13.55	12.63	913
4. LANDING TAXI	22.57	–	335	21.25	12.70	531.63	38,426
5. TAXI TURN	18.7	+2.0	321	20.62	12.79	13.66	987
6. TAXI TURN	14.9	-3.2	312	19.86	12.94	15.68	1,134
					TOTAL	883.60	63,867

* SHOT PEENED

NOTES:

1. Twenty-five (25) blocks required for complete test representing 50,000 roll miles.

2. The tire is to be deflated after each block and reinflated prior to start of next block.

3. Each condition will be applied once per block for the indicated number of cycles per the sequence given.

2-40

2.2.2 Crack Growth

Cracks can form in a wheel due to a number of operational hazards that can cause pitting such as stress corrosion, poor maintenance procedures and foreign objects hitting the wheel. The most common type of pitting is caused by stress corrosion. While it can occur in an area of the wheel which permits visual inspection, it usually occurs in the flange area at the bead seat. Since the tire covers this area, the only time that an inspection can be made is during tire change.

In order to determine the smallest feasible site for Electro Discharge Machining (EDM) notches to be used as crack origins in crack growth testing of the wheels, eight aluminum dog bone coupons were prepared and tested. The shape of the EDM notches closely resemble those found in service, Figure 2-18. Various size notches were made in the specimens. The stresses imposed during the cyclic bending test closely matched the 53,428 most severe cycles in the long range transport wheel spectrum block as can be seen in Figure 2-19. Table 2-17 lists the various size semi-circular EDM notches used in the tests, the number of cycles to crack initiation and the number of cycles to failure. Figure 2-20 shows the cycles to initial crack propagation as a function of notch radius. Based on the testing, the 0.070 inch size will provide crack initiation within approximately one spectrum block.

A fractographic study was performed of crack growth rates in eight different wide bodies transport wheels that failed in service. In each case the crack origin is identified and a scanning electron microscope is employed at typically 3000X magnification to photograph the fracture surface at various distances from the origin (measured in the thickness direction) and to measure the spacings of fracture surface markings. There is ample evidence that one mark is caused each flight, due to the ground-air-ground cycle. Thus the spacing between marks is equal to the crack growth per flight in the thickness (depth) direction.
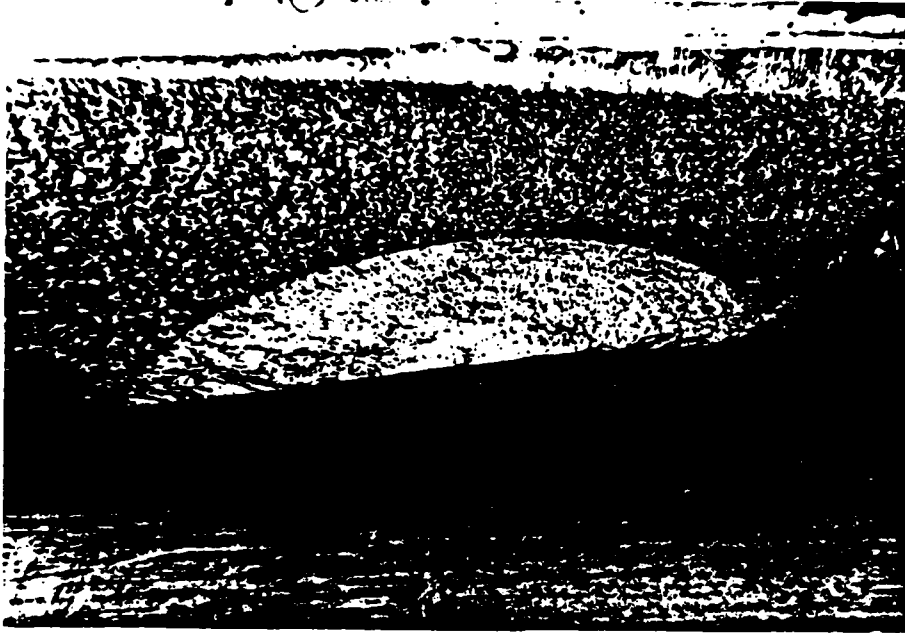
Figure 2-18.   Fracture Surface of a Wheel Flange Showing
               Typical Semi-Elliptical Surface Crack
               Where Cracking Originated.

Figure 2-21 shows the results of a linear regression analysis done on the measured spacings of these marks for each of the eight wheels. The growth rate per flight, da/dF, was (approximately) linear with crack depth, except in Wheel Number 7, where the sudden increase occurred at a depth of 0.13 inch where cracks from two nearby origins coalesced.

Since the maximum of the ground-air-ground cycle occurs during take-off taxi, the crack growth rate is sensitive to the take-off weight of the airplane. Therefore the eight aircraft are separated into two groups according to typical take-off weight. A statistical analysis is done for each separate group. Figure 2-22 shows the 95 percent crack probability-level growth rates for each of these two groups.

These crack growth rate curves were then integrated to predict growth of a 0.030-inch deep crack. Figure 2-23 shows the results for 95 percent proba-
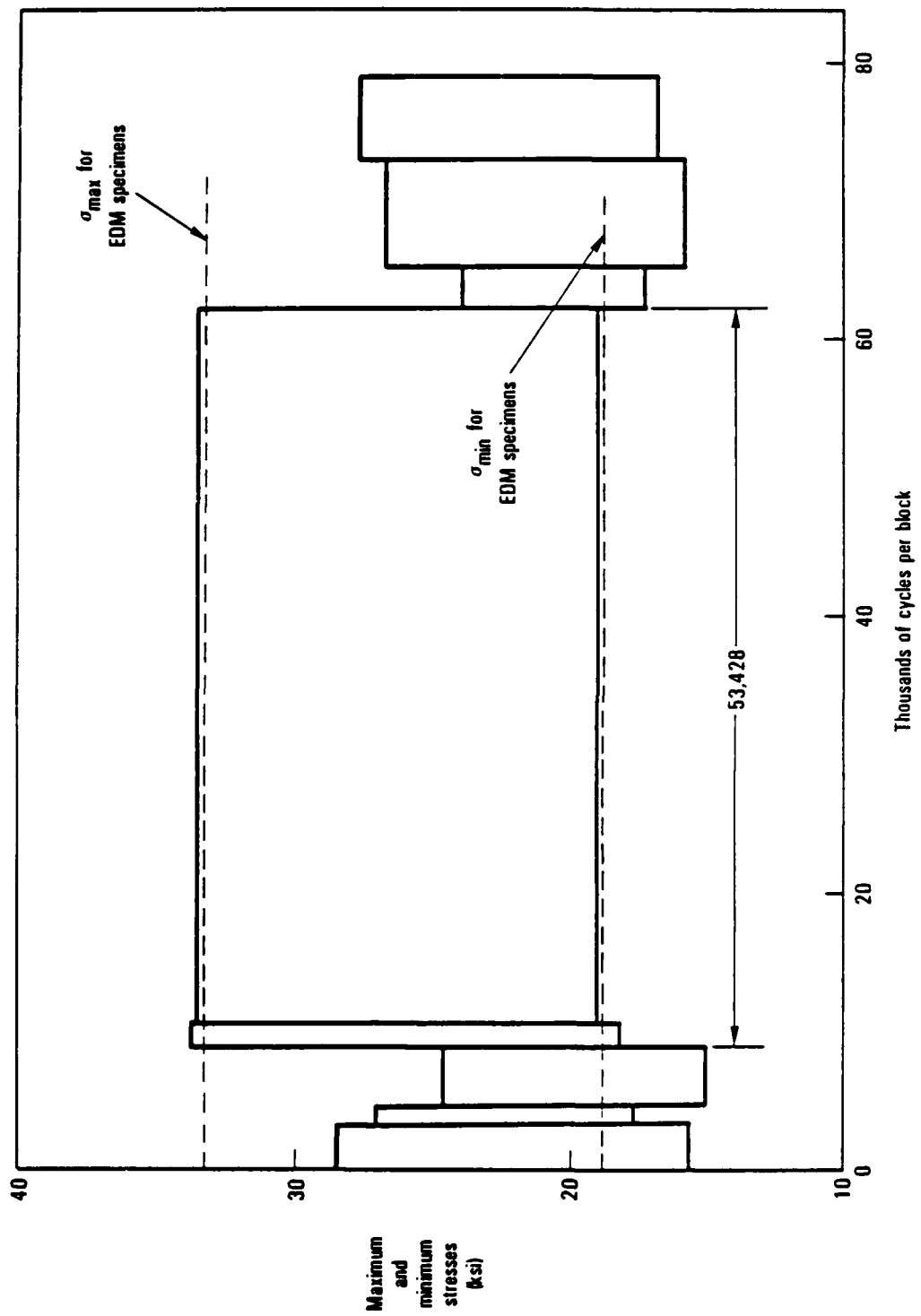
Figure 2-19. Long-Range Transport Wheel Test Spectrum and Stresses
Used in Testing EDM-Notched Specimens
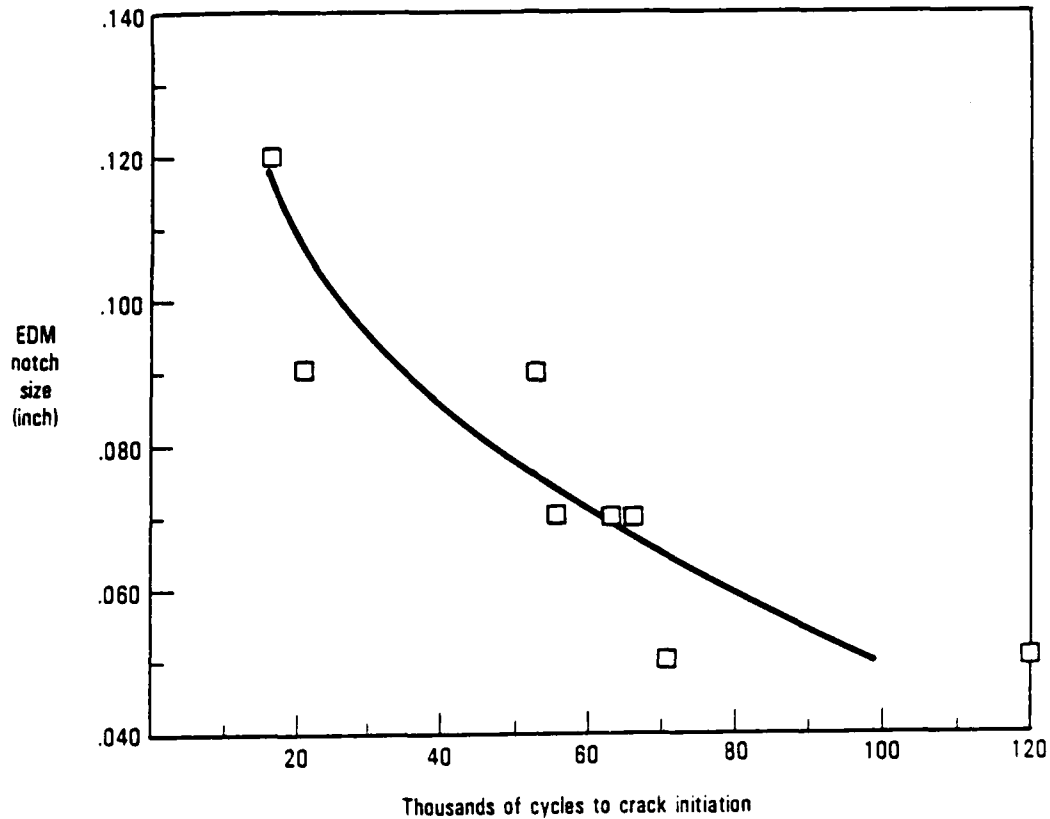
Figure 2-20. Time to Crack Initiation for Dogbone Specimens
with EDM Notches of Various Sizes

TABLE 2-17. RESULTS OF CRACK GROWTH TESTS

SUPPLIER OF EDM NOTCH	NOTCH RADIUS	INITIAL PROPAGATION	CYCLES TO FAILURE
F&G TOOL	.050	120,000	337,000
F&G TOOL	.070	56,000	220,000
F&G TOOL	.070	66,000	228,000
F&G TOOL	.090	53,000	202,000
F&G TOOL	.090	21,000	192,000
F&G TOOL	.120	17,000	136,000
METCUT	.050	71,000	238,000
METCUT	.070	63,000	230,000
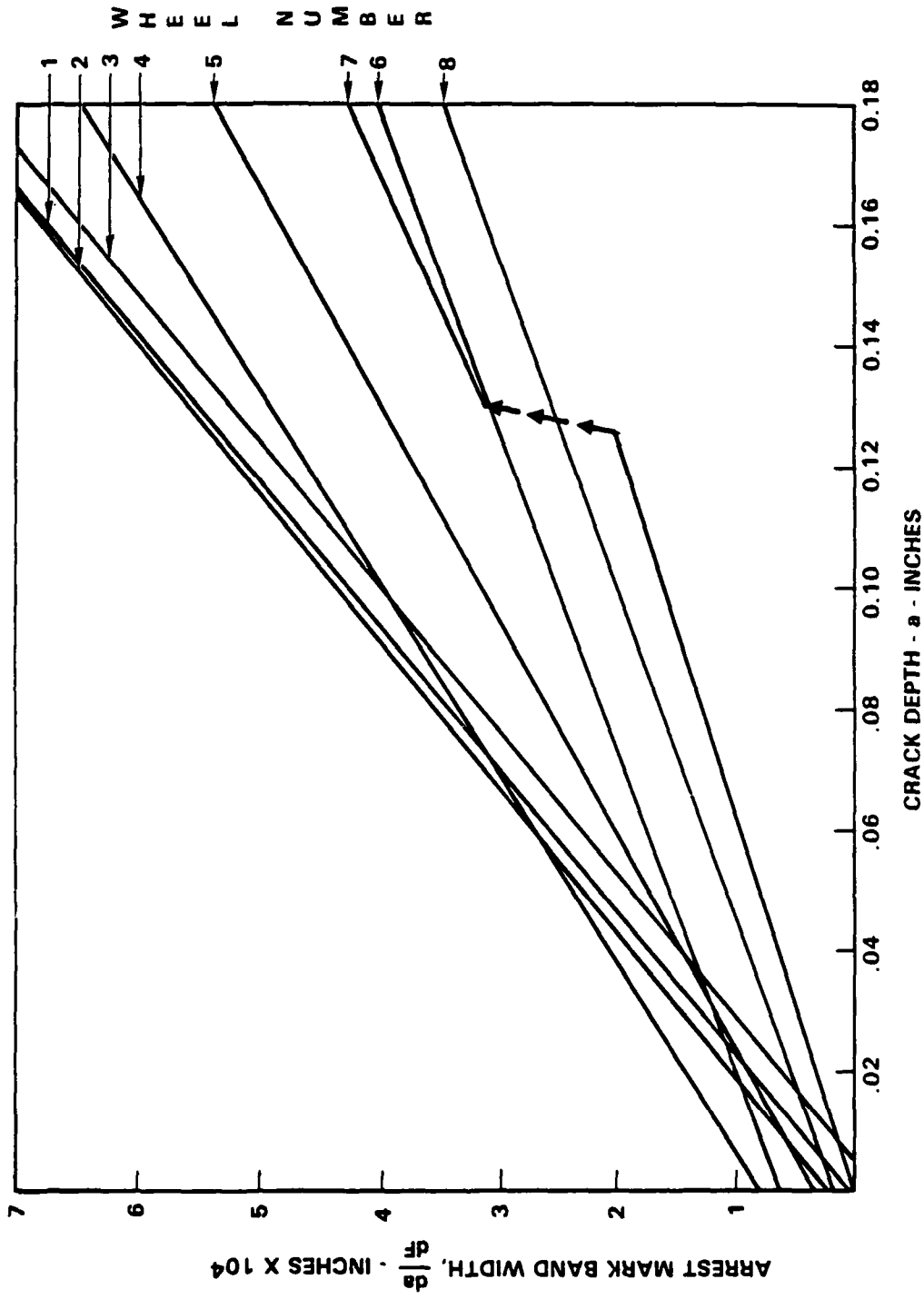
Figure 2-21. Linear Regression Plots of Arrest Mark Spacing Versus Crack Depth
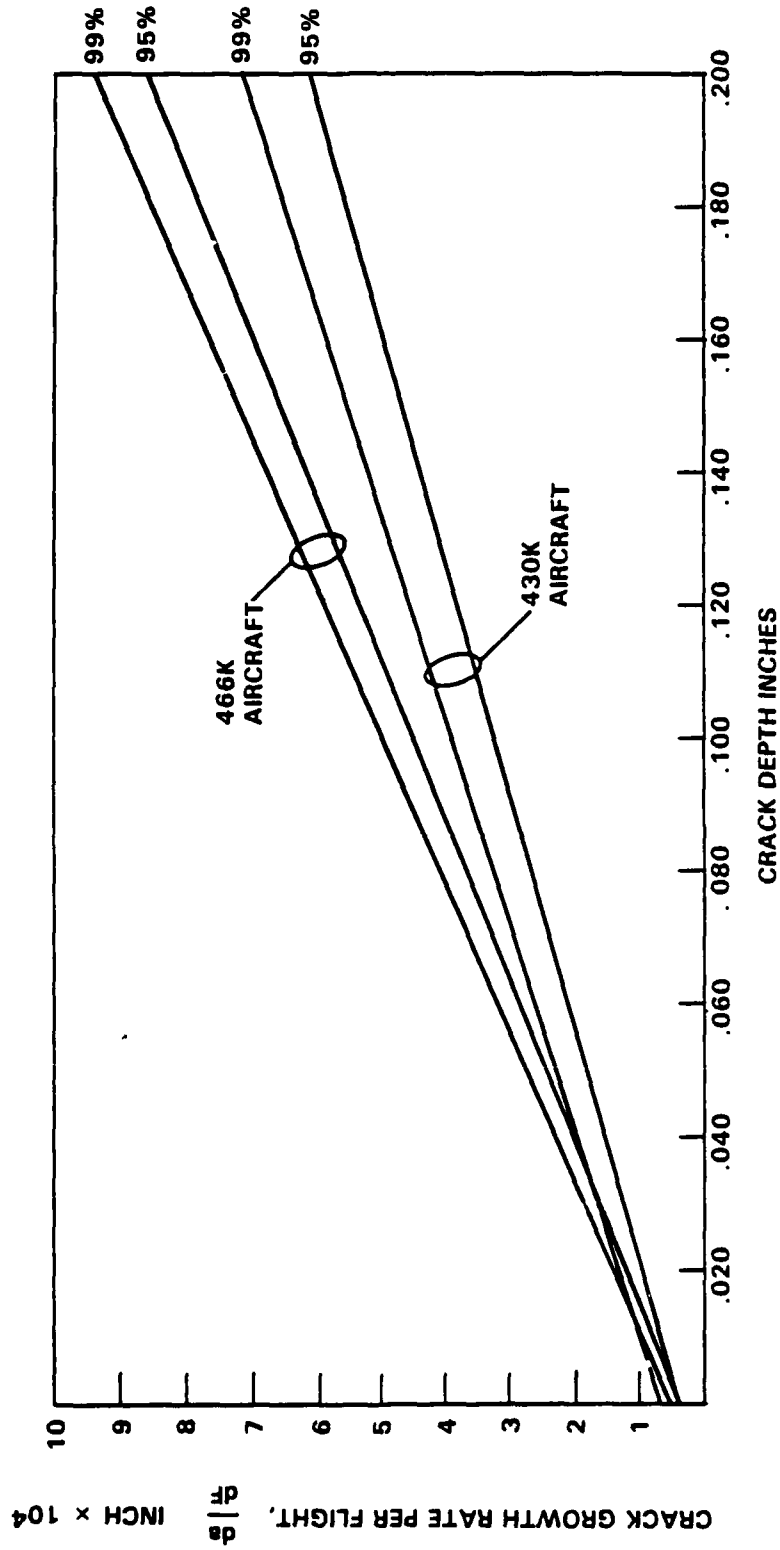
Figure 2-22. Linear Regression Plots of Crack Growth Rate per Flight

2-46
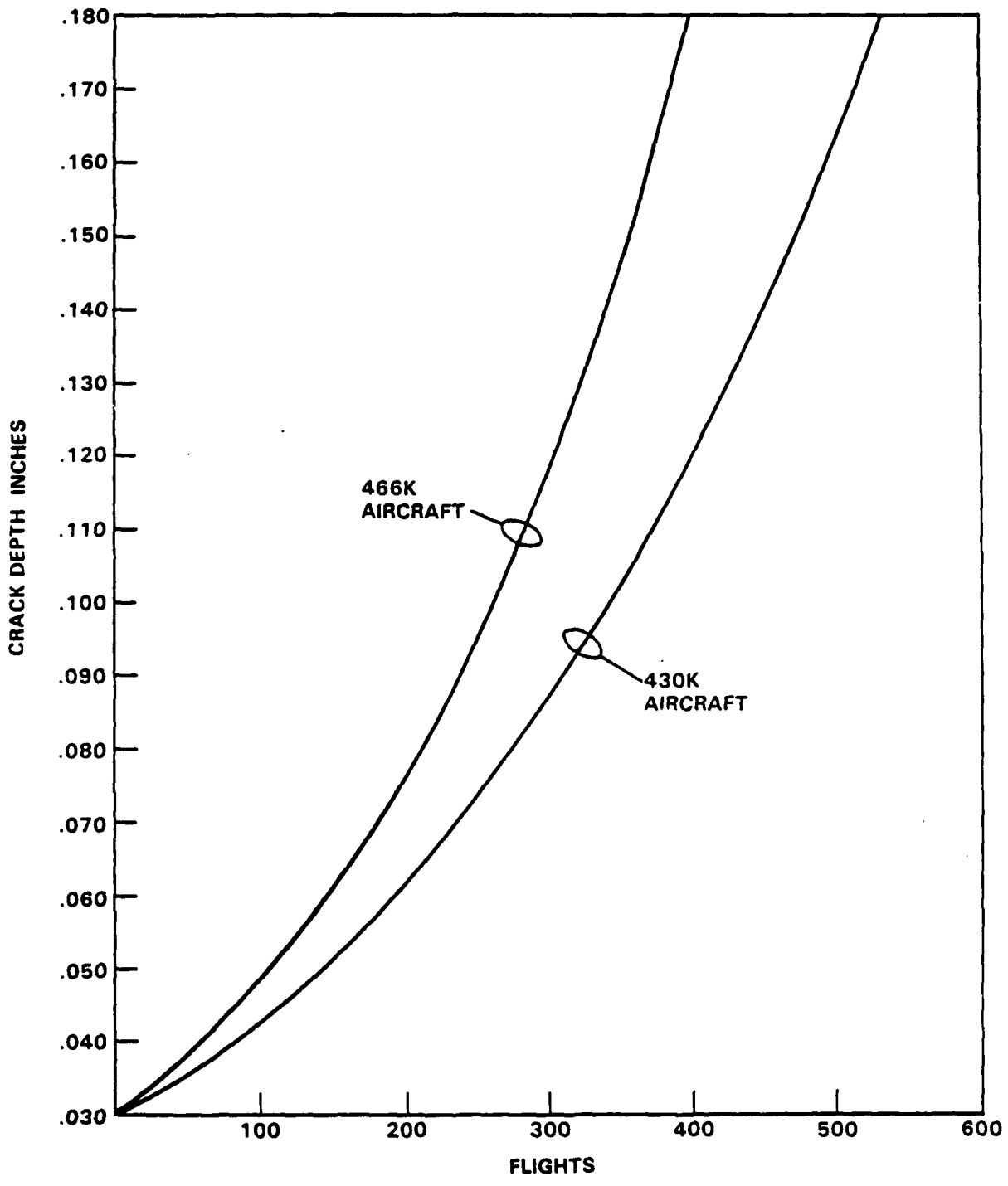
Figure 2-23. Plots of Crack Depth Versus Flights
Based on 95 Percent Level of Probability

2-47

bility and 50 percent confidence. On this basis, only five percent of service cracks in wheels would be expected to crack faster.

The difference between the data means from Figure 2-21 and the 95 or 99 percent probability lines in Figure 2-22 is a meaningful scatterband width. Because it is established by service cracking data, this scatterband accounts for all the pertinent statistical parameters such as those related to variations in material properties, service usage and manufacturing quality.

Of concern during operations is a crack developing in the wheel to the extent that failure occurs before an inspection can be made. Locations that can be inspected without removal of the tire can be monitored as necessary. However, cracks originating in areas such as the tubewell, bead seat and flange locations usually occur in areas which are not inspectable unless the tire is removed. Cracks originating in the tubewell area although not readily inspectable usually show up as a loss in tire pressure. However, cracks in the bead seat and flange areas, which are most common, do not loose tire pressure and are only usually detected in an inspection during tire changes. Accordingly, it must be assured that if a crack develops, that it will not grow sufficiently to result in failure prior to the next tire change.

By introducing a flaw in the critical area of the wheel, the crack growth rate can be determined by dynamometer tests using a loading spectrum representing service operations. The spectrum is developed from the wheel load operational spectrum for the wheel. The spectrum must take into account the need to change the loads more often in order to make a more even distribution of the larger loads over the shorter test period. Tables 2-18 through 2-22 show the spectra for the long range, medium range and short haul transports, and patrol and fighter airplanes, respectively. The 148 flights is representative of the number of flights in between tire changes due to wear. The 148 flights is from service experience with one model airplane and will vary between airplanes. In a new design or a redesign of an alder airplane the number of flights between tire changes must be estimated from past experience. In estimating the number of flights between tire changes for wear, it is best to be optimistic on wear life.

TABLE 2-18. WHEEL CRACK GROWTH SPECTRUM, LONG-RANGE TRANSPORT

	CONDITION	LOADS - KIPS		TIRE PRESS PSI	* TUBEWELL STRESS - KSI		CYCLES PER FLIGHT	CYCLES PER BLOCK
		RADIAL	LATERAL		MAX	MIN		
1.	TAKEOFF TAXI	63.0	-	239	22.07	5.06	230	3,404
2.	TAKEOFF TAXI	50.0	-	237	19.75	6.25	390	5,772
3.	TAKEOFF TAXI	43.4	-	209	17.80	6.08	70	1,036
4.	TAKEOFF TURN	56.7	-9.3	236	26.71	7.11	8	118
5.	TAKEOFF TURN	56.7	6.4	202	17.43	3.01	20	296
6.	LANDING TAXI	51.3	-	219	20.07	5.09	320	4,736
7.	LANDING TAXI	51.1	-	192	18.13	4.33	320	4,736
8.	LANDING TAXI	50.8	-	166	16.86	3.14	275	4,070
9.	LANDING TURN	41.5	-10.3	249	25.74	9.79	1	15
						TOTAL	1634	24,183

* SHOT PEENED

NOTES:

1. Ten (10) blocks required for one tire change (148 flights).

2. If crack has not grown to a critical length, repeat the test until it does. The number of repeats will be used to determine the number of tire changes in between eddy current inspections.

TABLE 2-19. WHEEL CRACK GROWTH SPECTRUM, MEDIUM-RANGE TRANSPORT

	CONDITION	LOADS - KIPS		TIRE PRESS PSI	* FLANGE STRESS - KSI		CYCLES PER FLIGHT	CYCLES PER BLOCK
		RADIAL	LATERAL		MAX	MIN		
1.	TAKEOFF TAXI	62.0	-	221	37.04	20.05	100	1,480
2.	TAKEOFF TAXI	54.2	-	223	35.70	20.80	200	2,960
3.	TAKEOFF TURN	44.0	3.5	206	33.50	19.60	300	4,440
4.	TAKEOFF TURN	45.9	-5.5	205	29.44	18.59	40	592
5.	TAKEOFF TURN	41.3	-3.5	205	29.28	19.06	20	296
6.	LANDING TAXI	49.6	-	206	32.60	19.00	1,000	14,800
7.	LANDING TURN	39.3	10.8	215	38.20	21.80	2	30
8.	LANDING TURN	39.2	5.1	222	35.40	22.00	200	2,960
9.	LANDING TURN	40.8	-3.0	212	30.20	20.00	14	207
10.	LANDING TURN	35.9	-3.0	215	29.54	20.64	40	592
						TOTAL	1,916	28,357

* SHOT PEENED

NOTES:

1. Ten (10) blocks required for one tire change (148 flights).

2. If crack has not grown to a critical length, repeat the test until it does. The number of repeats will be used to determine the number of tire changes in between eddy current inspections.

TABLE 2-20. WHEEL CRACK GROWTH SPECTRUM, SHORT HAUL TRANSPORT

	CONDITION	LOADS - KIPS		TIRE PRESS PSI	* FLANGE STRESS - KSI		CYCLES PER FLIGHT	CYCLES PER BLOCK
		RADIAL	LATERAL		MAX	MIN		
1.	TAKEOFF TAXI	40.3	-	186	28.22	17.17	450.0	6,660
2.	TAKEOFF TURN	35.5	0.3	186	27.07	17.44	20.0	296
3.	TAKEOFF TURN	30.4	0.2	186	26.03	17.76	20.0	296
4.	TAKEOFF TURN	35.4	-0.1	177	26.15	16.40	20.0	296
5.	LANDING TAXI	36.9	-	184	27.25	17.14	450.0	6,660
6.	LANDING TURN	35.6	-2.4	192	29.42	18.42	0.3	4
7.	LANDING TURN	36.5	-2.3	188	28.95	17.75	0.3	4
8.	LANDING TURN	27.8	1.0	182	24.67	17.36	20.0	296
9.	LANDING TURN	34.1	-2.3	191	28.92	18.39	5.0	74
10.	LANDING TURN	33.5	-0.1	176	25.63	16.39	40.0	592
						TOTAL	1,025.6	15,178

* SHOT PEENED

NOTES:

1. Ten (10) blocks required for one tire change (148 flights).

2. If crack has not grown to a critical length, repeat the test until it does. The number of repeats will be used to determine the number of tire changes in between eddy current inspections.

TABLE 2-21. WHEEL CRACK GROWTH SPECTRUM, PATROL AIRPLANE

	CONDITION	LOADS - KIPS		TIRE PRESS PSI	"O" RING SEAL STRESS - KSI		CYCLES PER FLIGHT	CYCLES PER BLOCK
		RADIAL	LATERAL		MAX	MIN		
1.	TAKEOFF TAXI	35.2	–	246	41.81	31.94	900	13,320
2.	TAKEOFF TAXI	27.7	–	209	39.18	31.41	630	9,324
3.	TAKEOFF TAXI	24.4	–	206	37.13	30.29	570	8,436
4.	TAKEOFF TURN	26.8	0.3	211	38.12	29.25	30	444
5.	TAKEOFF TURN	33.4	-3.3	240	37.40	33.17	10	148
6.	LANDING TAXI	24.4	–	232	38.75	31.91	280	4,144
7.	LANDING TAXI	24.4	–	225	38.35	31.50	300	4,440
8.	LANDING TAXI	21.9	–	215	37.17	31.04	600	8,880
9.	LANDING TAXI	20.2	–	203	36.08	30.41	800	11,840
10.	LANDING TURN	22.6	5.3	218	44.20	28.99	2	30
11.	LANDING TURN	22.6	5.3	206	40.79	28.17	20	296
12.	LANDING TURN	24.9	0.3	206	37.43	30.09	70	1,036
						TOTAL	4,212	62,338

NOTES:

1. Ten (10) blocks required for one tire change (148 flights).

2. If crack has not grown to a critical length, repeat the test until it does. The number of repeats will be used to determine the number of tire changes in between eddy current inspections.

2-52

TABLE 2-22. WHEEL CRACK GROWTH SPECTRUM, TACTICAL AIRPLANE

	CONDITION	LOADS - KIPS		TIRE PRESS PSI	* FLANGE STRESS - KSI		CYCLES PER FLIGHT	CYCLES PER BLOCK
		RADIAL	LATERAL		MAX	MIN		
1.	TAKEOFF TAXI	29.3	-	379	25.41	14.45	89	1,317
2.	TAKEOFF TAXI	29.3	-	327	22.60	11.65	227	3,359
3.	TAKEOFF TAXI	25.6	-	324	21.45	11.82	326	4,825
4.	TAKEOFF TAXI	25.6	-	282	19.22	9.58	326	4,825
5.	TAKEOFF TAXI	25.6	-	262	18.18	8.54	252	3,730
6.	TAKEOFF TURN	28.8	-1.5	354	24.82	13.55	10	148
7.	TAKEOFF TURN	26.0	-1.3	252	16.61	8.46	50	740
8.	TAKEOFF TURN	33.7	6.6	360	29.38	14.70	1	15
9.	TAKEOFF TURN	30.6	6.7	320	26.49	12.88	5	74
10.	TAKEOFF TURN	21.7	5.8	252	11.56	8.85	50	740
11.	LANDING TAXI	17.6	-	334	19.86	13.08	370	5,476
12.	LANDING TAXI	17.0	-	241	13.52	7.45	50	740
13.	LANDING TURN	14.5	3.1	251	11.90	9.42	50	740
						TOTAL	1,806	26,729

* SHOT PEENED

NOTES:

1. Ten (10) blocks required for one tire change (148 flights).

2. If crack has not grown to a critical length, repeat the test until it does. The number of repeats will be used to determine the number of tire changes in between eddy current inspections.

2.3 COMPARISON OF TSO AND PROPOSED WHEEL TEST SPECTRA

A comparison is made between the test spectrum given in Table 2-12 and that given in TSO 26C. Since the test spectrum given in Table 2-12 has been compared with a flight-by-flight spectra on a damage basis and accepted because the damage was close to being the same, the test spectrum given in Table 2-12 represents what is to be expected in service operations.

These test spectra were required to produce fatigue crack growth rates approximately equivalent to the rates that would be encountered during operations. The operational spectra generally consist of a couple of hundred different load levels and a few thousand load cycles per flight which have to be reduced to manageable and economical test spectra.

The fatigue crack growth rates per flight are calculated for the complete operational and the developed test spectra, so that they can be compared (see Figures 2-24 through 2-28), by calculating the rates for spectra having discrete magnitudes. In addition to calculating the contribution of each discrete loading per flight, the contribution of each significant discrete loading in percent of the total growth rate is listed. This listing of the percent of contribution to rate makes possible the substitution of discrete loadings on a basis of these percentages.

The following simple example illustrates how these substitutions are made:

Load Level (Discrete)	Growth/Flight	% of Total
. . .	. . .	. . .
$S_{(n-k)}$	(Not listed	.23
$S_{(n-k+1)}$	here for	.10
$S_{(n-k+2)}$	simplicity)	.16
$S_{(n-k+3)}$		.21
$S_{(n-k+4)}$		.08
. . .	. . .	. . .

(At stress intensity/load = constant = $(K/P)c$)

2-54
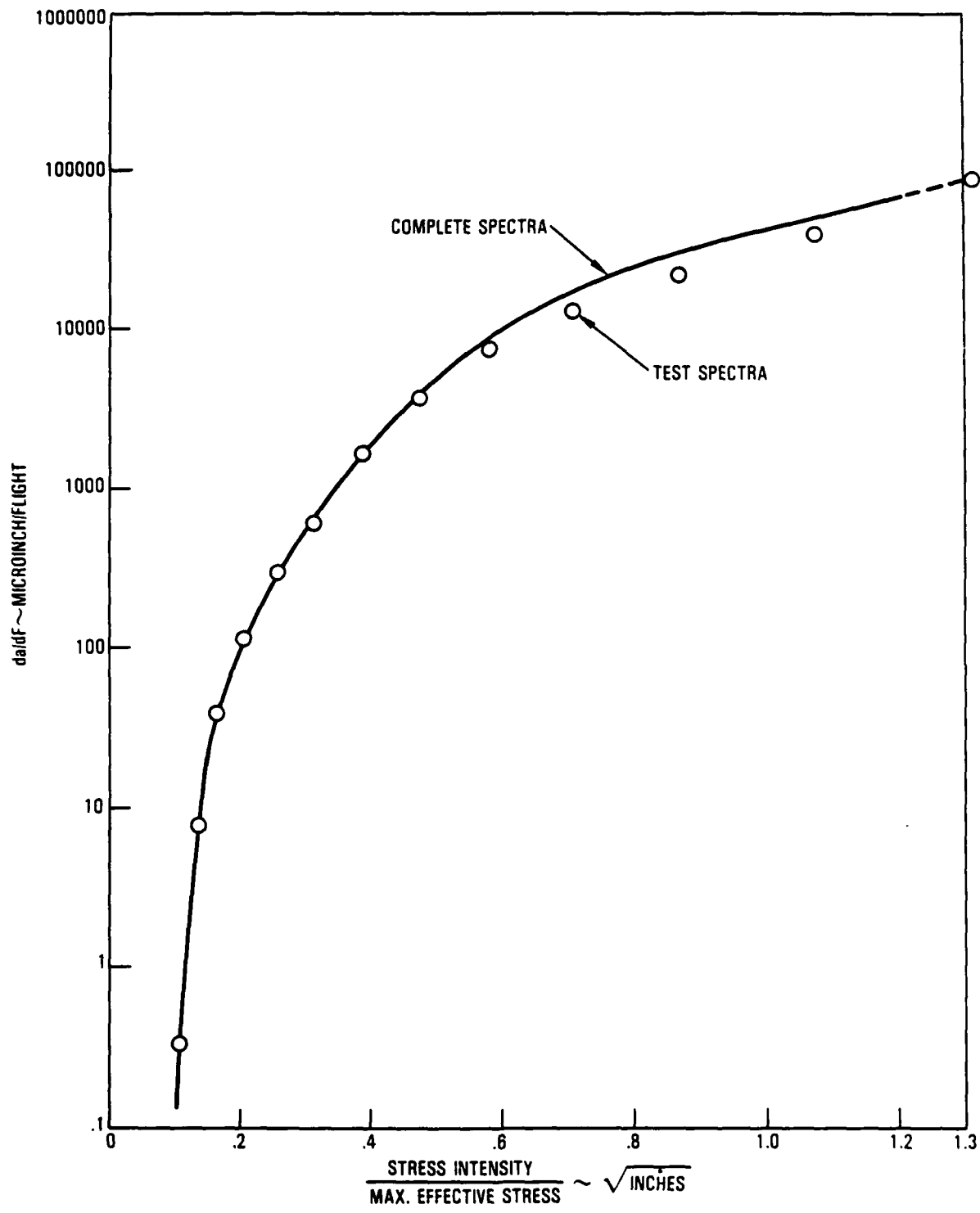
Figure 2-24. Comparison of da/dF for Complete and Truncated Test Spectra for Long Range Transport Main Landing Gear Wheel, Tubewell Area

2-55
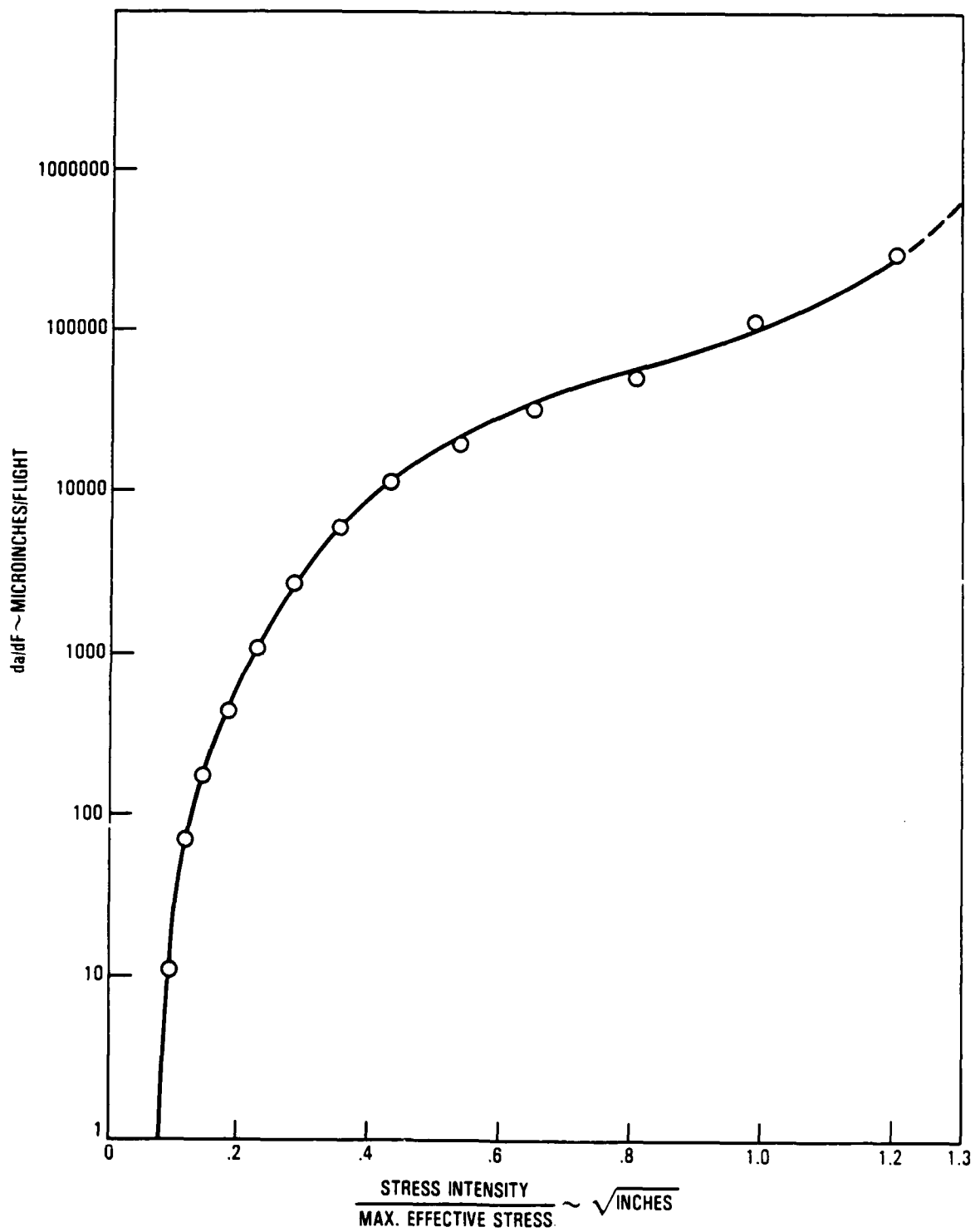
Figure 2-25. Comparison of da/dF for Complete and Truncated Test Spectra for Medium Range Transport Main Landing Gear Wheel, Flange Area

2-56
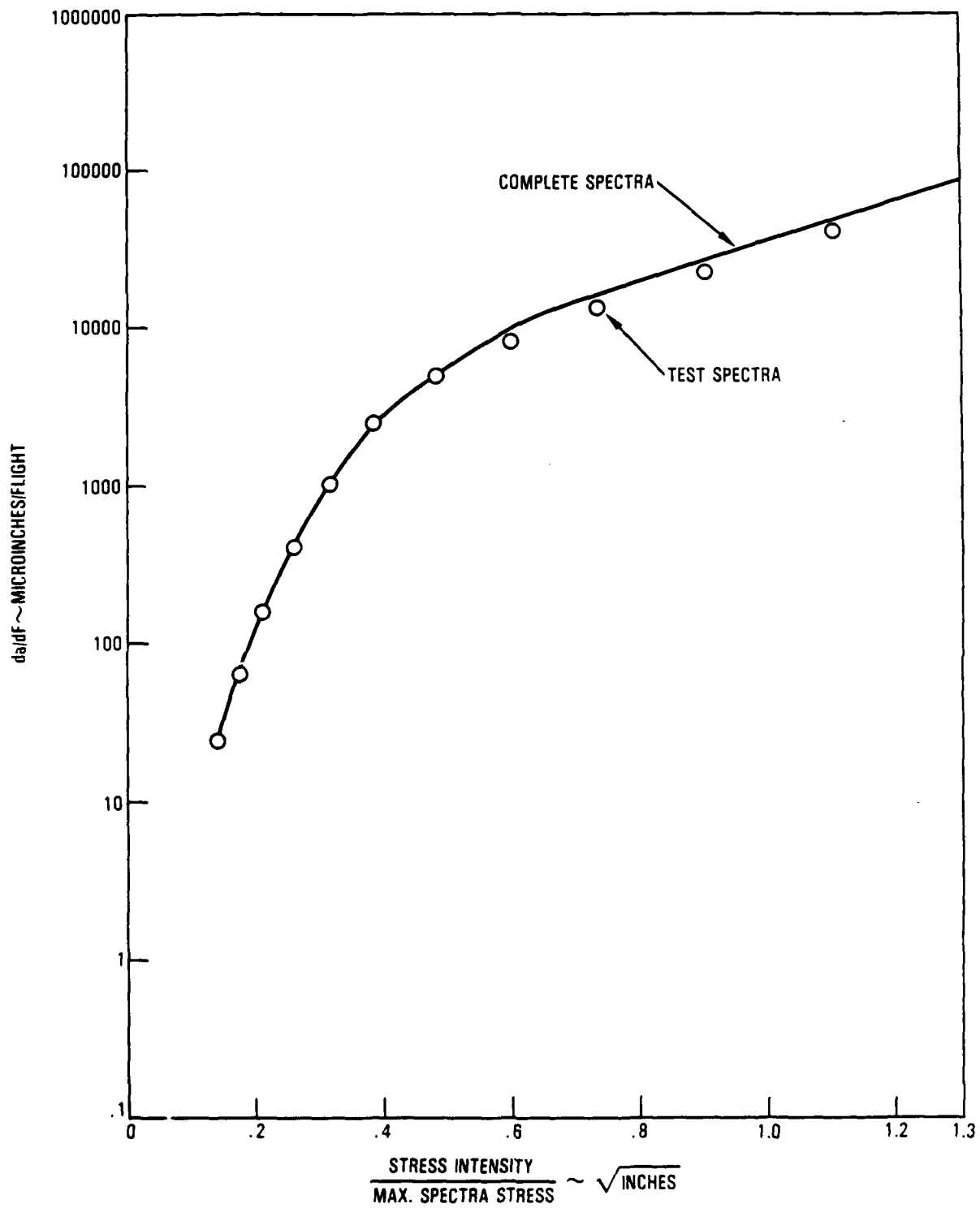
Figure 2-26. Comparison of da/dF for Complete and Truncated Test Spectra for Short Range Transport Main Landing Gear Wheel, Flange Area

2-57
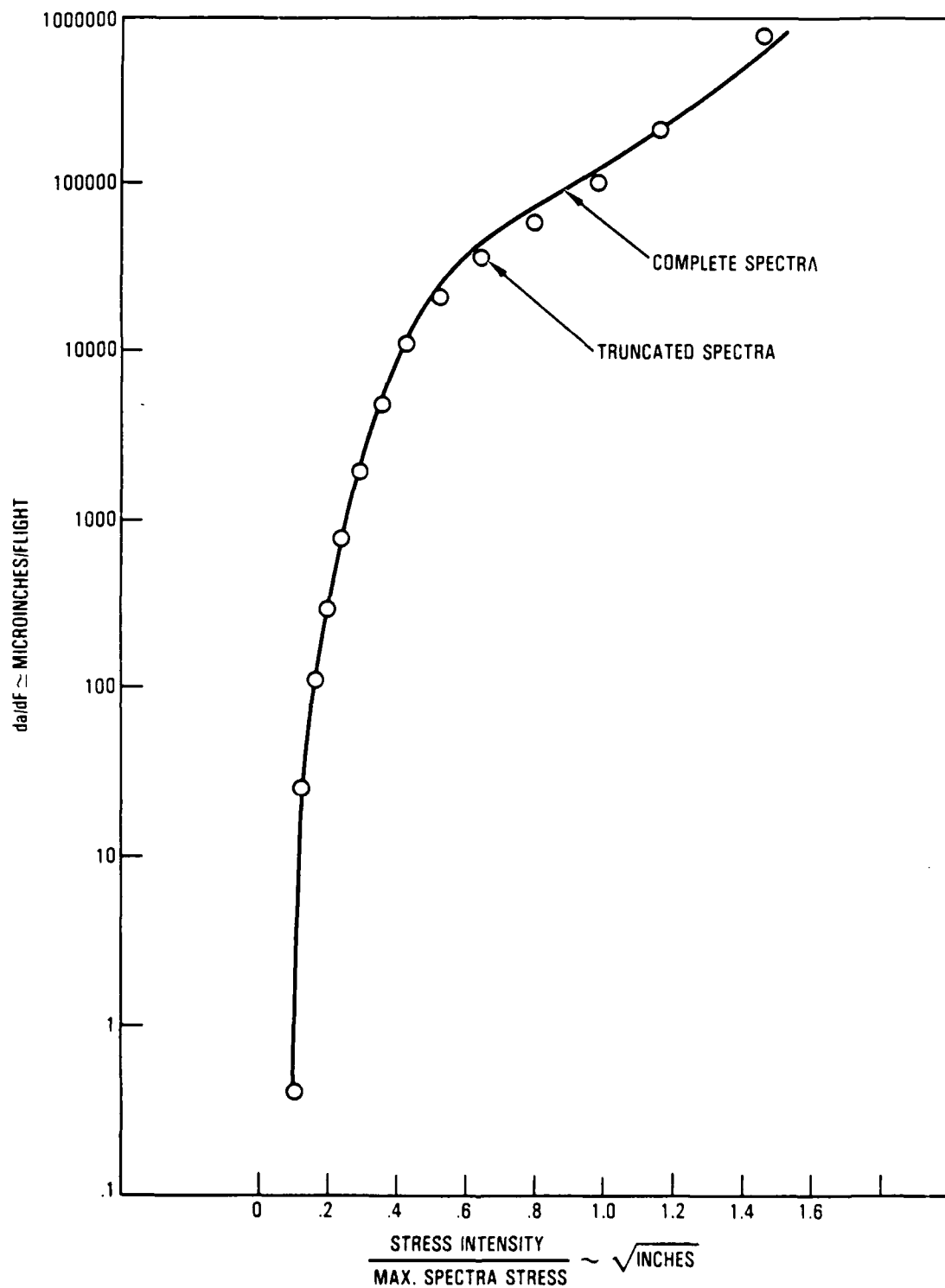
Figure 2-27. Comparison of da/dF for Complete and Truncated Test Spectra for P-3 Main Landing Gear Wheel, O-Ring Seal Groove
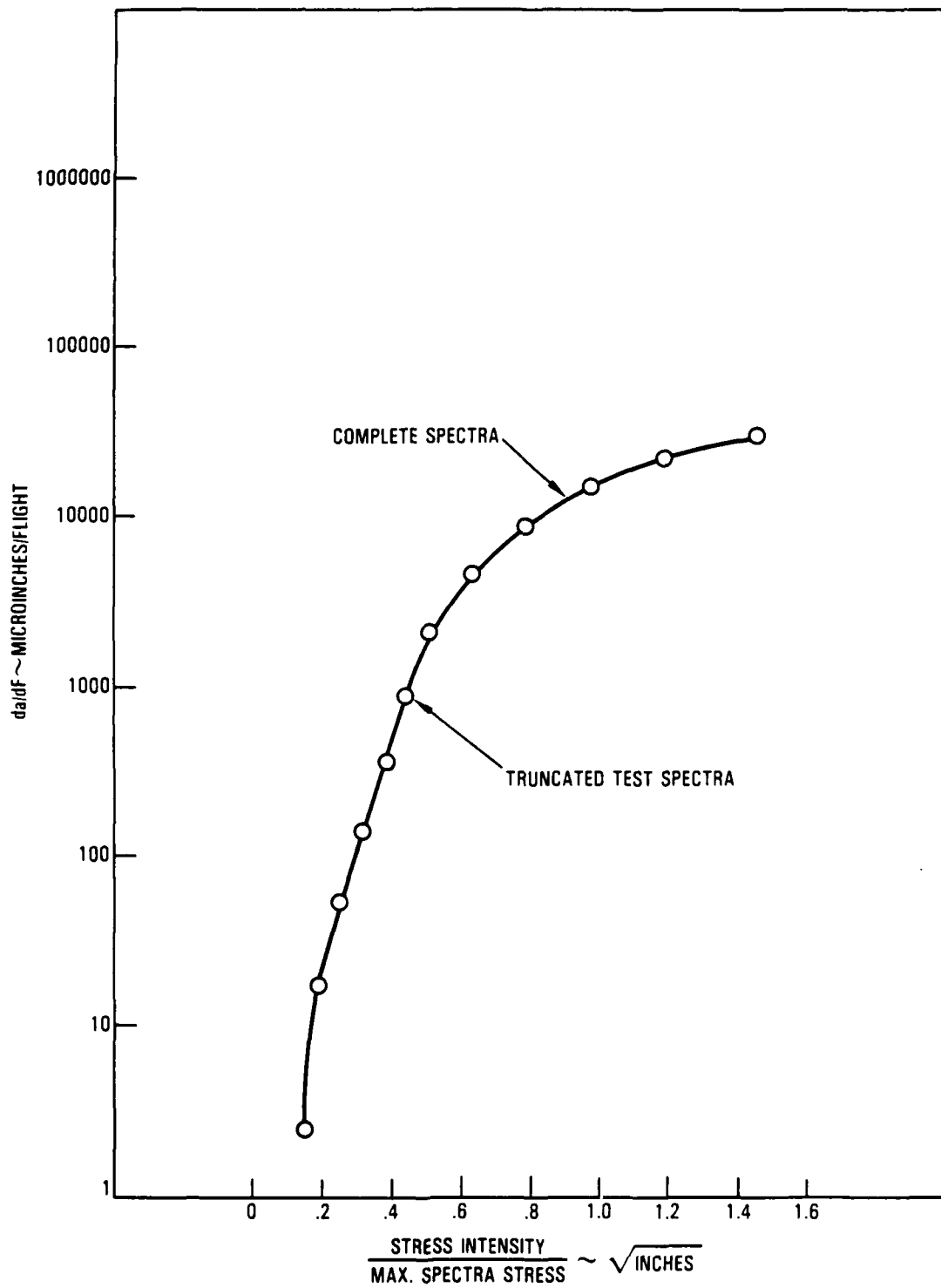
Figure 2-28. Comparison of da/dF for Complete and Truncated Test Spectra for F4E Main Landing Gear Wheel, Flange Area

2-59

The above listing shows that the total cycles of the $S_{(n-k+1)}$ discrete loading contributes approximately .10% of the total crack growth per flight at $(K/P)c$. The same definition applies for the other magnitudes of discrete loadings. Therefore, if the $S_{(n-k+1)}$ load level is to be the only applied load level for the above group of loadings, then the cycles $(N_{(n-k+1)})$ of the $S_{(n-k+1)}$ loading have to be increased to produce the crack growth brought about by the loadings to be removed. This is simply:

$$\left[\frac{(.23 + .16 + .21 + .08)}{.10}\right] \left(N_{(n-k+1)}\right) = \left(N_{(n-k+1)}\right) (\text{Added}).$$

Then, the application of $(N_{(n-k+1)}) + (N_{(n-k+1)})$ (Added) cycles of the $S_{(n-k+1)}$ loading magnitude will produce approximately the same crack growth as all of the loadings in the example group.

The criteria generally used for development of the test spectra are:

o The fatigue crack growth rate for the test and complete spectra should be approximately equal over the length of the da/dF curve. (Exact equality is impossible to achieve because loading levels and cycles are both reduced. Adjustments are made through iterative trials to provide a small degree of conservatism in the low da/dF region. Further "fine tuning" adjustments to vary the degree of conservatism, based on the outcome of initial future testing, can be very easily accomplished because the basic datasets have been stored for later use.)

o Loadings in the test spectra should have representation from the loading segments causing the majority of cracking.

o Maximum and minimum loadings from the complete spectra should be included in the test spectra.

The contributions to cracking for the five complete wheel spectra are primarily from the takeoff and landing straight spectra segments.

Table 2-23 lists the contributions of the straight taxi segments to
cracking at approximately the midrange of the da/dF curves. Totals vary from
89.1 percent for the short range transport to 96.0 percent for the F4E
tactical airplane. Comparisons of total cycles in the operational and test
spectra are made in Table 2-24.

TABLE 2-23. CONTRIBUTIONS TO da/dF OF STRAIGHT TAXI IN COMPLETE SPECTRA

SPECTRA	PERCENT OF TOTAL CRACKING DUE TO STRAIGHT TAXI SEGMENTS		
	Take Off	Landing	Total
Short Range Transport @ .585 (Figure 2-24)	50.6	38.5	89.1
Medium Range Transport @ .410 (Figure 2-25)	50.5	43.4	93.9
Long Range Transport @ .465 (Figure 2-26)	61.7	32.2	93.9
P-3 Patrol @ .410 (Figure 2-27)	45.1	49.7	94.8
F4E Fighter @ .512 (Figure 2-28)	88.5	7.5	96.0

TABLE 2-24. COMPARISONS OF TOTAL CYCLES IN COMPLETE AND TEST SPECTRA

SPECTRA	CYCLES/FLIGHT IN SPECTRA		TEST COMPLETE
	COMPLETE	TEST	
Short Range Transport	1540	1025	.666
Medium Range Transport	3027	1916	.633
Long Range Transport	2963	1634	.551
P-3 Patrol	6020	4212	.700
F4E Fighter	3282	1806	.550

The wheel roll tests required by the present TSO 26C uses a straight roll at the maximum static load for 2000 miles plus a lateral load of 0.15 times the maximum static load for 100 miles in each direction. The tire pressure is that recommended for the maximum static load and does not vary as a result of tire heat. The corresponding stresses for the tests are given in Table 2-25. Since Table 2-25 is for the same outboard wheel segment as that used in Table 2-6, a comparison of the wheel stresses in the critical areas for the TSO and predicted operational loads can be made as shown in Table 2-26. The stresses from application of the TSO and the 50,000 roll mile operational loads are approximately the same with the operational loads being slightly lower when considering the difference between maximum and minimum stresses. However, when the number of cycles for the operational spectrum is compared with the number of cycles for the TSO, there is a large difference as can be seen in Table 2-27. The number of straight rolls and the number of turns in Table 2-6 have been combined. As can be seen, there are over ten times as many straight roll cycles and over six times as many turn cycles in the operational spectrum as there are in the TSO spectrum. Since it is impractical to apply that many cycles in a test, the number of cycles is reduced by adjusting the loads as described in 2.2 above.

Table 2-12 shows the test spectrum that represents the operational spectrum shown in Table 2-6. The number of cycles per block times 50 blocks are less than one-half of the operational cycles and a little over four times that of the TSO requirement, which indicates that the TSO test requirements are very unconservative.

A comparison of the long-range transport wheel damage shows that the TSO requirements results in a damage of 0.034 while the proposed test spectrum has a damage of 0.526. The lower value for the TSO results indicates that the TSO requirements do not adequately test the wheel.

TABLE 2-25. TSO 26C ROLL TEST

| AREA | CONDITION | LOAD KIPS | | ROLL DIST. MILES | CYCLES | STRESS*-KSI | |
		RADIAL	LATERAL			MAX	MIN
FLANGE	STATIC	63.75	--	2000	836,134	19.5	11.5
	LATERAL	63.75	+9.56	100	41,807	18.2	10.5
	LATERAL	63.75	-9.56	100	41,807	25.1	10.5
WEB	STATIC	63.75	--	2000	836,134	18.5	7.0
	LATERAL	63.75	+9.56	100	41,807	27.4	0.4
	LATERAL	63.75	-9.56	100	41,807	25.4	-6.2
TUBEWELL	STATIC	63.75	--	2000	836,134	18.4	2.8
	LATERAL	63.75	+9.56	100	41,807	21.8	2.8
	LATERAL	63.75	-9.56	100	41,807	15.2	-0.9

*Tire Pressure 205 PSI

TABLE 2-26. COMPARISON OF TSO, AND OPERATIONAL STRESSES,
LONG-RANGE TRANSPORT

| CRITICAL AREA | CONDITION | STRESSES - KSI | | | |
| | | TSO | | OPERATIONAL | |
		MAX	MIN	MAX	MIN
FLANGE	Straight Roll	19.5	11.5	21.71	13.86
	Right Turn	25.1	10.5	26.16	12.86
	Left Turn	18.2	10.5	17.09	10.91
WEB	Straight Roll	18.5	7.0	20.80	11.64
	Right Turn	25.4	-6.2	25.09	-2.92
	Left Turn	27.4	0.4	26.92	8.01
TUBEWELL	Straight Roll	18.4	2.8	22.07	5.06
	Right Turn	15.2	-0.9	18.31	4.17
	Left Turn	21.8	2.8	26.71	7.11

TABLE 2-27. NUMBER OF CYCLES FOR EACH CONDITION

CONDITION	TOTAL NUMBER OF CYCLES*	
	TSO	OPERATIONAL
STRAIGHT ROLL	836,134	8,804,100
RIGHT TURN	41,807	390,100
LEFT TURN	41,807	175,800
TOTAL	919,748	9,370,000
*One cycle is one revolution		

2.4 REVIEW OF INSPECTION PROCEDURES

The ability to detect flaws by Non Destructive Inspection (NDI) is
necessary for a workable damage tolerance design philosophy. Known
capabilities for the detection of flaws in both production and in-service
environments allow for the assurance of structural integrity within operating
intervals defined by predicted fracture and fatigue behavior. Flaw detection
by NDI is probabilistic, however, and it is influenced by a number of factors
such as NDI method, material type, part configuration, environment and
inspector proficiency. The assignment of values to detection probabilities
and flaw sizes in damage tolerance criteria must therefore reflect a careful
consideration of numerous influences on the NDI processes.

The objective of this NDI assessment is to seek out and to identify the
capability of current NDI techniques in finding flaws in wheels, including the
flaw size these techniques are capable of finding.

2.4.1 NDI Methods

In this section, the available NDI methods which can be used to detect
the flaw in wheels are presented.

2.4.1.1 Dye Penetrant

The principle of the use of dye penetrant is very simple. The component is cleaned and sprayed with a colored or fluorescent dye, which seeps into any open surface cracks. After allowing sufficient time for penetration, excess dye is wiped away and the surface is dusted with developer. The developer acts like blotting paper, and defects are revealed as lines of dye against the white chalky background of the developer.

The method is economical and is widely used. It has sensitivity to a surface crack with surface opening, but the sensitivity diminishes severely for "tight" cracks; i.e., cracks with surface closure, or surface cracks contaminated with foreign material.

2.4.1.2 Eddy Current

When a coil carrying an alternating current is placed near a metal surface, eddy currents are induced at the metal surface. The penetration depth of the eddy currents is determined by the frequency of the current and the magnetic permeability and electrical conductivity of the metal. As the coil is scanned over the metal surface containing a defect within the penetration depth, the flow of eddy currents is distorted and the associated magnetic field changes. This field links the search coil, so the coil senses the defect or crack as a local change in its impedance. The sensitivity of the technique to cracks depends on the surface conditions and homogeneity of the material. It estimates the flaw severity by comparing the magnitude of the response to the response for a standard using a known flaw.

Automatic eddy current appears to be the most reliable technique known for inspecting the flaw in an aluminum wheel. The probe is automatically advanced along the surface and rotated, typically about 0.025-inch per revolution. This way the probe covers all locations on the wheel, eliminating a major source of human error. With the use of shielded probes, the automatic eddy current method can be used by a skilled inspector to reliably find cracks in the range of 0.025-inch radial depth.

2.4.1.3 Ultrasonic

Ultrasonic flaw detection uses a piezoelectric transducer radiating a beam of pulsed sound waves into the structure to be inspected. The transducer is scanned over the surface so that the ultrasonic beam searches the interior volume of the structure. Defects (and geometrical features of the component) reflect the incident pulse, returning a greater or lesser amount of energy to the transducer, which also acts as a receiver. After a delay corresponding to the return time of the pulsed signal, a defect echo is detected. Normally, the defect echoes are amplified, rectified, smoothed, and a graph of echo amplitude is displayed on the Cathode Ray Tube (CRT) screen as a function of time.

The ultrasonic method is sensitive for finding subsurface flaws, cracks induced by corrosion pits, and cracks in a bushed hole without removing the bushing.

2.4.1.4 Radiography

Radiography is another method for detecting subsurface cracks. A source of x-rays or gamma rays is placed on one side of the component and a suitably sensitive photographic film on the other. Flaws are revealed by their lower absorption of x-ray and the consequent increased blackening of the film by rays that have passed through the defect. The sensitivity of this method is poor compared to other NDI methods. Unless the radiation beam strikes the crack almost tangentially, there is negligible differential absorption between rays passing through the crack and those through adjacent sound material and the crack may be undetectable on the film. Furthermore, radiography requires special necessary safety precautions, and is difficult to apply in service in remote or hot environments.

2.4.2 Results of the NDI Survey

The dye penetrant method is least costly. For eddy current and ultrasonic methods, the initial investment is expensive, but the subsequent inspections are relatively economical.

Dye penetrant, manual eddy current, and manual ultrasonic methods will not reliably detect cracks under 0.10-inch in radial length. Radiographic methods tend to be significantly less sensitive. For a wheel with a bushing in place, only the ultrasonic or radiographic methods can be used for surface flaws in the hole bore, the most common initial crack geometry for that case.

Tight cracks have a strong influence on detectability by some methods, including ultrasonic, visual and penetrant, but not eddy current. It is found that 0.06-inch deep cracks are usually detectable at fastener holes by use of a portable ultrasonic scanner without disassembly or fastener removal. However, detectability improved to 01020-inch deep cracks when tension was applied to the specimen to open up the tight cracks. Unfortunately, the application of tension load to a wheel during inspection is seldom feasible.

Flaw detection by NDI is probabilistic and is influenced by NDI method, material, part configuration, crack location, orientation and tightness, surface condition including the presence of corrosion products, inspection environment, and inspector proficiency. Of these, inspector proficiency appears to be the most difficult reliability problem. New NDI technology is required which must reduce operator dependency, optimize simplicity, mesh with the work environment, and provide reproducible results.

2.4.3 Service Experience

A review has been made of wide bodied transport wheels retired from the first quarter of 1979 through the third quarter of 1984. New inspection procedures, using eddy current equipment, were introduced into the field in 1981. As an example of some of the results of the inspection procedure, the dramatic effect on the number of wheels retired for broken flanges can be seen in Figure 2-29. In contrast, Figure 2-30 shows the increase in number of wheels retired as a result of detecting cracks. The drop off in number of wheels retired for cracks indicates the effectiveness of the inspection program in detecting cracks at the wheel salvageable level.
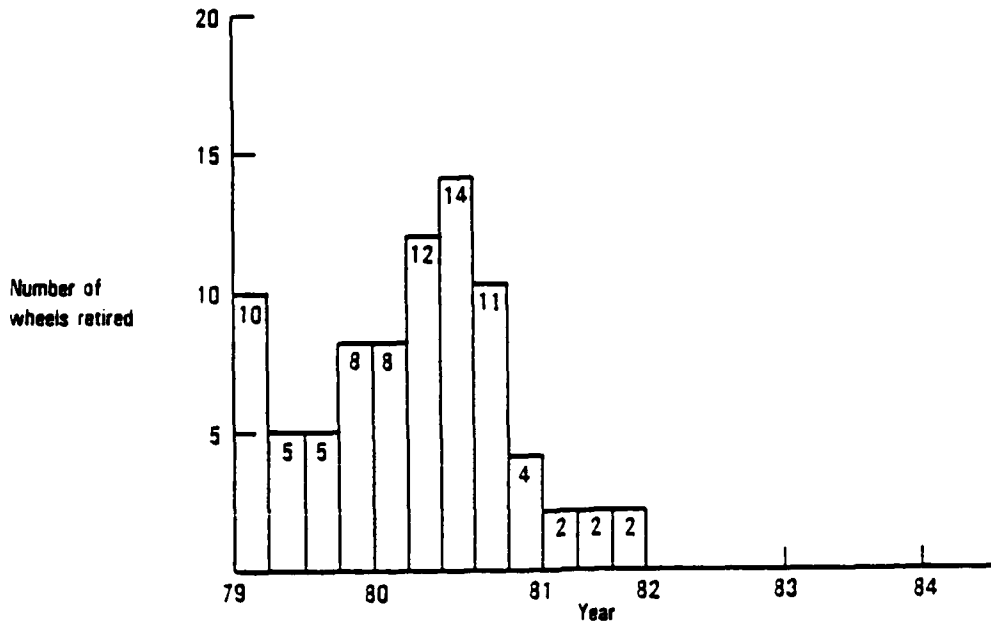
Figure 2-29. Number of Broken Flange Retirements, 10-1213 Outboard Half
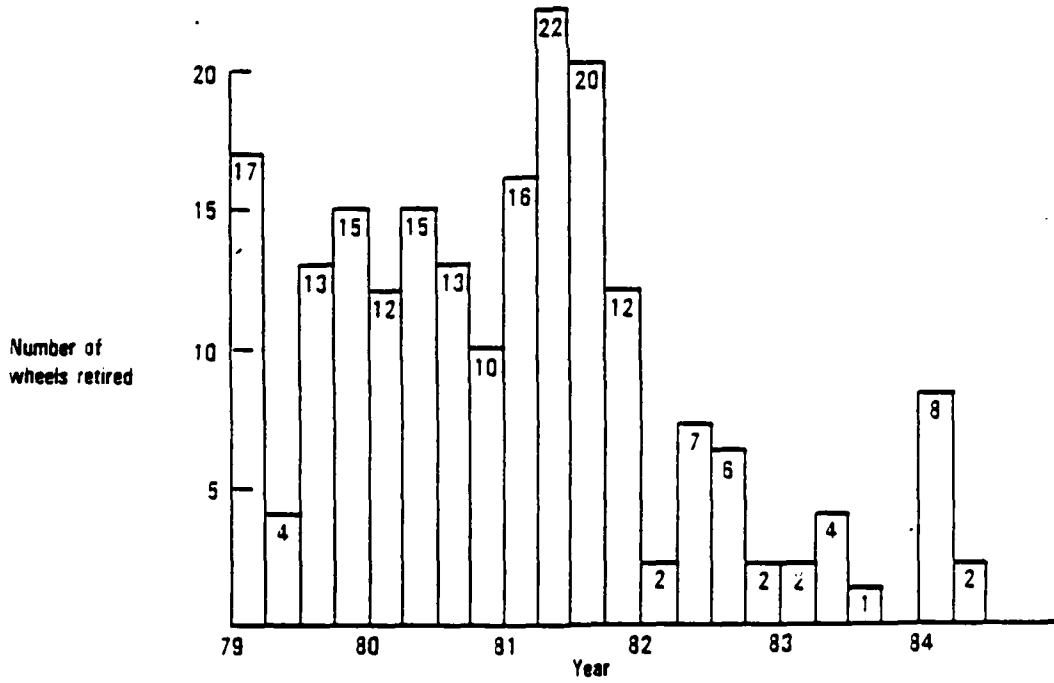
Figure 2-30. Number of Cracked Flange Retirements, 10-1213 Outboard Half

2-68

2.5 COST EFFECTIVENESS STUDIES

In developing new requirements, the cost-effectiveness aspects need also to be examined in addition to the safety aspects. In an effort to provide a safe wheel, the requirements should not be so conservative that they add unnecessary weight to the wheel. The ideal test spectrum should duplicate the environment expected in service for the proposed roll life of the wheel without an increase in life cycle cost over the methods now used.

Usually, if a wheel manufacturer is selected to provide a wheel for a new airplane, that wheel will be used on the airplane throughout the airplane's life. Thus the manufacturer strives to furnish the lightest wheel at the least cost. As a minimum the wheel has to meet TSO requirements. However, most airframe manufacturers add additional requirements generally dealing with the roll life of a wheel when exposed to certain loads and combinations of loads. These requirements are linked to warranties.

There are at least two areas of interest in minimizing wheel failures during operations and thus improving the safety. The first is by providing a wheel test procedure that more nearly represents the operational conditions and ascertains the life of the wheel. The second pertains to inspection procedures. The most common material used in the manufacture of wheels is 2014-T6 aluminum which is susceptible to stress corrosion. The pits from stress corrosion will result in cracks that may not be detectable during visual inspections. The impact of these two areas on the cost of a wheel is explored. In addition, a roll-on-rim requirement has been added which has resulted in an impact on costs.

2.5.1 Test Procedure

A test program that closely represents the service conditions and life that the wheel will be exposed to, will initially add about one percent to the wheel acquisition price. However, if a certificated wheel tested to an inadequate spectrum develops a structural problem, the cost in warranty, redesign, changed forgings and retest could add 10 to 15 percent to the

2-69

manufacturer's cost of the wheel. In addition the user will suffer a loss for his share of the warranty and would require an increase in inventory to cover the failures. Also a wheel failure can cause damage to the airplane either from parts of the wheel itself and/or from tire failure resulting from the wheel failure. It is difficult to assess what the additional cost will be for the user since it depends on the warranty agreement, the rate of failures and the amount of damage to the airplane.

2.5.2 Inspection Procedure

As previously discussed, stress corrosion can result in the premature retirements of wheels either from failure or from the depth of the crack being beyond salvage. Failure can cause other damage such as punctured fuel tanks, which can jeopardize safety, tire failures, and damage to engines and airplane structure. Even though wheels develop cracks, if they are within limits. corrective action can be taken. The incidents of failure and unsalvagable cracks can be reduced by setting proper inspection procedures and using reliable crack detecting equipment. The initial investment for eddy current equipment is in the order of $25,000. However, considering that the cost of a new wheel is about $6000, the salvage of four wheels will almost pay for the equipment. It takes about one hour to set up the wheel for tests and another half hour to run the test and analyze the results. Thus the operating costs are less than thirty cents per landing.

An inspection procedure using eddy current inspection techniques was started in early 1981 for the users of a wide bodied transport. The results of the inspection are shown in Figures 2-29 and 2-30. After the year 1981 there have been no wheels retired because of broken flanges. In addition, the number of wheels retired for crack flanges is reduced by more than 75 percent. The latter performance is attributed to the inspection procedure detecting cracks prior to them exceeding rework tolerances.

2.5.3 Roll-On-Rim Requirement

The present roll-on-rim requirement is designed to provide a wheel roll capability in the event of a tire loss. The test, as now stipulated, is

2-70

performed on a dynamometer at 10 miles per hour for a roll of approximately 1,100 feet. In actuality tire failures that result in the complete loss of the tire either precede or occur during a rejected takeoff (RTO) on a concrete surface under heavy braking and high contact pressure. The difference in environment between a dynamometer and an actual runway defeats the intended purpose of the requirement. With a coefficient of friction about 0.3 for aluminum on a concrete runway, the average wear of aluminum, under a bearing pressure of about 4,000 psi, is about 0.26 pounds per 100 feet of slide. Thus for a 2,000-foot braking distance 5.2 pounds of flange material will be removed, which will wear well within the tubewell area.

To meet the roll-in-rim requirement, the weight of one main wheel for a wide bodied transport is increased by five pounds. The increase of 40-pounds per the airplane is equivalent to a reduction in revenue of one-fourth of a passenger. From the foregoing discussion it appears that the roll-on-rim requirement is not cost-effective.

SECTION 3

CONCLUSIONS

Subject to the results of Phase II tests and analysis, the following conclusions are drawn:

o It is feasible to develop a practical fatigue test spectrum for wheels that more readily duplicates the loads that will be imposed on the wheels during operations.

o It is feasible to develop a practical crack growth test spectrum for wheels using loads applications truncated from operational loads spectra.

o A crack growth rate that is consistent with the tire change interval is necessary to assure safe operations.

o The operational fatigue spectra developed in the program is more severe in fatigue damage than the present test requirements under TSO-C26c.

REFERENCES

1. "Converting Fatigue Loading Spectra for Flight-by-Flight Testing of Aircraft and Helicopter Components," Journal of Testing and Evaluation, JTEVA, Vol. 4, No. 4, July 1976, pp 231-247 (with L. Young).

Appendix A

Load Spectra

TABLES

Table

TABLE A-1. LONG-RANGE TRANSPORT LOAD SPECTRUM
FOR A TAKEOFF WEIGHT OF 0.940 TIMES
DESIGN GROSS WEIGHT FOR 5.2 PERCENT
OF FLIGHTS

| | EVENT | WHEEL LOAD - KIPS | | | SPEED MPH | TIRE CONTAINED GAS | | SINGLE FLIGHT CYCLES* |
		RADIAL	LATERAL	DRAG		TEMP °F	PRESS PSI	
TAKEOFF	90' LFT TURN	54.4	6.0	--	10	101.1	200.4	0.59
	90' RT TURN	56.7	6.4	--	10	104.5	201.6	0.80
	1500' TAXI	55.6	--	--	25	112.3	204.4	6.16
	150' LFT TURN	54.6	4.1	--	10	115.9	205.7	0.98
	3000' TAXI	55.6	--	--	25	134.1	212.2	12.32
	150' LFT TURN	54.6	4.1	--	10	137.2	213.3	0.98
	9000' TAXI	55.6	--	--	25	187.6	231.3	36.96
	65' RT TURN	56.7	9.3	--	10	189.8	232.1	0.64
	65' RT TURN	56.7	9.3	--	10	199.5	235.6	0.64
	7010' T.O.	63.0	--	--	0-170	207.6	238.5	28.70
	9.4 Hour Flight							
LANDING	1805' LDG	50.8	--	--	160	6.1	166.4	7.42
	3619' BRK	46.4	--	9.7	160-25	19.7	171.3	14.81
	1800' TAXI	42.8	--	--	25	44.3	180.1	7.33
	150' LFT TURN	35.5	3.4	--	10	47.3	181.2	0.97
	65' LFT TURN	34.8	11.0	--	10	49.4	181.9	0.43
	5000' TAXI	36.2	--	--	25	71.8	189.9	20.21
	150' RT TURN	36.7	3.1	--	10	73.1	190.4	1.17
	3000' TAXI	36.2	--	--	25	85.3	194.8	12.12
	150' LFT TURN	35.5	3.4	--	10	87.4	195.5	0.97
	1500' TAXI	36.2	--	--	25	93.9	197.8	6.06
	90' LFT TURN	35.3	5.1	--	10	95.1	198.2	0.58
	35' RT TURN	36.7	9.6	--	10	96.5	198.8	0.44

*1 cycle equals 1 revolution of the wheel and based on 5.2 percent of
all flights.

A-1

TABLE A-2. LONG-RANGE TRANSPORT LOAD SPECTRUM
FOR A TAKEOFF WEIGHT OF 0.846 TIMES
DESIGN GROSS WEIGHT FOR 17.4 PERCENT
OF FLIGHTS

| | EVENT | WHEEL LOAD – KIPS | | | SPEED MPH | TIRE CONTAINED GAS | | SINGLE FLIGHT CYCLES* |
		RADIAL	LATERAL	DRAG		TEMP °F	PRESS PSI	
TAKEOFF	90' LFT TURN	49.0	5.4	--	10	101.1	200.4	1.98
	90' RT TURN	51.1	5.8	--	10	102.7	201.0	2.68
	1500' TAXI	50.0	--	--	25	110.5	203.8	20.62
	150' LFT TURN	49.2	3.7	--	10	113.6	204.9	3.29
	3000' TAXI	50.0	--	--	25	130.2	210.8	41.24
	150' LFT TURN	49.2	3.7	--	10	133.3	211.9	3.29
	9000' TAXI	50.0	--	--	25	181.8	229.3	123.71
	65' RT TURN	51.1	8.4	--	10	184.9	230.3	2.14
	65' RT TURN	51.1	8.4	--	10	194.9	233.9	2.14
	6310' T.O.	56.7	--	--	0-170	203.1	236.9	86.46
	6.8 Flight Hours							
LANDING	1819' LDG	51.2	--	--	160	32.1	175.7	25.02
	3647' BRK	46.8	--	9.8	160-25	45.1	180.4	49.94
	1800' TAXI	43.2	--	--	25	69.7	189.2	24.52
	150' LFT TURN	35.8	3.4	--	10	72.8	190.3	3.24
	65' LFT TURN	35.1	11.1	--	10	74.9	191.0	1.43
	5000' TAXI	36.5	--	--	25	97.2	199.0	67.62
	150' RT TURN	37.0	3.1	--	10	98.5	199.5	3.92
	3000' TAXI	36.5	--	--	25	110.8	203.9	40.57
	150' LFT TURN	35.8	3.4	--	10	112.8	204.6	3.24
	1500' TAXI	36.5	--	--	25	119.3	206.9	20.28
	90' LFT TURN	35.6	5.1	--	10	120.6	207.3	1.95
	35' RT TURN	37.0	9.7	--	10	122.0	207.9	1.46

*1 cycle equals 1 revolution of the wheel and based on 17.4 percent of
 all flights.

TABLE A-3.   LONG-RANGE TRANSPORT LOAD SPECTRUM
FOR A TAKEOFF WEIGHT OF 0.818 TIMES
DESIGN GROSS WEIGHT FOR 12.2 PERCENT
OF FLIGHTS

| | EVENT | WHEEL LOAD - KIPS | | | SPEED MPH | TIRE CONTAINED GAS | | SINGLE FLIGHT CYCLES* |
		RADIAL	LATERAL	DRAG		TEMP °F	PRESS PSI	
TAKEOFF	90' LFT TURN	47.3	5.3	--	10	100.4	200.1	1.39
	90' RT TURN	49.4	5.6	--	10	101.9	200.7	1.88
	1500' TAXI	48.4	--	--	25	109.9	203.6	14.46
	150' LFT TURN	47.5	3.5	--	10	113.1	204.7	2.31
	3000' TAXI	48.4	--	--	25	120.9	207.5	28.91
	150' LFT TURN	47.5	3.5	--	10	124.3	208.7	2.31
	9000' TAXI	48.4	--	--	25	172.9	226.1	85.74
	65' RT TURN	49.4	8.1	--	10	176.0	227.2	1.50
	65' RT TURN	49.4	8.1	--	10	186.7	231.0	1.50
	6100' T.O.	54.8	--	--	0-170	194.9	233.9	58.28
	3.6 Flight Hours							
LANDING	1922' LDG	56.1	--	--	160	83.5	194.1	18.52
	3945' BRK	51.3	--	--	160-25	96.8	198.8	37.88
	1800' TAXI	47.3	--	--	25	121.3	207.6	17.19
	150' LFT TURN	40.0	3.4	--	10	124.4	208.7	2.27
	65' LFT TURN	39.8	10.9	--	10	126.4	209.4	1.00
	5000' TAXI	42.5	--	--	25	148.8	217.4	47.41
	150' RT TURN	41.3	3.0	--	10	150.1	217.9	2.75
	3000' TAXI	42.5	--	--	25	162.3	222.3	28.45
	150' LFT TURN	40.0	3.4	--	10	164.3	223.0	2.27
	1500' TAXI	42.5	--	--	25	170.9	225.3	14.22
	90' LFT TURN	39.6	5.2	--	10	172.0	225.7	1.37
	35' RT TURN	41.5	10.3	--	10	173.3	226.2	1.02

*1 cycle equals 1 revolution of the wheel and based on 12.2 percent of
all flights.

TABLE A-4. LONG-RANGE TRANSPORT LOAD SPECTRUM
FOR A TAKEOFF WEIGHT OF 0.736 TIMES
DESIGN GROSS WEIGHT FOR 12.2 PERCENT
OF FLIGHTS

	EVENT	WHEEL LOAD - KIPS			SPEED MPH	TIRE CONTAINED GAS		SINGLE FLIGHT CYCLES*
		RADIAL	LATERAL	DRAG		TEMP °F	PRESS PSI	
TAKEOFF	90' LFT TURN	43.2	5.1	--	10	100.4	200.1	1.39
	90' RT TURN	44.3	5.5	--	10	101.9	200.7	1.88
	1500' TAXI	43.4	--	--	25	108.1	202.9	14.46
	150' LFT TURN	42.5	3.6	--	10	110.3	203.7	2.31
	3000' TAXI	43.4	--	--	25	123.9	208.6	28.91
	150' LFT TURN	42.5	3.6	--	10	126.5	209.5	2.31
	9000' TAXI	43.4	--	--	25	167.9	224.3	85.74
	65' RT TURN	44.1	7.5	--	10	170.0	225.0	1.50
	65' RT TURN	44.1	7.5	--	10	179.5	228.4	1.50
	4787' T.O.	50.1	--	--	0-170	184.1	230.1	45.92
	3.6 Flight Hours							
LANDING	1816' LDG	51.1	--	--	160	78.0	192.1	17.43
	3641' BRK	46.7	--	9.8	160-25	85.7	194.9	34.83
	1800' TAXI	43.1	--	--	25	100.3	206.1	17.17
	150' LFT TURN	35.7	3.4	--	10	118.3	206.5	2.27
	65' LFT TURN	35.0	11.1	--	10	121.3	207.6	1.00
	5000' TAXI	36.4	--	--	25	140.7	214.7	47.41
	150' RT TURN	36.9	3.1	--	10	145.0	216.1	2.75
	3000' TAXI	36.4	--	--	25	154.3	219.4	28.45
	150' LFT TURN	35.7	3.4	--	10	159.3	221.2	2.27
	1500' TAXI	36.4	--	--	25	165.8	223.5	14.22
	90' LFT TURN	35.5	5.1	--	10	167.0	224.0	1.37
	35' RT TURN	36.9	9.7	--	10	168.5	224.5	1.02

*1 cycle equals 1 revolution of the wheel and based on 12.2 percent of
all flights.

A-4

TABLE A-5. LONG-RANGE TRANSPORT LOAD SPECTRUM
FOR A TAKEOFF WEIGHT OF 0.729 TIMES
DESIGN GROSS WEIGHT FOR 26.5 PERCENT
OF FLIGHTS

| | EVENT | WHEEL LOAD - KIPS | | | SPEED MPH | TIRE CONTAINED GAS | | SINGLE FLIGHT CYCLES* |
		RADIAL	LATERAL	DRAG		TEMP °F	PRESS PSI	
TAKEOFF	90' LFT TURN	42.8	5.1	--	10	100.4	200.1	3.02
	90' RT TURN	43.8	5.4	--	10	101.9	200.7	4.08
	1500' TAXI	43.0	--	--	25	108.1	202.9	31.40
	150' LFT TURN	42.1	3.6	--	10	110.4	203.7	5.01
	3000' TAXI	43.0	--	--	25	124.0	208.6	62.81
	150' LFT TURN	42.1	3.6	--	10	126.4	209.4	5.01
	9000' TAXI	43.0	--	--	25	167.8	224.2	188.42
	65' RT TURN	43.6	7.4	--	10	169.8	224.9	3.26
	65' RT TURN	43.6	7.4	--	10	179.3	228.3	3.26
	4739' T.O.	49.6	--	--	0-170	182.6	229.5	98.69
	1.0 Flight Hours							
LANDING	1922' LDG	56.1	--	--	160	146.5	216.6	40.19
	3945' BRK	51.3	--	12.6	160-25	154.2	219.4	82.20
	1800' TAXI	47.3	--	--	25	168.8	224.6	37.30
	150' LFT TURN	40.0	3.4	--	10	186.8	231.0	4.93
	65' LFT TURN	39.8	10.9	--	10	189.8	232.1	2.17
	5000' TAXI	42.5	--	--	25	209.2	239.0	102.88
	150' RT TURN	41.3	3.0	--	10	213.5	240.6	5.97
	3000' TAXI	42.5	--	--	25	222.8	243.9	61.74
	150' LFT TURN	40.0	3.4	--	10	227.8	245.7	4.93
	1500' TAXI	42.5	--	--	25	233.7	247.8	30.86
	90' LFT TURN	39.6	5.2	--	10	234.9	248.2	2.97
	35' RT TURN	41.5	10.3	--	10	236.3	248.7	2.21

*1 cycle equals 1 revolution of the wheel and based on 26.5 percent of
all flights.

A-5

TABLE A-6. LONG-RANGE TRANSPORT LOAD SPECTRUM
FOR A TAKEOFF WEIGHT OF 0.652 TIMES
DESIGN GROSS WEIGHT FOR 26.5 PERCENT
OF FLIGHTS

| | EVENT | WHEEL LOAD - KIPS | | | SPEED MPH | TIRE CONTAINED GAS | | SINGLE FLIGHT CYCLES* |
		RADIAL	LATERAL	DRAG		TEMP °F	PRESS PSI	
TAKEOFF	90' LFT TURN	37.5	5.1	--	10	101.2	200.4	3.02
	90' RT TURN	39.2	5.5	--	10	102.8	201.0	4.08
	1500' TAXI	38.6	--	--	25	108.3	203.0	31.40
	150' LFT TURN	37.5	3.2	--	10	110.0	203.6	5.01
	3000' TAXI	38.6	--	--	25	121.6	207.7	62.81
	150' LFT TURN	37.5	3.2	--	10	123.2	208.3	5.01
	9000' TAXI	38.6	--	--	25	156.7	220.3	188.42
	65' RT TURN	39.1	7.2	--	10	158.2	220.8	3.26
	65' RT TURN	39.1	7.2	--	10	167.1	224.0	3.26
	3927' T.O.	44.9	--	--	0-170	170.5	225.2	81.49
	1.0 Flight Hours							
LANDING	1816' LDG	51.1	--	--	160	136.4	213.0	37.82
	3641' BRK	46.7	--	9.8	160-25	150.2	217.9	75.58
	1800' TAXI	43.1	--	--	25	174.7	226.7	37.26
	150' LFT TURN	35.7	3.4	--	10	177.8	227.8	4.93
	65' LFT TURN	35.0	11.1	--	10	179.8	228.5	2.17
	5000' TAXI	36.4	--	--	25	202.2	236.5	102.88
	150' RT TURN	36.9	3.1	--	10	203.5	237.0	5.97
	3000' TAXI	36.4	--	--	25	215.8	241.4	61.74
	150' LFT TURN	35.7	3.4	--	10	217.8	242.1	4.93
	1500' TAXI	36.4	--	--	25	224.3	244.5	30.86
	90' LFT TURN	35.5	5.1	--	10	225.5	244.9	2.97
	35' RT TURN	36.9	9.7	--	10	226.8	245.3	2.21

*1 cycle equals 1 revolution of the wheel and based on 26.5 percent of
 all flights.

A-6

TABLE A-7. MEDIUM-RANGE TRANSPORT LOAD SPECTRUM
FOR A TAKEOFF WEIGHT OF 0.958 TIMES
DESIGN GROSS WEIGHT FOR 15.2 PERCENT
OF FLIGHTS

| | EVENT | WHEEL LOAD – KIPS | | | SPEED MPH | TIRE CONTAINED GAS | | SINGLE FLIGHT CYCLES* |
		RADIAL	LATERAL	DRAG		TEMP °F	PRESS PSI	
TAKEOFF	90' LFT TURN	46.8	5.2	--	10	100.0	205.0	1.72
	90' RT TURN	48.8	5.5	--	10	100.1	205.0	2.52
	1500' TAXI	47.8	--	--	25	100.1	205.4	18.68
	150' LFT TURN	47.0	3.5	--	10	101.6	205.6	2.89
	3000' TAXI	47.8	--	--	25	106.8	207.5	37.38
	150' LFT TURN	47.0	3.5	--	10	108.3	208.0	2.89
	9000' TAXI	47.8	--	--	25	134.6	217.7	112.13
	65' RT TURN	48.8	8.0	--	10	136.7	218.4	2.02
	65' RT TURN	48.8	8.0	--	10	138.6	219.2	2.02
	6030' T.O.	54.2	--	--	0-170	150.1	223.4	75.62
	5.6 Hour Flight							
LANDING	1770' LDG	49.8	--	--	160	43.9	184.4	22.10
	3550' BRK	45.5	--	9.6	160-25	45.7	185.0	44.13
	1800' TAXI	42.0	--	--	25	56.9	189.2	22.30
	150' LFT TURN	34.8	3.3	--	10	60.7	190.5	2.86
	65' LFT TURN	34.1	10.8	--	10	62.2	191.1	1.22
	5000' TAXI	35.5	--	--	25	87.8	200.5	61.53
	150' RT TURN	36.0	3.0	--	10	92.1	202.1	3.65
	3000' TAXI	35.5	--	--	25	107.2	207.6	36.92
	150' LFT TURN	34.8	3.3	--	10	110.3	208.7	2.86
	1500' TAXI	35.5	--	--	25	117.7	211.5	18.45
	90' LFT TURN	34.6	5.0	--	10	119.4	212.1	1.70
	35' RT TURN	36.0	9.5	--	10	120.8	212.6	1.41

*1 cycle equals 1 revolution of the wheel and based on 15.2 percent of
all flights.

TABLE A-8. MEDIUM-RANGE TRANSPORT LOAD SPECTRUM
FOR A TAKEOFF WEIGHT OF 0.900 TIMES
DESIGN GROSS WEIGHT FOR 10.9 PERCENT
OF FLIGHTS

	EVENT	WHEEL LOAD – KIPS			SPEED MPH	TIRE CONTAINED GAS		SINGLE FLIGHT CYCLES*
		RADIAL	LATERAL	DRAG		TEMP °F	PRESS PSI	
TAKEOFF	90' LFT TURN	43.8	5.3	--	10	100.0	205.0	1.23
	90' RT TURN	45.9	5.5	--	10	100.1	205.0	1.81
	1500' TAXI	44.9	--	--	25	100.9	205.3	13.40
	150' LFT TURN	44.0	3.5	--	10	101.4	205.5	2.07
	3000' TAXI	44.9	--	--	25	106.0	207.2	26.79
	150' LFT TURN	44.0	3.5	--	10	107.3	207.7	2.07
	9000' TAXI	44.9	--	--	25	130.7	216.3	80.38
	65' RT TURN	45.8	7.3	--	10	132.5	216.9	1.45
	65' RT TURN	45.8	7.3	--	10	134.3	217.5	1.45
	5280' T.O.	51.4	--	--	0-170	140.9	220.0	47.50
	1.9 Hour Flight							
LANDING	1900' LDG	55.5	--	--	160	73.9	195.5	17.17
	3900' BRK	50.7	--	12.5	160-25	75.2	195.9	35.07
	1800' TAXI	46.8	--	--	25	84.1	199.1	16.11
	150' LFT TURN	39.5	3.4	- -	10	92.5	202.2	2.06
	65' LFT TURN	39.3	10.8	--	10	93.7	202.7	0.88
	5000' TAXI	42.0	--	--	25	115.0	210.5	44.54
	150' RT TURN	40.8	3.0	--	10	118.9	211.9	2.63
	3000' TAXI	42.0	--	--	25	132.7	217.0	26.72
	150' LFT TURN	39.5	3.4	--	10	136.0	218.2	2.06
	1500' TAXI	42.0	--	--	25	143.9	221.1	13.36
	90' LFT TURN	39.2	5.1	--	10	145.8	221.7	1.23
	35' RT TURN	41.0	10.2	--	10	147.3	222.3	1.02

*1 cycle equals 1 revolution of the wheel and based on 10.9 percent of
all flights.

TABLE A-9. MEDIUM-RANGE TRANSPORT LOAD SPECTRUM
FOR A TAKEOFF WEIGHT OF 0.847 TIMES
DESIGN GROSS WEIGHT FOR 30.2 PERCENT
OF FLIGHTS

| | EVENT | WHEEL LOAD - KIPS | | | SPEED MPH | TIRE CONTAINED GAS | | SINGLE FLIGHT CYCLES* |
		RADIAL	LATERAL	DRAG		TEMP °F	PRESS PSI	
TAKEOFF	90' LFT TURN	42.0	5.0	--	10	100.0	205.0	3.41
	90' RT TURN	43.0	5.3	--	10	100.1	205.0	4.98
	1500' TAXI	42.2	--	--	25	100.8	205.3	37.12
	150' LFT TURN	41.3	3.5	--	10	101.3	205.5	5.74
	3000' TAXI	42.2	--	--	25	105.4	207.0	74.23
	150' LFT TURN	41.3	3.5	--	10	106.5	207.4	5.74
	9000' TAXI	42.2	--	--	25	127.3	215.0	222.69
	65' RT TURN	42.8	7.3	--	10	128.9	215.6	4.02
	65' RT TURN	42.8	7.3	--	10	130.4	216.2	4.02
	4650' T.O.	48.7	--	--	0-170	135.8	218.1	115.97
	0.6 Hour Flight							
LANDING	1900' LDG	55.5	--	--	160	116.3	211.0	47.78
	3900' BRK	50.7	--	12.5	160-25	117.5	211.4	97.52
	1800' TAXI	46.8	--	--	25	124.5	214.0	44.79
	150' LFT TURN	39.5	3.4	--	10	126.9	214.9	5.74
	65' LFT TURN	39.3	10.8	--	10	127.9	215.2	2.45
	5000' TAXI	42.0	--	--	25	145.5	221.7	123.73
	150' RT TURN	40.8	3.0	--	10	148.6	222.8	7.31
	3000' TAXI	42.0	--	--	25	159.9	227.0	74.24
	150' LFT TURN	39.5	3.4	--	10	162.3	227.8	5.74
	1500' TAXI	42.0	--	--	25	168.0	229.9	37.12
	90' LFT TURN	39.2	5.1	--	10	169.4	230.4	3.41
	35' RT TURN	41.0	10.2	--	10	170.5	230.8	2.84

*1 cycle equals 1 revolution of the wheel and based on 30.2 percent of
 all flights.

A-9

TABLE A-10. MEDIUM-RANGE TRANSPORT LOAD SPECTRUM
FOR A TAKEOFF WEIGHT OF 0.787 TIMES
DESIGN GROSS WEIGHT FOR 10.4 PERCENT
OF FLIGHTS

| | EVENT | WHEEL LOAD - KIPS | | | SPEED MPH | TIRE CONTAINED GAS | | SINGLE FLIGHT CYCLES* |
		RADIAL	LATERAL	DRAG		TEMP °F	PRESS PSI	
TAKEOFF	90' LFT TURN	38.2	5.2	--	10	100.0	205.0	1.18
	90' RT TURN	39.9	5.6	--	10	100.0	205.0	1.73
	1500' TAXI	39.3	--	--	25	100.6	205.2	12.78
	150' LFT TURN	38.2	3.3	--	10	101.0	205.4	1.98
	3000' TAXI	39.3	--	--	25	104.4	206.6	25.56
	150' LFT TURN	38.2	3.3	--	10	105.3	207.0	1.98
	9000' TAXI	39.3	--	--	25	123.1	213.5	76.69
	65' RT TURN	39.8	7.3	--	10	124.4	214.0	1.38
	65' RT TURN	39.8	7.3	--	10	125.8	215.0	1.38
	4000' T.O.	45.7	--	--	0-170	129.7	216.4	44.80
	1.9 Hour Flight							
LANDING	1750' LDG	49.4	--	--	160	69.3	194.2	15.10
	3520' BRK	45.1	--	10.0	160-25	70.3	194.6	30.22
	1800' TAXI	41.6	--	--	25	77.2	197.1	15.39
	150' LFT TURN	34.5	3.3	--	10	79.6	198.0	1.97
	65' LFT TURN	33.8	10.8	--	10	80.6	198.4	0.84
	5000' TAXI	35.3	--	--	25	98.3	204.9	42.41
	150' RT TURN	35.7	3.0	--	10	101.4	206.0	2.51
	3000' TAXI	35.3	--	--	25	112.8	210.2	25.45
	150' LFT TURN	34.5	3.3	--	10	115.3	211.1	1.97
	1500' TAXI	35.3	--	--	25	121.1	213.3	12.72
	90' LFT TURN	34.3	5.0	--	10	122.5	213.8	1.18
	35' RT TURN	35.7	9.5	--	10	123.7	214.2	0.98

*1 cycle equals 1 revolution of the wheel and based on 10.4 percent of
all flights.

TABLE A-11. MEDIUM-RANGE TRANSPORT LOAD SPECTRUM
FOR A TAKEOFF WEIGHT OF 0.745 TIMES
DESIGN GROSS WEIGHT FOR 33.3 PERCENT
OF FLIGHTS

| | EVENT | WHEEL LOAD - KIPS | | | SPEED MPH | TIRE CONTAINED GAS | | SINGLE FLIGHT CYCLES* |
		RADIAL	LATERAL	DRAG		TEMP °F	PRESS PSI	
TAKEOFF	90' LFT TURN	36.2	5.0	--	10	100.0	205.0	3.76
	90' RT TURN	37.7	5.3	--	10	100.0	205.0	5.53
	1500' TAXI	37.2	--	--	25	100.6	205.2	40.93
	150' LFT TURN	35.9	3.3	--	10	100.9	205.3	6.33
	3000' TAXI	37.2	--	--	25	104.0	206.5	81.85
	150' LFT TURN	35.9	3.3	--	10	104.8	206.8	6.33
	9000' TAXI	37.2	--	--	25	120.8	212.9	245.55
	65' RT TURN	37.7	7.3	--	10	122.0	213.4	4.33
	65' RT TURN	37.7	7.3	--	10	123.3	213.9	4.33
	3600' T.O.	43.5	--	--	0-170	126.4	215.0	99.07
	0.6 Hour Flight							
LANDING	1750' LDG	49.6	--	--	160	102.1	206.0	48.55
	3530' BRK	45.3	--	10.3	160-25	102.8	206.3	97.37
	1800' TAXI	41.8	--	--	25	108.0	208.2	49.42
	150' LFT TURN	34.7	3.3	--	10	109.8	208.8	6.33
	65' LFT TURN	34.0	10.8	--	10	111.5	209.5	2.70
	5000' TAXI	35.3	--	--	25	124.9	214.4	136.13
	150' RT TURN	35.9	3.0	--	10	127.3	215.3	8.06
	3000' TAXI	35.3	--	--	25	136.0	218.5	81.68
	150' LFT TURN	34.7	3.3	--	10	137.9	219.2	6.33
	1500' TAXI	35.3	--	--	25	142.4	220.8	40.84
	90' LFT TURN	34.5	5.0	--	10	143.5	221.2	3.76
	35' RT TURN	35.9	9.5	--	10	144.4	221.5	3.13

*1 cycle equals 1 revolution of the wheel and based on 33.3 percent of
all flights.

A-11

TABLE A-12. SHORT HAUL TRANSPORT LOAD SPECTRUM
FOR A TAKEOFF WEIGHT OF 0.916 TIMES
DESIGN GROSS WEIGHT FOR 20 PERCENT
OF FLIGHTS

| | EVENT | WHEEL LOAD - KIPS | | | SPEED MPH | TIRE CONTAINED GAS | | SINGLE FLIGHT CYCLES* |
		RADIAL	LATERAL	DRAG		TEMP °F	PRESS PSI	
TAKEOFF	90' LFT TURN	34.9	0.4	--	10	100.0	175.0	2.38
	90' RT TURN	37.6	0.3	--	10	100.0	175.0	2.84
	1500' TAXI	36.6	--	--	25	100.7	175.0	24.88
	150' LFT TURN	35.4	0.1	--	10	101.2	175.4	3.94
	3000' TAXI	36.6	--	--	25	105.2	176.6	49.76
	150' LFT TURN	35.4	0.1	--	10	106.4	177.0	3.94
	9000' TAXI	36.6	--	--	25	127.3	183.5	149.28
	65' RT TURN	38.3	1.2	--	10	128.6	184.0	2.18
	65' RT TURN	38.3	1.2	--	10	129.9	184.4	2.18
	4340' T.O.	40.3	--	--	0-160	134.9	185.9	72.28
	1.0 Hour Flight							
LANDING	1777' LDG	38.5	--	--	155	98.8	174.6	29.54
	3124' BRK	34.2	--	7.4	155-25	99.2	174.7	51.68
	1800' TAXI	38.5	--	--	25	103.0	176.0	29.92
	150' LFT TURN	33.5	0.1	--	10	104.5	176.5	4.00
	65' LFT TURN	32.4	1.2	--	10	105.1	176.7	1.72
	5000' TAXI	35.2	--	--	25	117.6	180.6	82.82
	150' RT TURN	35.4	0.1	--	10	120.0	181.3	4.42
	3000' TAXI	35.2	--	--	25	129.3	184.3	49.69
	150' LFT TURN	33.5	0.1	--	10	131.5	185.0	4.00
	1500' TAXI	35.2	--	--	25	136.6	186.6	24.85
	90' LFT TURN	33.1	0.2	--	10	137.9	187.0	2.38
	35' RT TURN	36.9	2.5	--	10	138.7	187.2	1.40

0.5 HOUR TERMINAL TIME

*1 cycle equals 1 revolution of the wheel and based on 20 percent of
all flights.

TABLE A-13. SHORT HAUL TRANSPORT LOAD SPECTRUM
FOR A TAKEOFF WEIGHT OF 0.865 TIMES
DESIGN GROSS WEIGHT FOR 20 PERCENT
OF FLIGHTS

	EVENT	WHEEL LOAD - KIPS			SPEED MPH	TIRE CONTAINED GAS		SINGLE FLIGHT CYCLES*
		RADIAL	LATERAL	DRAG		TEMP °F	PRESS PSI	
TAKEOFF	90' LFT TURN	32.9	0.4	--	10	135.3	186.2	2.38
	90' RT TURN	35.5	0.3	--	10	135.2	186.1	2.84
	1500' TAXI	34.5	--	--	25	135.3	186.2	24.82
	150' LFT TURN	33.4	0.1	--	10	135.5	186.3	3.94
	3000' TAXI	34.5	--	--	25	137.8	187.0	49.64
	150' LFT TURN	33.4	0.1	--	10	138.1	187.1	3.94
	9000' TAXI	34.5	--	--	25	152.9	191.7	148.92
	65' RT TURN	36.1	1.1	--	10	153.8	192.0	2.18
	65' RT TURN	36.1	1.1	--	10	154.8	192.3	2.18
	4097' T.O.	38.0	--	--	0-160	158.2	193.4	68.06
	0.667 Hour Flight							
LANDING	1724' LDG	36.9	--	--	155	127.0	183.6	28.66
	2968' BRK	32.3	--	7.1	155-25	127.1	183.6	49.04
	1800' TAXI	36.9	--	--	25	129.0	184.2	29.92
	150' LFT TURN	32.1	0.1	--	10	129.7	184.4	3.92
	65' LFT TURN	31.1	1.2	--	10	130.0	184.5	1.72
	5000' TAXI	33.7	--	--	25	137.9	187.0	82.68
	150' RT TURN	34.0	0.1	--	10	139.4	187.5	4.38
	3000' TAXI	33.7	--	--	25	146.1	189.6	49.61
	150' LFT TURN	32.1	0.1	--	10	147.6	190.0	3.92
	1500' TAXI	33.7	--	--	25	151.4	191.2	24.80
	90' LFT TURN	31.8	0.2	--	10	152.3	191.5	2.36
	35' RT TURN	35.6	2.4	--	10	152.9	191.7	1.40

0.5 HOUR TERMINAL TIME

*1 cycle equals 1 revolution of the wheel and based on 20 percent of
all flights.

TABLE A-14. SHORT HAUL TRANSPORT LOAD SPECTRUM
FOR A TAKEOFF WEIGHT OF 0.820 TIMES
DESIGN GROSS WEIGHT FOR 20 PERCENT
OF FLIGHTS

	EVENT	WHEEL LOAD - KIPS			SPEED MPH	TIRE CONTAINED GAS		SINGLE FLIGHT CYCLES*
		RADIAL	LATERAL	DRAG		TEMP °F	PRESS PSI	
TAKEOFF	90' LFT TURN	31.5	0.4	--	10	148.2	190.2	2.36
	90' RT TURN	34.0	0.3	--	10	148.0	190.2	2.82
	1500' TAXI	33.1	--	--	25	147.8	190.1	24.78
	150' LFT TURN	32.0	0.1	--	10	147.9	190.1	3.92
	3000' TAXI	33.1	--	--	25	149.4	190.6	49.56
	150' LFT TURN	32.0	0.1	--	10	149.9	190.8	3.92
	9000' TAXI	33.1	--	--	25	161.0	194.2	148.68
	65' RT TURN	34.6	1.1	--	10	161.7	194.5	2.18
	65' RT TURN	34.6	1.1	--	10	162.5	194.7	2.18
	3925' T.O.	36.4	--	--	0-160	165.1	195.5	65.10
	0.667 Hour Flight							
LANDING	1656' LDG	35.3	--	--	155	131.9	185.1	27.42
	2813' BRK	31.4	--	6.8	155-25	131.9	185.1	46.40
	1800' TAXI	35.3	--	--	25	132.7	185.4	29.82
	150' LFT TURN	30.7	0.1	--	10	133.2	185.5	3.92
	65' LFT TURN	29.8	1.1	--	10	133.4	185.6	1.72
	5000' TAXI	32.2	--	--	25	138.9	187.3	82.54
	150' RT TURN	32.5	0.1	--	10	140.1	187.7	4.38
	3000' TAXI	32.2	--	--	25	145.3	189.3	49.52
	150' LFT TURN	30.7	0.1	--	10	146.6	189.7	3.92
	1500' TAXI	32.2	--	--	25	149.6	190.7	24.76
	90' LFT TURN	30.4	0.2	--	10	150.4	190.9	2.36
	35' RT TURN	34.1	0.3	--	10	150.8	191.1	1.40

0.5 HOUR TERMINAL TIME

*1 cycle equals 1 revolution of the wheel and based on 20 percent of
all flights.

A-14

TABLE A-15. SHORT HAUL TRANSPORT LOAD SPECTRUM
FOR A TAKEOFF WEIGHT OF 0.792 TIMES
DESIGN GROSS WEIGHT FOR 20 PERCENT
OF FLIGHTS

| | EVENT | WHEEL LOAD - KIPS | | | SPEED MPH | TIRE CONTAINED GAS | | SINGLE FLIGHT CYCLES* |
		RADIAL	LATERAL	DRAG		TEMP °F	PRESS PSI	
TAKEOFF	90' LFT TURN	30.2	0.3	--	10	146.4	189.7	2.36
	90' RT TURN	32.9	0.3	--	10	146.2	189.7	2.82
	1500' TAXI	31.6	--	--	25	146.0	189.6	24.74
	150' LFT TURN	30.6	0.1	--	10	146.1	189.6	3.92
	3000' TAXI	31.6	--	--	25	147.3	190.0	49.48
	150' LFT TURN	30.6	0.1	--	10	147.8	190.2	3.92
	9000' TAXI	31.6	--	--	25	157.8	193.3	148.44
	65' RT TURN	33.1	1.0	--	10	158.5	193.5	2.18
	65' RT TURN	33.1	1.0	--	10	159.2	193.7	2.18
	3754' T.O.	34.8	--	--	0-160	161.2	193.9	62.14
	1.0 Hour Flight							
LANDING	1632' LDG	33.0	--	--	155	119.1	181.2	26.96
	2593' BRK	29.4	--	6.3	155-25	119.1	181.2	42.68
	1800' TAXI	33.0	--	--	25	119.6	181.4	29.74
	150' LFT TURN	28.7	0.1	--	10	120.0	181.5	3.92
	65' LFT TURN	27.8	1.0	--	10	120.1	181.6	1.72
	5000' TAXI	30.2	--	--	25	125.0	183.2	82.36
	150' RT TURN	30.4	0.1	--	10	126.1	183.5	4.36
	3000' TAXI	30.2	--	--	25	130.9	185.0	49.42
	150' LFT TURN	28.7	0.1	--	10	132.1	185.4	3.92
	1500' TAXI	30.2	--	--	25	135.0	186.3	24.71
	90' LFT TURN	28.4	0.2	--	10	135.7	186.5	2.36
	35' RT TURN	31.9	2.2	--	10	136.2	186.7	1.40

0.5 HOUR TERMINAL TIME

*1 cycle equals 1 revolution of the wheel and based on 20 percent of
all flights.

TABLE A-16. SHORT HAUL TRANSPORT LOAD SPECTRUM
FOR A TAKEOFF WEIGHT OF 0.741 TIMES
DESIGN GROSS WEIGHT FOR 20 PERCENT
OF FLIGHTS

| | EVENT | WHEEL LOAD - KIPS | | | SPEED MPH | TIRE CONTAINED GAS | | SINGLE FLIGHT CYCLES* |
		RADIAL	LATERAL	DRAG		TEMP °F	PRESS PSI	
TAKEOFF	90' LFT TURN	28.2	0.3	--	10	133.0	185.7	2.36
	90' RT TURN	30.4	0.2	--	10	132.9	185.6	2.82
	1500' TAXI	29.6	--	--	25	132.8	185.6	24.70
	150' LFT TURN	28.6	0.1	--	10	132.9	185.7	3.92
	3000' TAXI	29.6	--	--	25	134.3	186.1	49.40
	150' LFT TURN	28.6	0.1	--	10	134.8	186.2	3.92
	9000' TAXI	29.6	--	--	25	144.8	189.4	148.20
	65' RT TURN	31.0	1.0	--	10	145.5	189.6	2.16
	65' RT TURN	31.0	1.0	--	10	146.1	189.8	2.16
	3510' T.O.	32.6	--	--	0-160	148.2	190.4	57.98
	0.667 Hour Flight							
LANDING	1585' LDG	31.4	--	--	155	119.3	181.3	26.14
	2439' BRK	28.0	--	6.0	155-25	119.3	181.3	40.08
	1800' TAXI	31.4	--	--	25	119.7	181.5	29.70
	150' LFT TURN	27.3	0.1	--	10	120.0	181.6	3.90
	65' LFT TURN	26.5	1.0	--	10	120.2	181.6	1.72
	5000' TAXI	28.7	--	--	25	124.5	183.0	82.22
	150' RT TURN	28.9	0.1	--	10	125.5	183.3	4.36
	3000' TAXI	28.7	--	--	25	129.9	184.7	49.33
	150' LFT TURN	27.3	0.1	--	10	131.0	185.0	3.90
	1500' TAXI	28.7	--	--	25	133.6	185.8	24.67
	90' LFT TURN	27.1	0.2	--	10	134.3	186.1	2.36
	35' RT TURN	30.3	2.1	--	10	134.7	186.2	1.40

*1 cycle equals 1 revolution of the wheel and based on 20 percent of
all flights.

TABLE A-17. PATROL AIRPLANE LOAD SPECTRUM
FOR A TAKEOFF WEIGHT OF 104,000 POUNDS
FOR 24.3 PERCENT OF FLIGHTS

	EVENT	WHEEL LOAD - KIPS			SPEED MPH	TIRE CONTAINED GAS		SINGLE FLIGHT CYCLES*
		RADIAL	LATERAL	DRAG		TEMP °F	PRESS PSI	
TAKEOFF	90' LFT. TURN	23.3	1.0	–	10	100.0	200.0	3.4
	90' RT. TURN	25.1	0.7	–	10	100.2	200.1	5.0
	1500' TAXI	24.4	–	–	25	102.9	201.0	37.0
	150' LFT. TURN	23.6	0.3	–	10	104.8	201.7	5.8
	3000' TAXI	24.4	–	–	25	116.9	206.1	74.0
	150' LFT. TURN	23.6	0.3	–	10	120.7	207.4	5.8
	9000' TAXI	24.4	–	–	25	160.5	221.7	222.0
	65' RT. TURN	25.6	2.6	–	10	165.1	223.3	4.0
	65' RT. TURN	25.6	2.6	–	10	169.4	224.8	4.0
	3,300' T.O.	26.9	–	–	0-150	182.5	229.5	81.4
FLIGHT	1.6 HRS., 210 KTS., ALT. 6 KFT.					146.2	216.5	–
	1.0 HRS., 230 KTS., ALT. 10 KFT.					126.0	209.3	–
	0.5 HRS., 150 KTS., GCA					122.0	207.9	–
	TOUCH & GO LDG.	22.1	–	–	150	121.9	207.8	68.3
	FLIGHT 9 MIN.	–	–	–	180	117.2	206.2	–
	TOUCH & GO LDG.	22.1	–	–	150	118.1	206.5	68.3
	FLIGHT 9 MIN.	–	–	–	180	116.4	205.9	–
LANDING	2,839' BRAKING	19.7	–	4.2	150-25	118.2	206.6	69.5
	1,800 TAXI	22.1	–	–	25	125.3	209.1	44.1
	150' LFT. TURN	19.2	0.3	–	10	128.1	210.1	5.7
	65' LFT. TURN	18.6	2.3	–	10	129.2	210.5	2.4
	5,000' TAXI	20.2	–	–	25	146.5	216.7	122.5
	150' RT. TURN	20.3	0.3	–	10	150.7	218.2	7.3
	3,000' TAXI	20.2	–	–	25	163.4	222.7	73.5
	150' LFT. TURN	19.2	0.3	–	10	166.5	223.9	5.7
	1,500' TAXI	20.2	–	–	25	173.3	226.3	36.7
	90' LFT. TURN	19.1	0.3	–	10	175.0	226.9	3.4
	35' RT. TURN	21.3	5.0	–	10	176.4	227.4	2.8

*1 cycle equals 1 revolution of the wheel and based on 24.3 percent of all flights.

A-17

TABLE A-17 (CONT'D). PATROL AIRPLANE LOAD SPECTRUM
FOR A TAKEOFF WEIGHT OF 104,000 POUNDS
FOR 24.3 PERCENT OF FLIGHTS

| | | WHEEL LOAD - KIPS | | | | TIRE CONTAINED GAS | | |
	EVENT	RADIAL	LATERAL	DRAG	SPEED MPH	TEMP °F	PRESS PSI	SINGLE FLIGHT CYCLES*
	2,400' T.O.	22.0	-	-	0-150	179.8	229.0	58.8
FLIGHT	FLIGHT 9 MIN.	-	-	-	180	160.2	222.0	-
	TOUCH & GO LDG.	21.8	-	-	150	159.1	221.6	67.7
	FLIGHT 9 MIN.	-	-	-	180	140.4	214.9	-
	TOUCH & GO LDG.	21.8	-	-	150	139.7	214.6	67.7
	FLIGHT 9 MIN.	-	-	-	180	126.4	209.8	-
	TOUCH & GO LDG.	21.8	-	-	150	126.3	209.8	67.7
	FLIGHT 9 MIN.	-	-	-	180	120.1	207.6	-
LANDING	2,756' BRAKING	19.5	-	4.2	150-25	120.9	207.9	67.5
	1,800' TAXI	21.8	-	-	25	126.1	209.7	44.1
	150' LFT. TURN	19.0	0.3	-	10	127.6	210.3	3.7
	65' LFT. TURN	18.4	2.3	-	10	128.2	210.5	1.6
	5,000' TAXI	20.0	-	-	25	143.8	216.1	122.5
	150' RT. TURN	20.1	0.3	-	10	145.9	216.9	3.7
	3,000' TAXI	20.0	-	-	25	158.5	221.4	73.5
	150' LFT. TURN	19.0	0.3	-	10	160.6	221.1	3.7
	1,500' TAXI	20.0	-	-	25	167.5	224.6	36.7
	90' LFT. TURN	18.8	0.3	-	10	169.2	225.2	3.4
	35' RT. TURN	21.1	5.0	-	10	170.6	225.7	2.8

*1 cycle equals 1 revolution of the wheel and based on 24.3 percent of
all flights.

TABLE A-18. TACTICAL AIRPLANE LOAD SPECTRUM
FOR A TAKEOFF WEIGHT OF 53,848 POUNDS
FOR 10 PERCENT OF FLIGHTS

| | WHEEL LOAD - KPS | | | | TIRE CONTAINED GAS | | |
EVENT	RADIAL	LATERAL	DRAG	SPEED MPH	TEMP °F	PRESS PSI	SINGLE FLIGHT CYCLES*
48' TAXI	25.6	-	-	5	100.0	250.0	0.6
90° LFT. TURN	25.1	1.3	-	5	100.1	250.0	0.6
800' TAXI	25.6	-	-	5	104.8	252.1	10.8
90° LFT. TURN	25.1	1.3	-	5	105.5	252.4	0.6
7,200' TAXI	25.6	-	-	30	170.4	281.5	97.6
90° LFT. TURN	25.1	1.3	-	5	178.8	285.5	0.9
120 SEC. HOLD	25.6	-	-	-	187.9	289.3	-
90° RT. TURN	26.0	1.3	-	5	188.5	289.6	1.1
150' TAXI	25.6	-	-	5	203.6	296.3	2.0
90° RT. TURN	26.0	1.3	-	5	209.5	299.0	0.8
80' TAXI	25.6	-	-	5	216.4	302.0	1.1
90° LFT. TURN	25.1	1.3	-	5	220.2	303.8	0.7
461' TAXI	25.6	-	-	20	228.5	307.5	6.2
90° RT. TURN	29.5	5.8	-	15	229.9	308.1	0.8
873' TAXI	25.6	-	-	15	244.9	314.8	11.8
90° RT. TURN	26.0	1.3	-	5	251.2	317.7	0.8
147' TAXI	25.6	-	-	5	257.1	320.3	2.0
60 SEC. HOLD	25.6	-	-	-	257.7	320.4	-
2,940 T.O.	25.6	-	-	0-170	264.2	323.5	39.8
1.58 HRS., 35,000' ALT.					227.3	307.0	-
5.0 MIN., S.L. GR. DN.					181.5	286.5	-

*1 cycle equals 1 revolution of the wheel and based on 10.0 percent of all flights.

TABLE A-18 (CONT'D). TACTICAL AIRPLANE LOAD SPECTRUM
FOR A TAKEOFF WEIGHT OF 53,848 POUNDS
FOR 10 PERCENT OF FLIGHTS

| | EVENT | WHEEL LOAD - KPS | | | SPEED MPH | TIRE CONTAINED GAS | | SINGLE FLIGHT CYCLES* |
		RADIAL	LATERAL	DRAG		TEMP °F	PRESS PSI	
LANDING	3,300' BRAKING	15.6	-	4.3	170-25	174.0	283.1	44.7
	4,500' TAXI	17.0	-	-	25	175.0	283.6	61.0
	90° RT. TURN	18.2	1.7	-	10	175.4	283.7	0.8
	680' TAXI	17.0	-	-	10	178.7	285.2	9.2
	90° RT. TURN	18.2	1.7	-	10	179.1	285.4	1.6
	90° LFT. TURN	16.8	0.4	-	5	179.9	285.7	0.9
	120 SEC. HOLD	17.0	-	-	-	180.1	285.8	-
	90° RT. TURN	17.3	0.4	-	5	180.7	286.1	1.1
	150' TAXI	17.0	-	-	5	181.9	286.7	2.0
	90° RT. TURN	17.3	0.4	-	5	182.4	286.9	0.8
	80' TAXI	17.0	-	-	5	183.0	287.2	1.1
	90° LFT. TURN	16.8	0.4	-	5	183.5	287.4	0.6
	400' TAXI	17.0	-	-	5	185.4	288.2	5.4
	90° LFT. TURN	16.8	0.4	-	5	185.8	288.4	0.8
	800' TAXI	17.0	-	-	5	188.0	289.4	10.8
	90° RT. TURN	17.3	0.4	-	5	188.4	289.5	1.1

*1 cycle equals 1 revolution of the wheel and based on 10.0 percent of
all flights.